ADDIS ABABA UNIVERSITY

COLLEGE OF NATURAL SCIENCES

SCHOOL OF EARTH SCIENCES

DEFORMATION HISTORY AND GEOCHEMISTRY OF NEOPROTEROZOIC ROCKS OF TAHTAILOGOMTI AREA, TIGRAI, NORTHERN ETHIOPIA

BY:

AZEB GEBREMICALE HAGOS

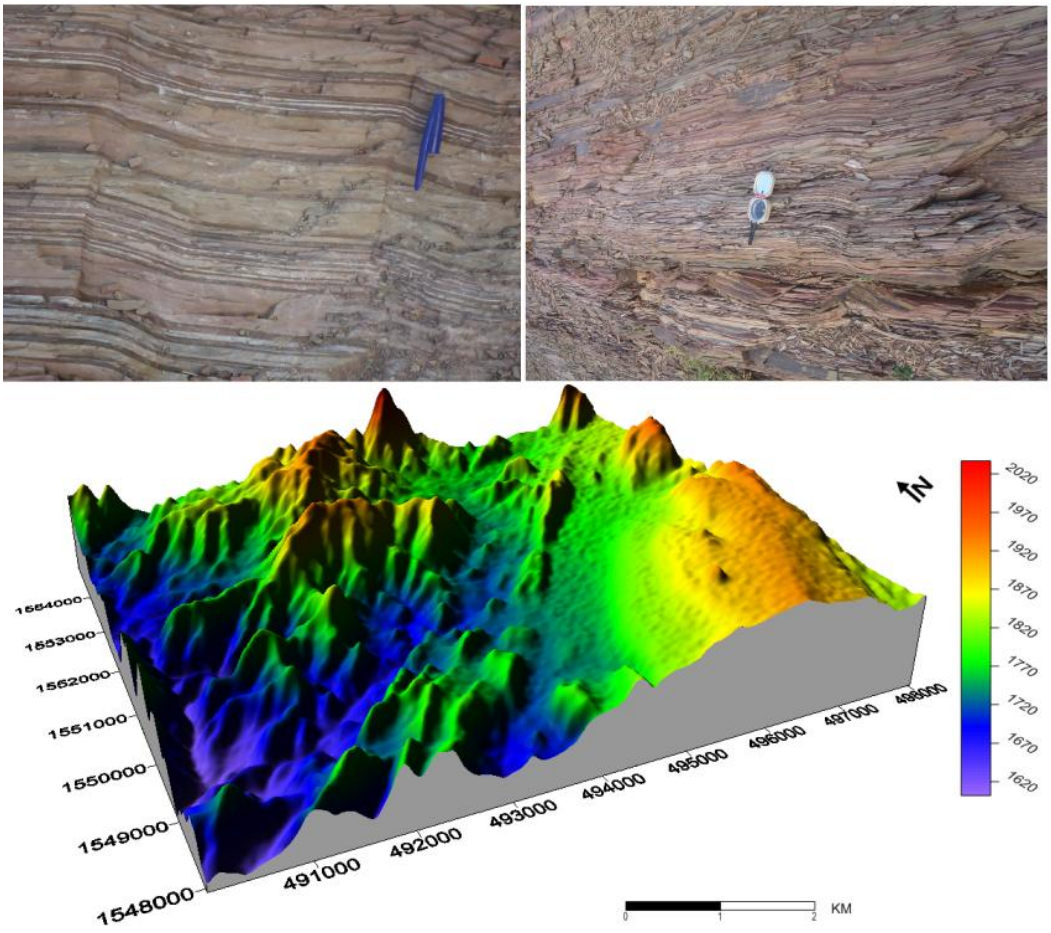

MAY, 2018

ADDIS ABABA UNIVERSITY
COLLEGE OF NATURAL SCIENCES
SCHOOL OF EARTH SCIENCES

DEFORMATION HISTORY AND GEOCHEMISTRY OF NEOPROTEROZOIC ROCKS OF TAHTAI LOGOMTI AREA, TIGRAI, NORTHERN ETHIOPIA

BY:

AZEB GEBREMICALE

ADVISOR: Dr. MULUGETA ALENE

A THESIS SUBMITTED TO SCHOOL OF EARTH SCIENCE, ADDIS ABABA UNIVERSITY, IN PARTIAL FULFILLMENT OF THE REQUIREMENTS FOR THE DEGREE OF MASTERS OF EARTH SCIENCES IN PETROLOGY

May 25, 2018
ADDIS ABABA, ETHIOPIA

ADDIS ABABA UNIVERSITY

COLLEGE OF NATURAL SCIENCES

SCHOOL OF EARTH SCIENCES

DEFORMATION HISTORY AND GEOCHEMISTRY OF NEOPROTEROZOIC ROCKS OF TAHTAI LOGOMTI AREA, TIGRAI, NORTHERN ETHIOPIA

By

Azeb Gebremicale Hagos

Approved by the Examining Committee

Dr. Balemwal Atnafu	_____	_____
Department Chairman and	Signature	Date
Graduate committee		
Dr. Mulugeta Alene Araya	_____	_____
Advisor	Signature	Date
Prof. Dereje Ayalew	_____	_____
Examiner	Signature	Date
Dr. Ameha Atnafu	_____	_____
Examiner	Signature	Date

MAY 25, 2018

ADDIS ABABA, ETHIOPIA

ADDIS ABABA UNIVERSITY

COLLEGE OF NATURAL SCIENCES

SCHOOL OF EARTH SCIENCES

This is to certify that this thesis is prepared by Azeb Gebremicale, entitled as: "Deformation history and geochemistry of Neoproterozoic rocks of Tahtai Logomti Area, Tigrai, Northern Ethiopia" and submitted in partial fulfillment of the requirement for the Degree of Master of Science in Petrology compiles with the regulations of the University and meets the accepted standards with respect to originality and quality.

Approved by the Examining Committee

Dr. Balemwal Atnafu	_____	_____
Head, School of Earth Science	Signature	Date
Dr. Mulugeta Alene	_____	_____
Advisor	Signature	Date
Prof. Dereje Ayalew	_____	_____
Examiner	Signature	Date
Dr. Ameha Atnafu	_____	_____
Examiner	Signature	Date

May 25, 2018

ADDIS ABABA, ETHIOPIA

Declaration of originality

I declare that the thesis entitled "Deformation history and geochemistry of Neoproterozoic rocks of Tahtai Logomti Area, Tigrai, and Northern Ethiopia" has been carried out by me under the supervision of Dr. Mulugeta Alene Araya, School of Earth Science, Addis Ababa University, during the year 2017-2018 as part of Masters of Science program in Petrology. It is my original work and has not been presented for a degree in any other university or institution, and that all sources of material used for the thesis have been duly acknowledged.

Azeb Gebremicale
Addis Ababa University
Addis Ababa
Date: 25/05/ 2018
Sign: ----------

Acknowledgment

I would like to thanks to Mekelle University and Ministry of Education of Ethiopia for giving me the chance to learn my master degree program.

In addition to, I would like also to acknowledge Addis Ababa University, School of Earth Science of for providing useful materials for my MSc study.

I am very gratefulness to my research advisor Dr. Mulugeta Alene for his close guidance/limitless support, valuable advices, comments and suggestions throughout the research work from the beginning to the end of the thesis was critical for the work and my future.

I gratefully thanks to my husband Mr. Teklay Gidey for his generous support, suggestion, encouragement and financial support and logistics throughout my research work.

My special thanks also go to my families for their encouragement, support, blessing and advice, especially for my brother Mr. Welday Gebremichael for his suggestion and support.

Finally, I would like to thanks the local peoples around Mai Kenetal and Tahtai Logomti area for their collaborated support during the field work.

Table of Content

Contents pages

List of Figures

List of Table

List of Acronyms

Act: Actinolite	ME-ICP06: Multi element inductive Coupled Plasma 06
ALS: Australian Laboratory Service	ME-MS81: Multi Element Mass Spectrometry81
ANS: Arabian Nubian Shield	mm: Millimeter
Bt: Biotite	MORB: Mid-ocean ridge basalt
CAB: Calc-alkaline basalt	Ms: Muscovite
Cal: Calcite	Op: Opaque
Chl: Chlorite	Pl: Plagioclase
D1: Deformational event 1	PPL: Plane Polarized Light
D2: Deformational event 2	ppm: part per million
D3: Deformational event 3	Px: Pyroxene
EAO: East African Orogeny	Qtz: Quartz
E-MORB: Enriched mid-ocean ridge basalt	REE: Rare Earth Element
Ep: Epidote	S0: Primary bedding
Fig.: Figure	S1: primary foliation
GCDKit: Geochemical data kit tool	Ser: Sericite
GPS: Global Position System	W.G: West Gondwana
HREEs: Heavy rare earth elements	WPB: With plate basalt
LILEs: Large ion lithophile elements	XPL: Cross polarized light
LOI: Loss on Ignition	
MB: Mozambique Belt	

Abstract

The Tahtai Logomti area is dominated by the Neoproterozoic basement rocks of Northern Ethiopia, occurred between the Adwa and Mai Kenetal blocks and covered by metavolcano-sedimentary rocks which belong to the Tambien and Tsaliet Groups and are part of the Arabian Nubian Shield. In this study, the integrated petrographic, structural and geochemical analyses were used to understand the metamorphism, deformation history and paleo-tectonic setting of the area. Basic to acidic metavolcanic, basic to intermediate metavolcanoclastic, meta-agglomerate and metatuff rock units characterized in the Tsaliet Group, whereas lower slate, lower metalimestone, upper slate and upper metalimestone are part of the Tambien Group. The quartz veins and acidic dike that has different orientations cut the metavolcani/clastic and metasedimentary rock units. Most of the units of the study area are characterized by volcanic origin parent rocks. The field observation lithologies, structural and petrographic interpretation of the rocks show that the area was affected by lower greenschist facies metamorphism. The macro and microstructures identification and analysis show that the study area has been affected by at least three events of deformation: D1 and D2 ductile deformations and a later brittle phase of deformation (D3). The relationship between metamorphism and deformation can be recognized from the mineral assemblages and micro structural features in the petrographic part. The first event of deformation (D1) shows NE striking S1 foliation and M1 metamorphic event and also pencil structure. It is represented by the development of mineral assemblages such as chlorite, actinolite, epidote, muscovite/sericite, plagioclase, calcite and recrystallized quartz. The second event of deformation is responsible for the development of low plunging folds, kink band folds and en echelon array veins. However, the third phase deformation (D3) is related to a different set of joints and faults that cut the regional foliation (S1) throughout each rock units.

The geochemical data plotted on different tectonic discrimination diagrams clearly indicates that the metavolcanic rocks of Tahtai Logomti area are characterized by calc-alkaline magma type and they were erupted in the volcanic arc setting. The general petrological and geochemical characteristics of the Tahtai Logomti metavolcanic rocks provides an important evidence to consider the area as part of the subduction-related arc accretion of the ANS.

Keywords: Deformation, foliation, metamorphism, metavolcanic, Neoproterozoic

CHAPTER ONE

1. Introduction

1.1. Background

The Gondwanaland was assembled during the Neoproterozoic time from two fragments, the West and East Gondwana along the Pan-African Mozambique Belt of East Africa (McWilliams, 1981). This idea is supported by the lithologic association's characteristic of the Mozambique Belt (MB) and the Arabian-Nubian Shield (ANS). The Pan African Mozambique Belt of East Africa is also called East African Orogen (EAO) (Stern, 1994). It consists of metamorphosed and deformed rocks of the higher grade Mozambique Belt in the south and the low grade Arabian-Nubian Shield in the northern part (Stern, 1994; Kroner and Stern, 2004). The fragments of Neoproterozoic rocks are now exposed in the African, Madagascar, Arabian and Indian Plates, once they were intact until the dispersal of Gondwanaland (Johnson et al., 2011). The ANS is part of the two major terranes in northern and eastern Africa that developed during the Neoproterozoic time (Kroner, 1985; Stern, 1994). It extends from Jordan and Israel in the north, through to Ethiopia and Sudan in the south (Berhe, 1990; Kroner et al., 1991; Stern, 1994; Teklay et al., 1998, 2001; Kroner and Stern, 2004). However, the Mozambique Belt is exposed in the south part and comprises mostly pre-Neoproterozoic crust with a Neoproterozoic early Cambrian tectonothermal overprint (Fritz et al., 2005; Collins, 2006).

The Ethiopia Neoproterozoic basement rocks are exposed in northern, western, southwestern, southern and eastern parts of the country. They are part of the southern ANS extension which is juvenile Neoproterozoic crust formed during the Mozambique Ocean closure accompanying greater Gondwana formation (Asrat et al., 2001; Stern, 1994, 2008; Fritz et al., 2013) (Fig.1.1). The low grade basement rocks of northern Ethiopia are subdivided into Tsaliet and Tambien Groups (Beyth, 1971). The former Group is older, mainly contains metavolcanic/metavolcanoclastic sequence, agglomerates, tuffs and mafic to felsic volcanic flows while, Tambien Group is a younger unit, mainly exposed in a series of synclinal inliers overlying the Tsaliet Group. It consists of metasedimentary rocks of slate and carbonate succession.

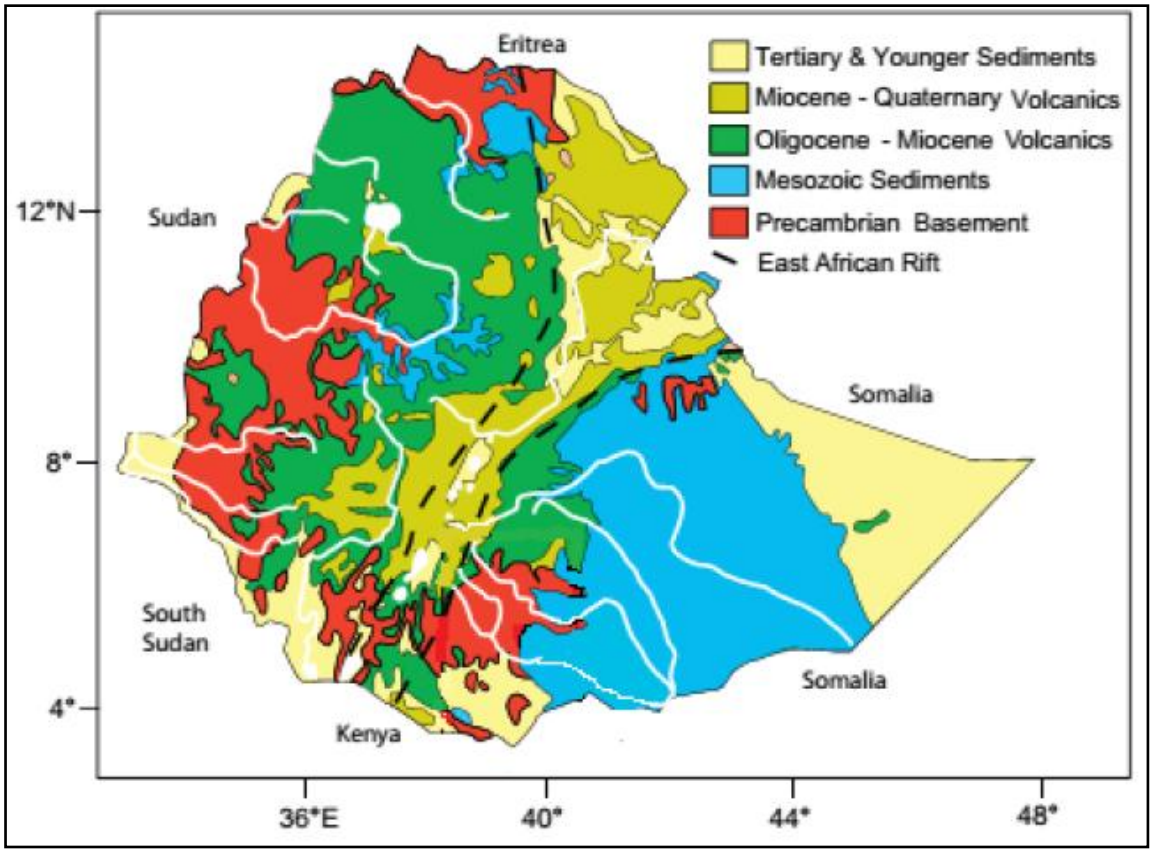

Figure1.1.Geological map of Ethiopia. The white lines and white irregular shapes are rivers and lakes, respectively. The map modified from Tefera et al. (1996) cited in Stern et al. (2012).

The Tsaliet and Tambien Groups recorded various tectonic structures that developed during the East African Orogen (Stern, 1994; Meert, 2003; Johnson and Woldehaimanot, 2003). Two phases of deformation in particular are commonly recognized in these rocks as D1 and D2 deformations (Alene, 1998; Alene and Sacchi, 2000). According to Sifeta et al. (2005), the provenance, weathering condition of the source area and tectonic setting of the sediment is determined by studies the geochemical of the metasedimentary rocks whereas, the tectonic setting of the volcanic rocks and its magma type are also determined and understand by studies the geochemistry of metavolcanic and micrograntic intrusion rocks (Alene et al., 2000). The present study area of the Tahtai Logomti area consists of both Tsaliet and Tambien groups of the northern Ethiopia rocks. The structural, petrography and geochemical studies of these rocks are important to evaluate the grade of metamorphism, phase of deformation and understand the tectonic evolution of the area.

1.2. Description of the study area

1.2.1. Location and accessibility of the study area

The study area is located in the Tahtai Logomti area, Tigrai, northern Ethiopia which is far about 930 km from Addis Ababa. Geographically, it is bounded by UTM coordinates of 490000m to 497000m E, and 1548000 m to 1555000 m N latitude and longitude, respectively with areal coverage about 49.24 km^2 (Fig. 1.2). It is accessed by the main asphalt road running from Mekelle to Adwa through Mai-Kenetal to the study area and it is accessed by different trails (Fig.1.2B).

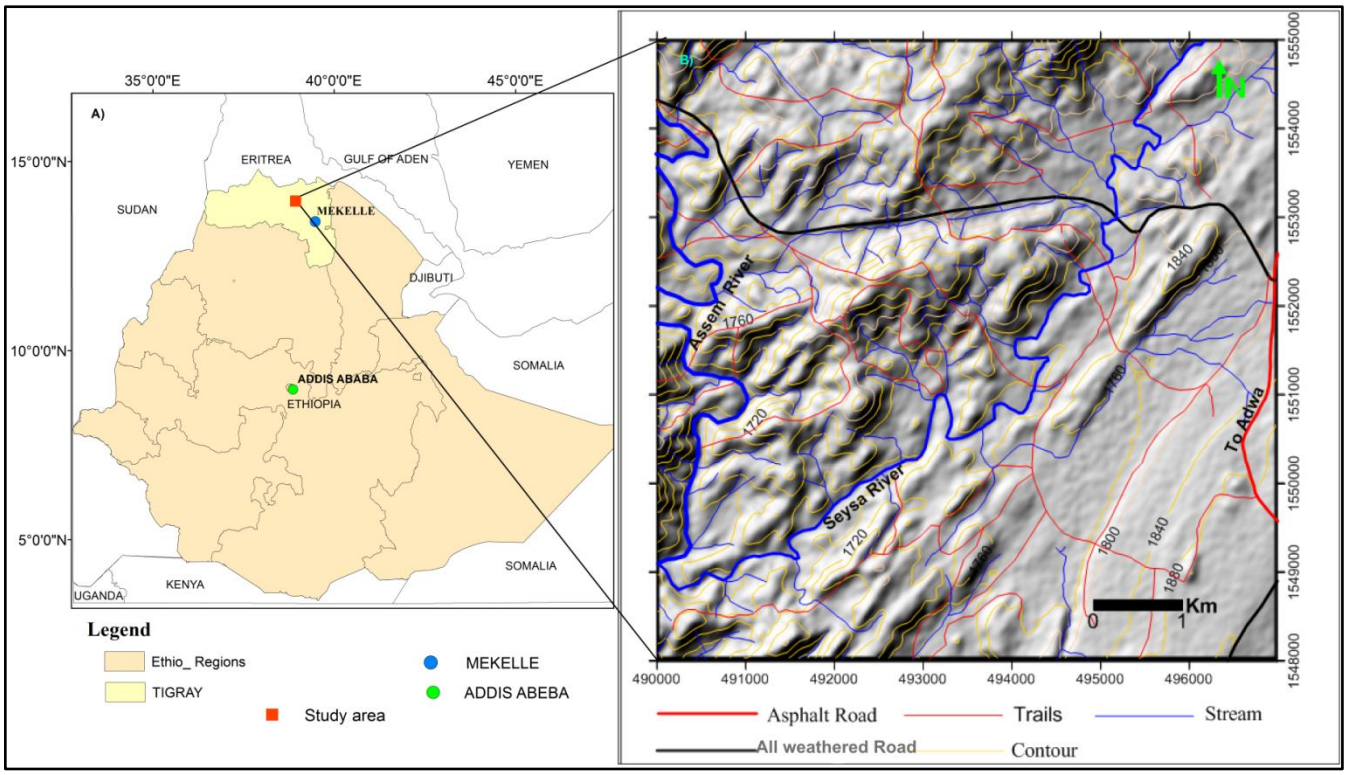

Figure1.2.Location and accessibility map of the study area extracted from DEM of Ethiopia using Global Mapper-11, extracted as map by Surfer 10 software (with a contour interval 40m).

1.2.2. Drainage pattern and physiography

The study area is characterized by sub parallel, radial and dendritic drainage patterns (Fig.1.3A). However, the main river shows meandering like flow. The area has minimum and maximum elevation of 1620 m and 2020 m above sea level respectively (Fig.1.3B)

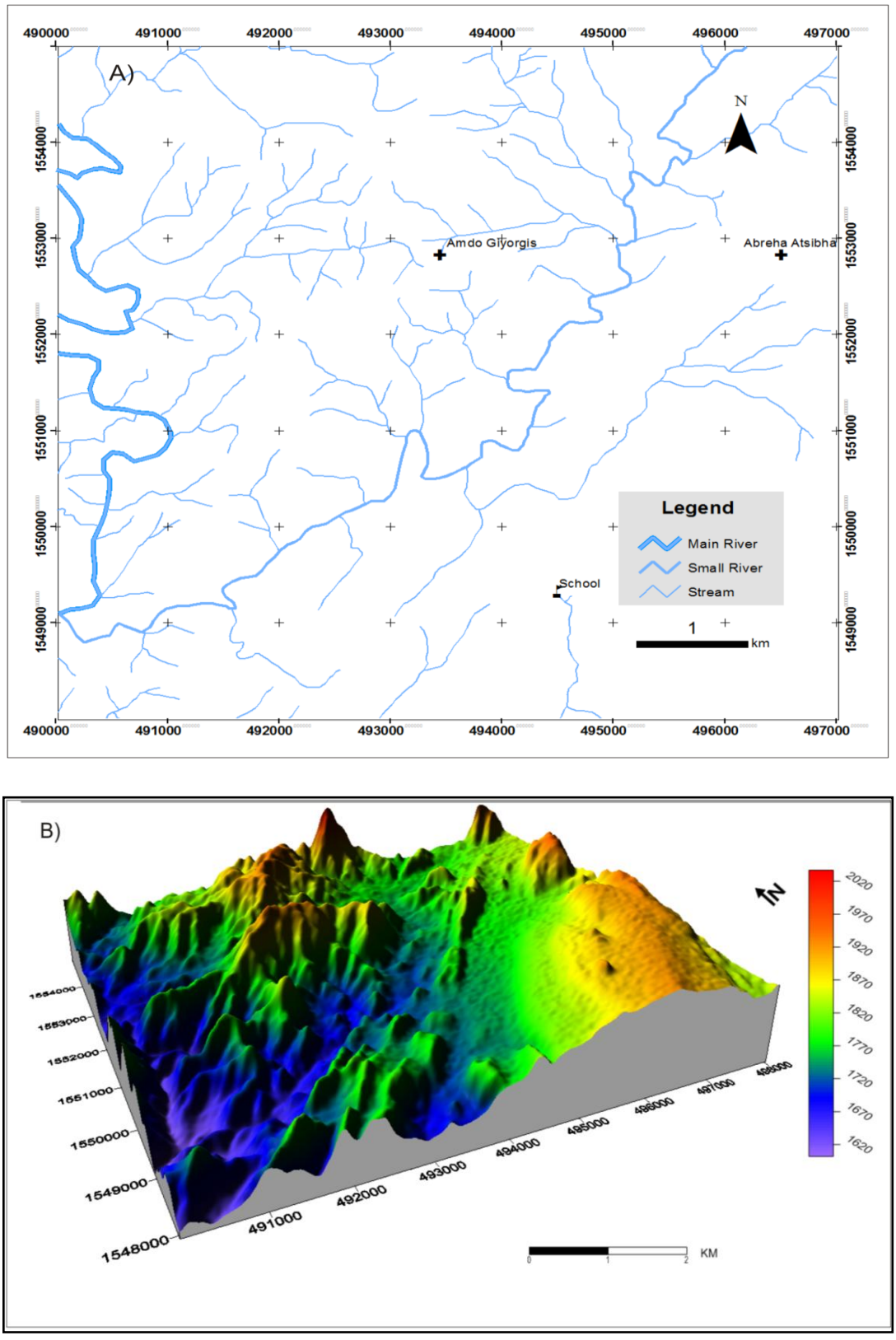

Figure 1.3. A) Drainage map of the study area. B) Physiographic map of the study area extracted from DEM of Ethiopia using Global Mapper-11 and changed to 3-D using Surfer software.

1.2.3. Climate condition and soil

The climatic condition of the study area is mainly dominated by semi arid to arid environments. The wet season commonly prevails in the months from May-August with total monthly rainfall 95.7-219.2mm. However, there is no rainfall during September, October, November, December, January and March months. Therefore, the dry season lasts from September to March with the maximum temperature varying from 26.2 up to 30.6 C^0 (From: National Meteorological Agency of Tigrai (NMAT)). The study area is covered by thin and poor fertile soil, but at the margin of the mainstream it is relatively thick and fertile and serves as agricultural crop production for the local people.

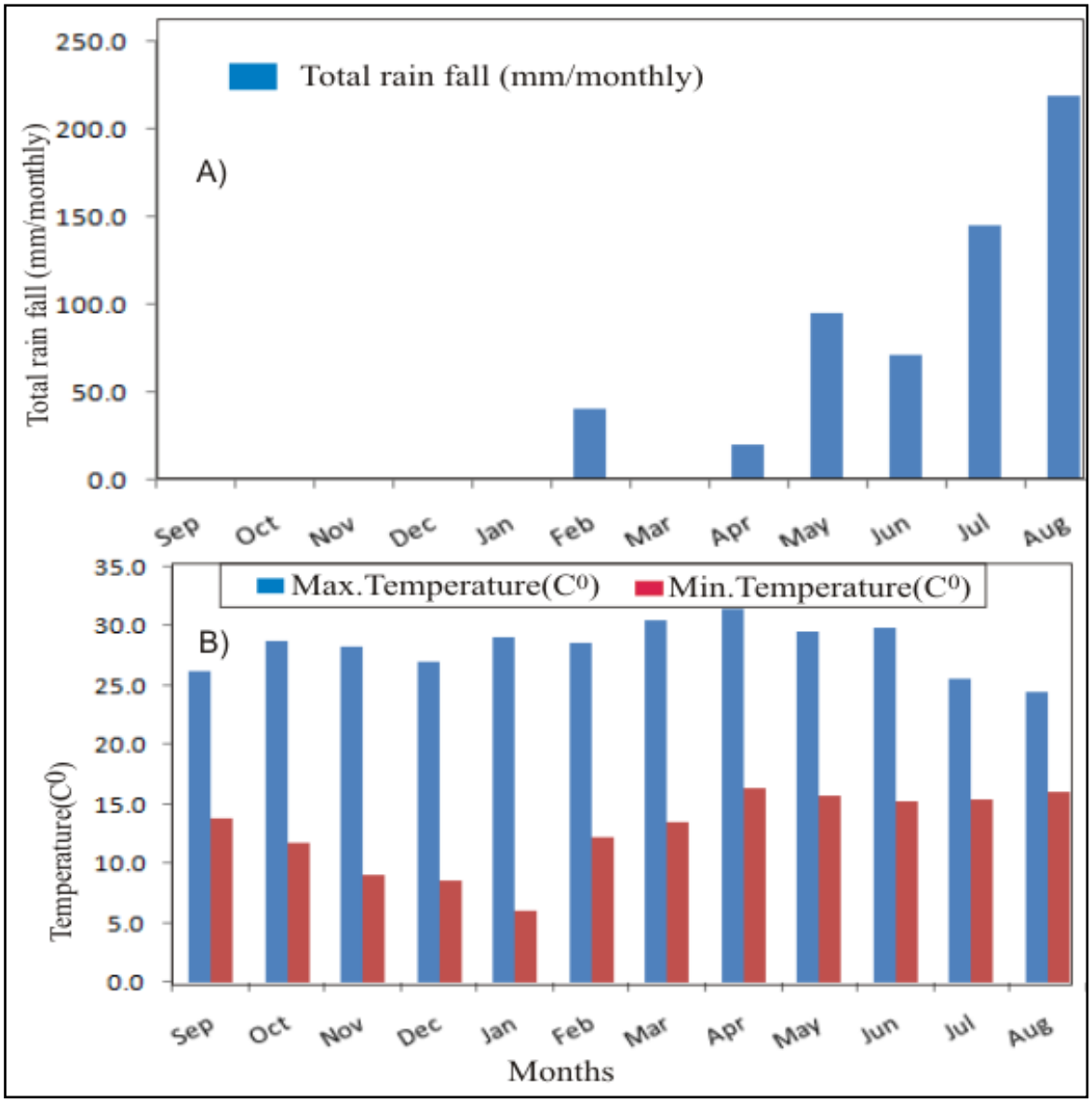

Figure1.4.A) A bar graph represents the average monthly rainfall and B) is also showing the minimum and maximum temperatures of Adwa and its surrounding area (Source: NMAT, 2017).

1.2.4. Vegetation

The study area is characterized by sparsely distributed vegetation coverage. It consists of acacia, bushes and shrub types of vegetations. The vegetation is mostly occurred nearly the streams and in the lowland areas, it consists big and small trees and they serve as invaluable shading for the local communities and animals during the hottest period.

1.2.5. Settlement

Large settlements are located either outside or near to the margin of the study area. Tahtai Logomti and its surrounding area are mostly sparsely populated. However, in the central and southeast part of the study area, it is densely populated than the southwestern and western parts. The livelihood of the people is entirely based on mixed and traditional agricultural practice that includes both crop cultivation and animal husbandry. Generally, the people commonly grow or cultivate different types of crops and cereals including sorghum, barley, teffe, maize and millet.

1.3. Statement of problem

The Precambrian geology of northern Ethiopia is defined by the presence of low grade metamorphic rocks (Johnson and Woldehaimanot, 2003), which consists series of thick heterogeneous volcano-sedimentary rocks (Asrat and Barbey, 2003). These rocks have good correlation with the low grade metamorphic terrane of southern and western Ethiopia and they comprise metavolcanic/metavolcano clasts, slate and carbonate (Beyth, 1971; Kazmin, 1972). The metavolcanics mineral assemblage represents peak regional metamorphism (pumpellyite-actinolite to lower greenschist facies) that was attained during the D1 deformation (Alene, 1998; Alene and Sacchi, 2000).

The previous researchers have worked on this region basement regarding geology and geochemistry of the rocks (Tadesse, 1997; Alene, 1998; Tadesse et al., 1999, 2000; Alene et al., 2000, 2006; Asrat and Barbey, 2003; Asrat et al., 2004; Miller et al., 2003, 2009). These researchers done regional geological mapping, lithological description on a small scale (less than 1:50,000) and also conducted geochemical analysis to determine the tectonic setting of the rocks. However, the present study focuses on detailed geological and structural mapping of lithological units at larger scale (1:25,000) and more specific petrographic studies to determine the metamorphic mineral assemblages, facies, metamorphic grade, metamorphic event and deformation phases in order to better understand the geological evolution of the rocks of the area.

1.4. Objectives

1.4.1. General objectives

The main objective of the study is to describe and understand the metamorphic mineral assemblages and its reactions, deformation history and geochemistry of the Tahtai Logomti area, Tigrai northern Ethiopia in line with the evolution of the ANS.

1.4.2. Specific objectives

- To produce detailed geological and structural map of the study area at 1:25,000 scale.
- To understand/determine the degree of metamorphism based on the mineral assemblages and differentiate the phases of deformation by examining the macro/micro structures in petrographic study.
- To understand the Paleotectonic setting based on the geochemistry (major, trace and rare earth elements) of the rocks in order to understand the geological evolution of the area.

1.5. Methodology

In order to achieve the above mentioned objectives, the following methodology has been used.

1.5.1. Data collection

Data from the literature, including geological and topographic maps, satellite imagery, relevant published and unpublished literatures related to the study area were collected. Lithological and structural data were also collected from the field. The GPS recording of each lithological unit was collected in order to compile the geological map of the area. These different exposures were described in terms of mineral composition, texture, rock fabric and outcrop-scale geological structures (folds, faults). Representative fresh rock samples were also collected from each lithological unit for thin section and geochemical analysis. Outcrop photographs and location were taken by using GPS and camera at each sample station. A topographic map with 1:25,000 scale has been used as a base map during field traverses. The topomap has been supplemented with a satellite imagery, which is downloaded from website www.golvis.USGS.gov.

1.5.2. Petrographic analysis

Total of 19 samples were sliced into two parts by using a rock cutter at the thin section laboratory of the Geological Survey of Ethiopia (GSE), Addis Ababa central laboratory (one piece each for thin section,

one piece for geochemical analysis and the remaining is placed as reserve). Nineteen samples were prepared for thin sections at this laboratory; however ten samples were used for geochemical analysis at Australia laboratory science (ALS). The rock samples prepared for thin section are described using transmitted light microscope in the petrographic laboratory of School of Earth Science, Addis Ababa University.

1.5.3. Structural data analysis

All the structural data that have been collected from different lithological units for different structural elements such as foliation, folds and fractures are plotted and analyzed using stereographic projection software and Arc GIS software. The geological and structural maps are generated using Arc GIS software, which show different lithological units and structures.

1.5.4. Geochemical data analysis

Ten samples were selected for geochemical analysis to determine the concentration of the major, rare earth element and trace elements. These samples are submitted to the Australian Laboratory Science (ALS) to determine the concentration of the elements.

1.5.5. Data processing

The Enhanced thematic satellite images were digitally processed by using SURFER-10, ENVI-4.5, ArcGIS-10 software packages to increase the resolution and to produce true ground color in order to determine the lithological contacts and structures. The Geological map and cross-section were produced using Surfer-10, Global mapper-11and ArcGIS-10 at 1:25,000 scale.

1.6. Significance of the research

As mentioned earlier, the Neoproterozoic basement rocks of northern Ethiopia have been studied by many researchers at smaller scales. However, the present study focuses on the detailed large scale geological and structural mapping (1:25,000), understanding of the phases of deformation, metamorphic events and tectonic environment by using the geochemical data therefore, this study is important to fill the existing gap regarding the area. Mostly, this present study is important to determine the metavolcanic and metasedimentary rocks of the Adwa block and western limb of the Mai Kenetal syncline. This new result of geological, structural mapping and stratigraphic section of the area make a contribution to determine the tectonic history of the Precambrian rocks of the Tigrai region,

specially the study area. In addition to that, this study is important for future individual researchers and organization.

1.7. Review of previous work

Many geological investigations have been carried out in northern Ethiopia by several authors (e.g. Beyth, 1971,1972; Kazmin, 1975; Kazmin et al., 1978; Garland, 1980; Tefera et al., 1996; Alene, 1998; Alene et al., 2000, 2006; Tadesse,1997;Tadesse et al., 1999, 2000; Sifeta et al., 2005; Miller et al., 2009; Swanson-Hysell et al., 2015; Ayele and Gangadharan, 2016). According those researchers, most Precambrian rocks of northern Ethiopia belong to two major stratigraphic groups. These are Tsaliet and Tambien Groups with minor, locally important and younger stratigraphic formations, including Didikama, Sheraro and Matheows formations in younging stratigraphic sequences (Beyth, 1971; Kazmin, 1972; Kazmin et al., 1978; Garland 1980; Tefera et al., 1996). The Tsaliet Group is characterized by greenschist facies metamorphism of originally volcanic and volcaniclastic rocks. The Tambien Group is mainly exposed in several synclinal inliers: Mai-Kenetal, Tsedia, Chehmit and Negash synclines (Alene et al., 2006; Garland, 1980). It consists of metamorphosed argillite and carbonate units. The two groups of rocks are recorded the tectonic structures that are developed due to rifting, arc accretion and terrain amalgamation processes in the East African Orogen during Neoproterozoic time (Stern, 1994; Meert, 2003; Johnson and Woldehaimanot, 2003). According to Alene (1998) and Alene and Sacchi (2000), these groups of rocks show D1 and D2 phase of deformation and it correlates with post-accretion structures of the ANS (Abdelsalam and Stern, 1996).

Six tectono-stratigraphic blocks were identified in west-central Tigrai: the Sheraro, Adi-Hageray, Adi-Nebrid, Chila, Adwa and Mai-Kenetal blocks from west to east (Tadesse, 1997). Shiraro and Mai-Kenetal blocks are dominated by weakly metamorphosed and deformed, post accretionary clastic and carbonate deposits. The Adi-Hageray block occurred near the eastern Shiraro block and it consists of extensively deformed, greenschist facies, metasedimentary and metavolcanic rocks. The Chila block contains mainly sedimentary in origin rocks, however the Adi Nebrid block is metavolcanic (intermediate to acidic lava, pyroclastics) and metasedimentary rocks. The Adwa block comprises low grade, intermediate to acidic metavolcanic, chert, pyroclastic and metasedimentary rocks. According to Tadesse et al. (1999), Alene et al. (2000) and Sifeta et al. (2005), the metavolcanic rocks of the northern Ethiopia are parts of volcanic-arc basalt having calc-alkaline to tholeiitic affinity. They are part of the Arabian Nubian Shield extension which is juvenile Neoproterozoic crust formed during the Mozambique Ocean closure (Asrat et al., 2001; Stern, 1994, 2008; Fritz et al., 2013).

CHAPTER TWO

2. Regional geological setting

2.1. Geodynamic evolution of the East African Orogen

The East African Orogen (EAO) is one of the greatest collision zones in the world (Stern, 1994; Jacobs et al., 1998; Kroner et al., 2000). It comprises the Arabian-Nubian Shield in the northern and the Mozambique Belt in the southern (Stern, 1994).The tectonic evolution of the East African Orogeny involved the following stages (DeWit and Chewaka, 1981; Stern, 1994; Kroner and Stern, 2004) (Fig. 2.1):

1. Breakup and extension of Rodinia, (900-850 Ma),
2. Sea-floor spreading and formation of arcs and back-arc basins, terrane accretion (870 to 690 Ma),
3. Collision of plates or continent-continent collision and micro plates (from 630 to 600 Ma) and,
4. Crustal shortening (subduction and obduction), orogenic collapse and extension producing to the break-up of Gondwana during 600 to 540Ma.

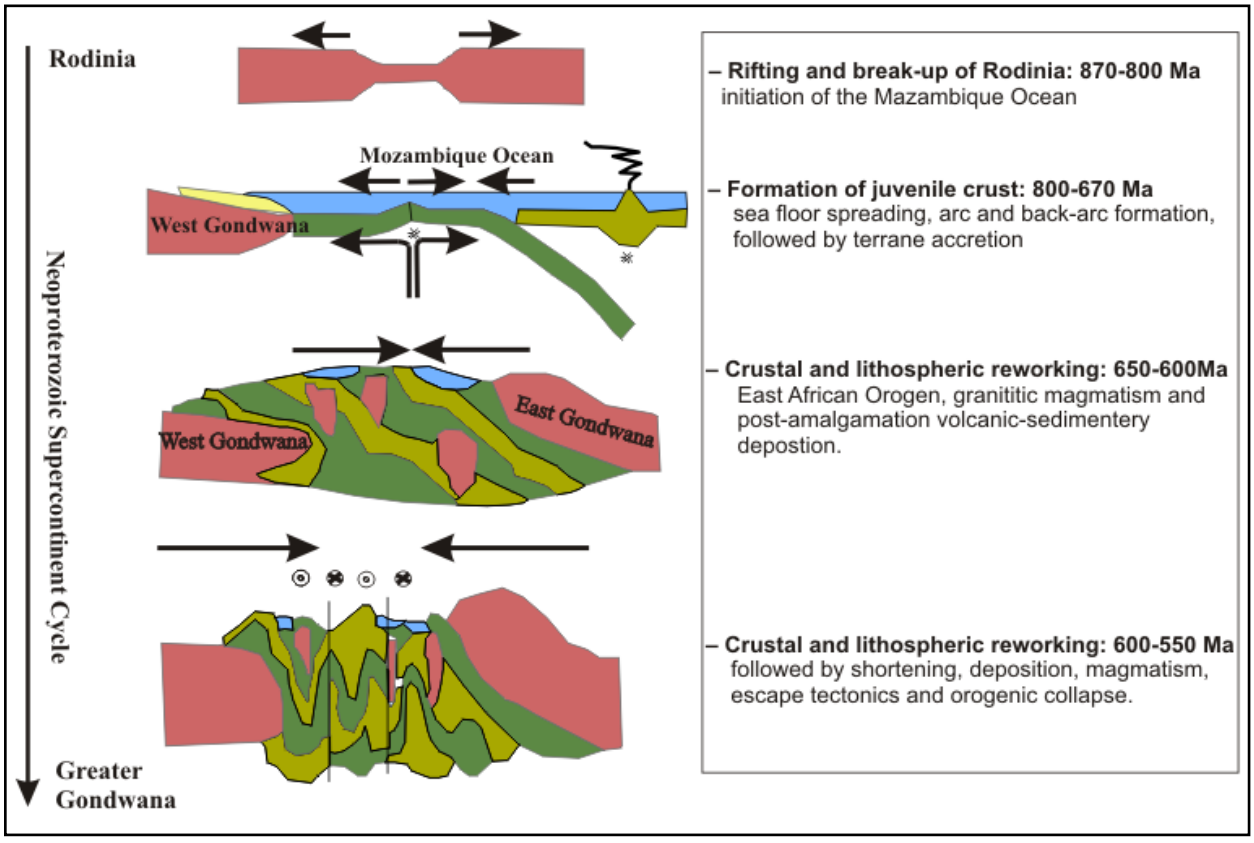

Figure 2.1. Schematic illustration of stages in the development of ANS showing its setting in the supercontinent cycle bracketed by the break-up of Rodinia and the assembly of Gondwana, modified from Stern and Johnson (2010) cited in Johnson et al. (2011).

2.1.1. Arabian Nubian Shield (ANS)

The Arabian Nubian Shield (ANS) is the suture zone between West and East Gondwana, which is found in the northern part of the East African Orogen (EAO), and formed during the amalgamation of the Gondwana supercontinent at the end of Neoproterozoic time (Vail, 1985; Stoeser and Camp, 1985; Johnson et al., 2011 and 2014). It is dominated by low grade volcano-sedimentary rocks in association with plutonic and ophiolitic remnants (Kroner et al., 1991; Stern, 1994; Abdelsalam and Stern, 1996; Shackleton, 1996; Allen and Tadesse, 2003; Cox et al., 2012). According to Patchett and Chase (2002), the Arabian-Nubian Shield (ANS) in NE Africa and Arabia is the largest land of juvenile continental crust of Neoproterozoic age on Earth. The ANS was subsequently buried by Phanerozoic sediments, but has been exposed due to uplift and erosion on the flanks of the Red Sea. It consists of three main geological units (Vail, 1983). These are: metavolcanic and metasedimentary terranes, gneissic terranes and mafic-ultramafic (ophiolitic) terranes which accreted during the orogeny time (Fig. 2.2).The gneissic terranes are located in the western, eastern and central parts of the ANS and comprise quartzo-feldspathic gneisses and migmatites of amphibolite grade which were reworked during the EAO. Many researchers interpreted, the early evolution of the ANS is due to accretion of island arcs and oceanic terranes (Vail, 1985; Stoeser and Camp, 1985; Abdelsalam and Stern, 1996; Johnson and Kattan, 2001). The volcano-sedimentary terranes occur between the gneissic terranes and include calc-alkaline basaltic and andestic lavas, tuffs, volcaniclastics and rhyolites. These terranes are intruded by various pre, syn and post-tectonic granitoids (Vail, 1985). The mafic-ultramafic suites comprise ophiolite assemblages, narrow discontinuous belts of dismembered serpentinites, gabbros, sheeted dikes, pillow lavas and ultramafic rocks. These mafic-ultramafic suites are interpreted to represent suture zones between intra oceanic plates or continent-island arc margins (Kröner, 1985; Vail, 1985; Berhe, 1990).

According to Abdelsalam and Stern (1996), ANS is divided into two deformation belts: (1) Related to arc-arc and arc-continent collisions (850-650 Ma), which are both associated with suture zone. The arc-arc deformation belts are manifested by the occurrence of E-W and N-S verging ophiolites in the northern and southern parts of the ANS whereas, the arc-continent deformation belts are related to the collision of East and West Gondwana and manifested by the E-W verging ophiolites and define the eastern and western boundaries. (2) Post accretionary structures (650-550 Ma) resulted from continuous shortening of the ANS and developed NW trending strike slip faults and shear zones during the waning

stages of ANS formation. The lateral transition between greenschist facies juvenile volcano-sedimentary sequences of the ANS and high-grade rocks of the Mozambique Belt occurs in Ethiopia. Northern Ethiopia and much of Eritrea plateau expose ANS-type of greenschist facies volcano-sedimentary sequences, whereas high-grade rocks are abundant in the southern, eastern and western part of Ethiopia (Avigad et al., 2007) (Fig.2.2).

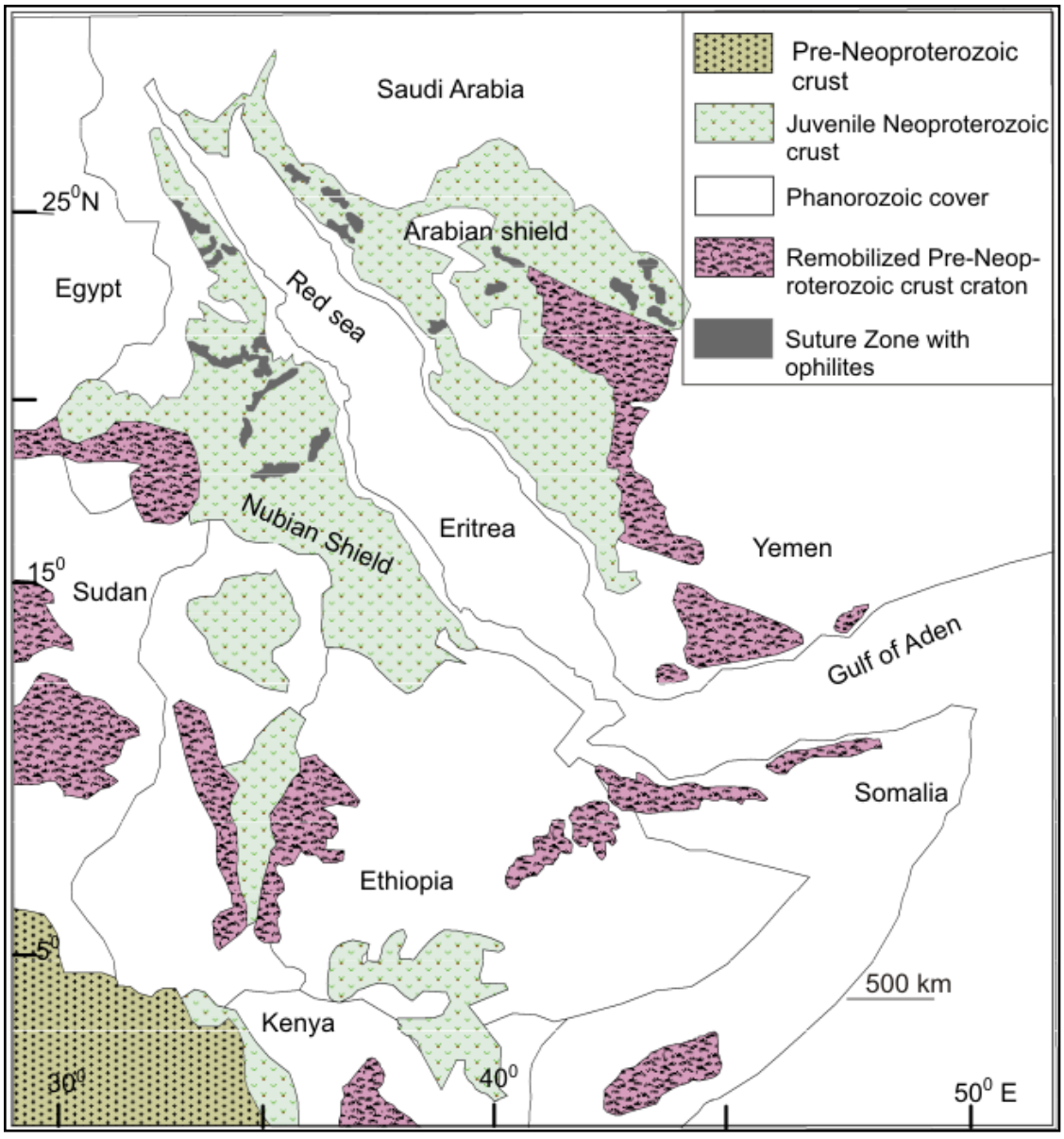

Figure 2.2.Map of the Arabian-Nubian Shield (modified from Stern, 2002) cited in Avigad et al. (2007).

2.1.2. Mozambique Belt

The Mozambique belt is the southern part of the East African Orogen (Fig.2.3) and essentially consists of medium to high-grade gneisses and voluminous granitoids (Kroner and Stern, 2004). It is a Neoproterozoic, polydeformed and collisional belt; it extends along the Eastern margin of the African continent from the Arabian-Nubian Shield into southern Ethiopia, Kenya and Somalia through Tanzania to Malawi, Mozambique and Madagascar (Shackleton, 1979; Kroner and Stern, 2004). It is strongly deformed and metamorphosed compare to ANS. Therefore, the main difference between them is a metamorphic grade of rocks now exposed at the surface, dominantly low for ANS and high for MB.

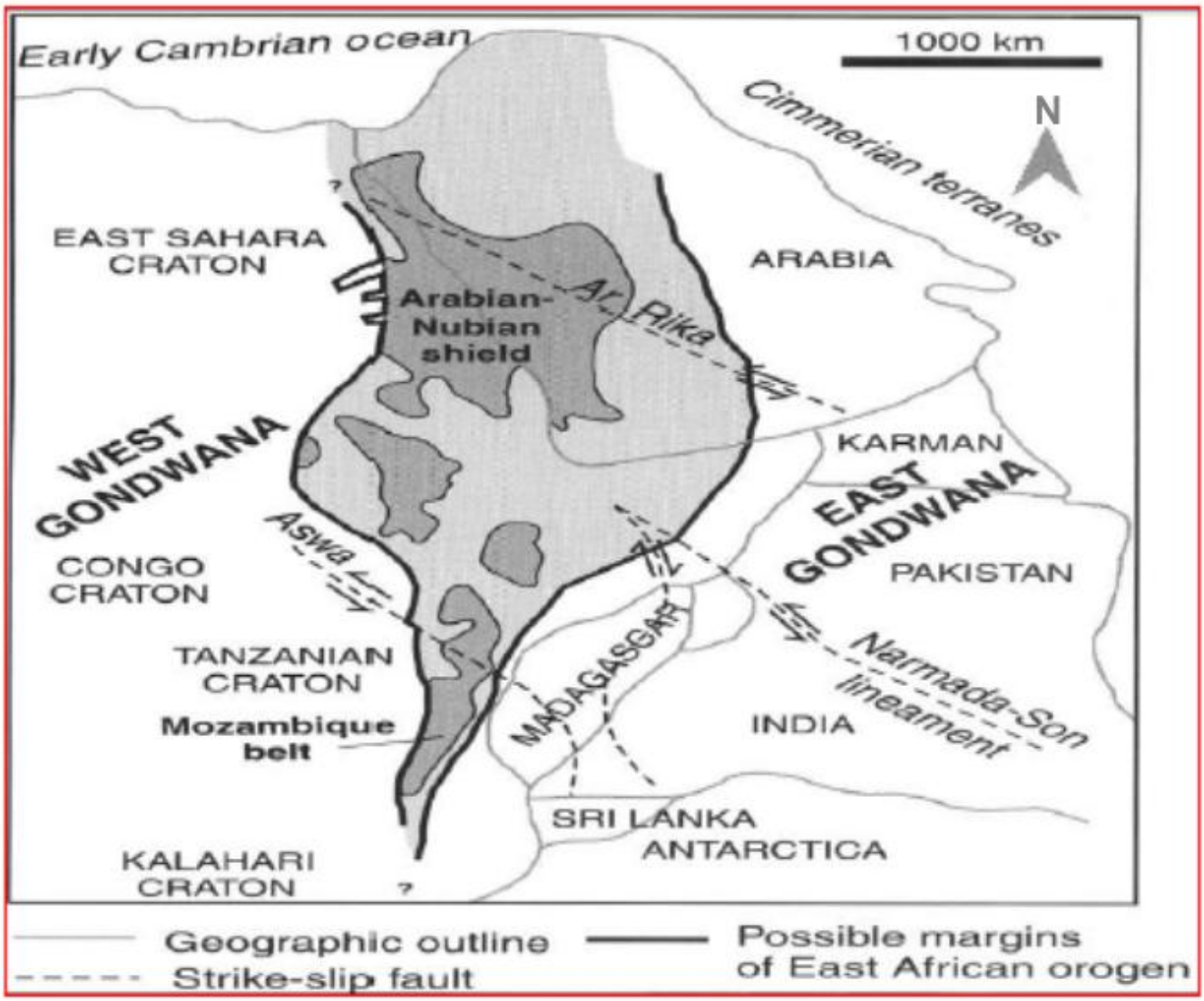

Figure 2.3. Map of the East African Orogen showing the location of the Arabian-Nubian Shield relative to the Mozambique Belt and adjacent cratonic margins (modified from Stern, 1994) cited in Johnson and Woldehaimanot (2003).

2.2. Geology of the Ethiopian basement rocks

The Ethiopian basement rocks are exposed in eastern, western, northern, and southern parts of the country (Kazmin, 1973; Tefera et al., 1996; Asrat et al., 2001) **(**Fig.2.4). These rock exposures are found in areas not intensively affected by Cenozoic volcanism and rifting and where the Phanerozoic cover rocks have been eroded away (Tefera et al., 1996). They have been studied by many researchers (Kazmin, 1971, 1975; Kazmin et al., 1978; Beyth, 1971, 1972; DeWit and Chewaka, 1981; Alemu, 1998; Tadesse, 1996, 1997; Tadesse et al., 1997, 1999, 2000; Alene et al., 2000, 2006; Tsige, 2005; Asrat et al., 2001, 2004; Yihunie and Hailu, 2007; Miller, 2009; Swanson-Hysell, 2015; Ayele and Gangadharan, 2016).

The previous studies suggested that the high grade rocks were Archean age basement underlying the Neoproterozoic volcano-sedimentary rocks (Kazmin et al., 1978), but the geochronology data so far indicated that the high-grade sequence is largely of Neoproteroic age (Asrat et al., 2001). Based on the compositional, deformational and metamorphic grade variations Kazmin (1971, 1975), subdivided the basement rocks of Ethiopia into Lower, Middle, and Upper Complexes. Recently, this subdivision has been revised and the rocks of Lower Complex turned out to be Late Proterozoic in age (Ayalew et al., 1990; Teklay et al., 1998; Gerra, 2000).

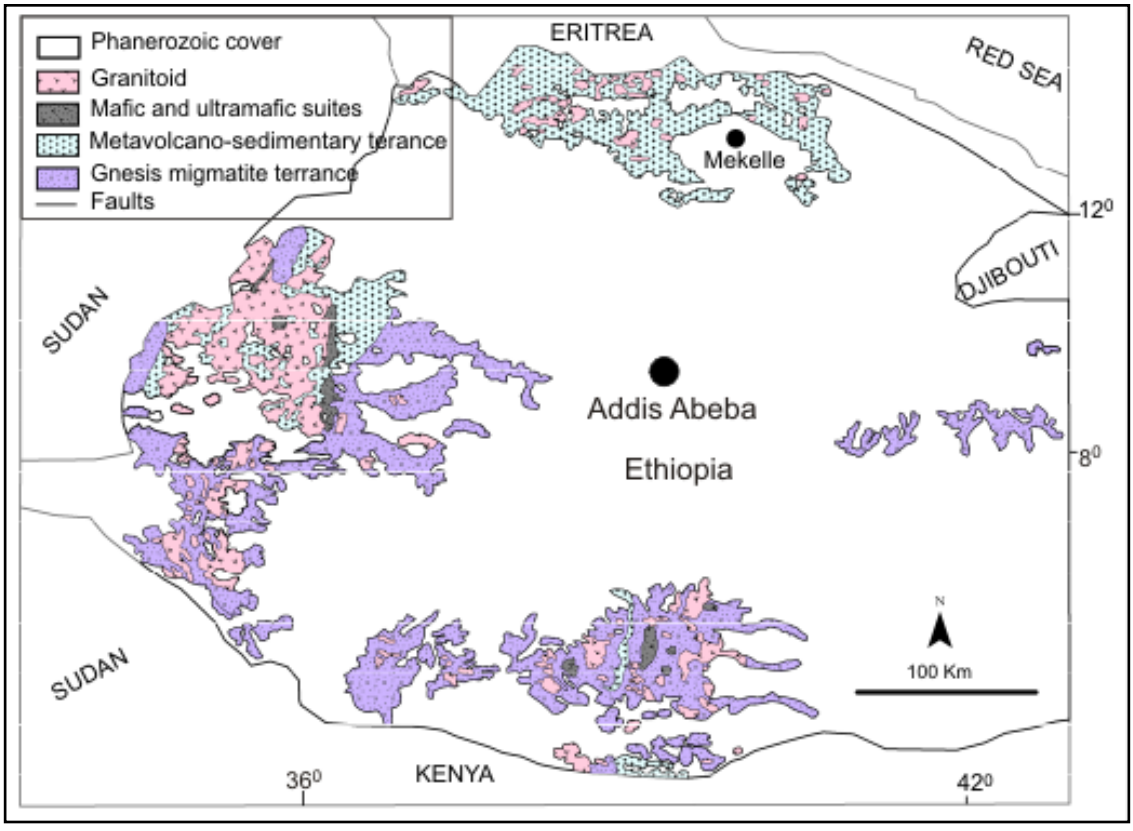

Figure 2.4. The distribution of the low-grade volcano-sedimentary sequences of the ANS, high-grade gneisses and migmatites of the Mozambique Belt in Ethiopia (modified from Asrat et al., 2001) cited in Gebresilassie (2009).

2.3. Precambrian rocks of Northern Ethiopia

The Precambrian rocks of northern Ethiopian are characterized by the low-grade volcanic, volcano-sedimentary, mafic and ultramafic rocks of ophiolitic character and plutonic rocks of typical Arabian-Nubian Shield rocks (Beyth, 1972; Kazmin, 1972; Tefera et al., 1996).These rocks indicate an accretion of compositionally different intra-oceanic island arcs (Tadesse et al., 1999). Likewise, the metamorphic terrain of Tigrai region is represented by a series of thick, inhomogeneous volcano-sedimentary assemblages, which belong to the Arabian-Nubian Shield (Stern and Dawoud, 1991; Tadesse et al., 1999; Asrat et al., 2001). As already mentioned earlier, it is dominantly characterized by steeply dipping and extensively folded, low-grade metamorphic rocks intruded by various granitic and mafic intrusions (Asrat, 1997; Tadesse, 1997; Alemu, 1998; Tadesse et al., 2000). The Precambrian rocks of this region are grouped into: (i) Tsaliet Group, (ii) Tambien Group, (iii) Didikama Formation, (iv) Shiraro Formation and (v) Matheows Formation in younging stratigraphic (Beyth, 1971; Kazmin, 1972; Kazmin et al., 1978; Garland, 1980; Tefera et al., 1996). The new physical stratigraphic data and the high-precision U-Pb dates from intercalated tuffs lead to a new stratigraphic framework for the Tambien Group that confirms identification of negative δ13C values from Assem Formation limestone with the ca. 800 Ma Bitter Springs carbon isotope stage. Integration with data from the Fifteen mile Group of northwestern Canada constitutes a positive test for the global synchroneity of the Bitter Spring Stage and constrains the stage to have started after 811.51 ± 0.25 Ma and to have ended before 788.72 ± 0.24 Ma.

According to Tadesse (1997), the northern part of Ethiopia also consists of six tectono-stratigraphic blocks. These are Adwa, Mai Kenetal, Chila, Sheraro, Adi Nebrid and Adi Hageray blocks. The present study area is located between the Mai Kenetal and Adwa blocks. The Mai Kenetal block is composed of variegated slates and weakly metamorphosed limestone units whereas, the Adwa block is comprises low grade, metavolcanic (intermediate to acidic, pyroclastics) and metasediment units. A series of NE-SW synclinal basins filled with weakly metamorphosed and deformed shale and limestone unconformably overlie Adwa rocks (Beyth, 1972). The rocks of Adwa block are intruded by composite granitoids of batholitic size (Kazmin, 1972; Beyth, 1972).In Mai Kenetal block, five units were identified by Tadesse (1997). These are: Tselim Imni limestone, Bliato limestone and slate, Logomti

slate, Filafil limestone and Segali slate from top to bottom, however Alene et al. (2006) described as upper limestone, upper slate, lower limestone and lower slate units.

2.3.1. Tsaliet Group

The Tsaliet Group is well constrained in the Tigrai region, which covers most of the area of the region (Fig.2.5A) named after the Tsaliet River in Tigrai region (Beyth, 1971; Kazmin, 1972 and 1975; Garland, 1980). It consists of calc-alkaline, island arc related metavolcano-sedimentary rocks, including metavolcanic/volcanoclastic rocks, sericite-chlorite schist, slate, greywacke, intermediate to acidic welded tuffs, lapilli tuff, and agglomerates (Beyth, 1972; Beyth et al., 2003; Alene, 1998; Tadesse et al., 1999; Alene et al., 2000 and 2006). These rocks are green to purple schist containing stringers of quartz, epidote and calcite, interbedded with black, white, green and pink quartzite and pink to light green gneiss. The rocks contain strongly deformed bodies of early diorite and granodiorites and large late to post-tectonic intrusions of granite and granodiorite of batholithic dimensions (Fig.2.5 A and B). They have been faulted and tightly folded forming anticlinoriums and anticlines and also subjected to lower greenschist facies metamorphism (Tefera et al., 1996). According to Alene (1998) and Alene and Sacchi (2000), the mineral assemblages of this group indicate peak regional metamorphism at pumpellyite-actinolite to lower greenschist facies (245-375 C^0) and it was attained during D1 deformation. The associated sediments show sedimentary features such as graded bedding, current bedding and well preserved ripple marks (Beyth, 1971; Garland, 1980; Kazmin, 1972). This Group is unconformably overlain by the Tambien Group (Beyth, 1972) and it is affected by NE-SW trending shear zones with a sinistral strike-slip displacement (Tadesse et al., 1999).

2.3.2. Tambien Group

According to Miller et al. (2003) and Alene et al. (2006), the Tambien Group is mainly a shallow marine sedimentary cover of carbonates and mudstones locally topped by a diamictite, preserved in limited outcrops as complex synclinoria surrounded by Tsaliet Group metavolcanics. It exposed in different parts and preserved the NNE-trending upright/overturned synclinorium formed by D2 deformation (Sifeta et al., 2005; Alene et al., 2006; Miller et al., 2011). It exposed in Mai Kenetal, Tsedia, and Chehimit and Negash synclines and comprises lower slate, lower limestone and upper slate are exposed in the first three synclines with additional upper limestone lying on top of these in Mai-Kenetal syncline from oldest to youngest (Alene et al., 2006). It has a gradational contact with the underlying Tsaliet Group (Alene et al., 2006; Garland, 1980); however Beyth (1972) described as

probably unconformable contact. It is divided into the Arequa Formation (lower unit) and Mai Kenetal limestone (upper unit) (Garland, 1980).

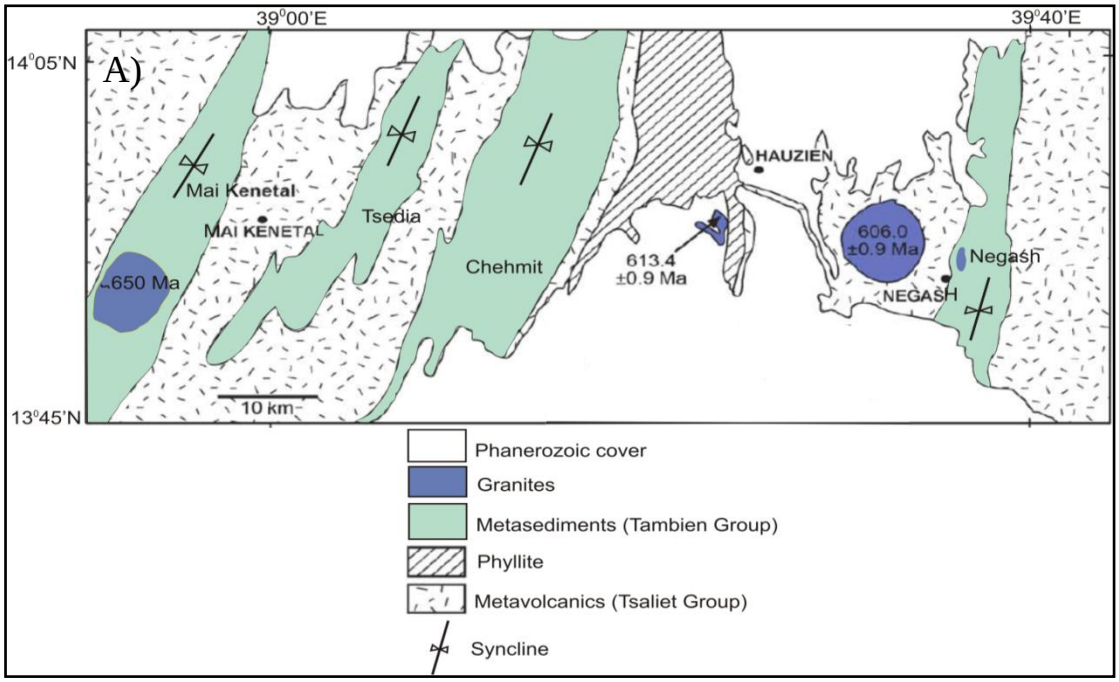

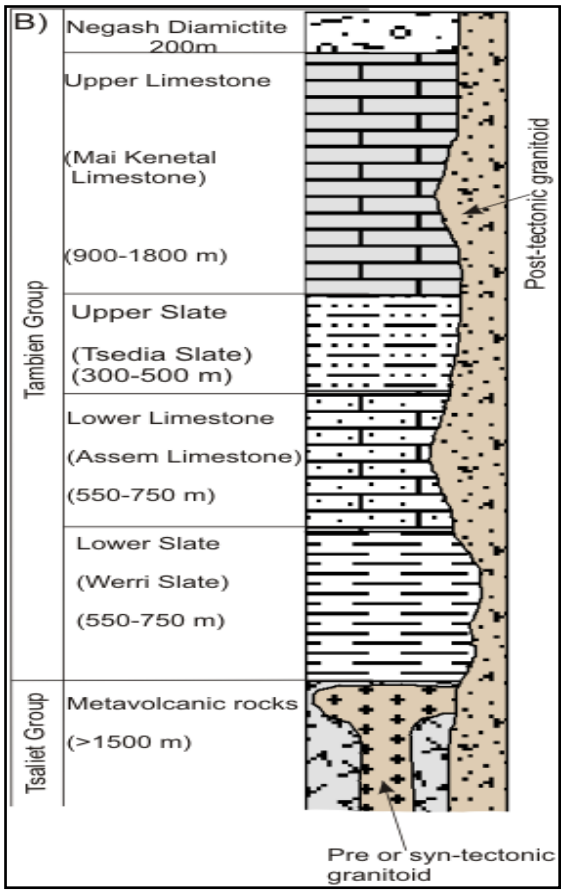

Figure 2.5. A) Geological map of Mai Kenetal-Negash area in Central Tigrai modified after Alene (1998). The age of the pre D2 intrusives are from Miller et al. (2003) for the Negash and Hauzien and Beyth (1972) for the Mai Kenetal granites (Alene et al., 2006). B) Stratigraphic section of Tigrai basement rocks showing relationship between the Tsaliet and Tambien Group rocks. The pre or syn-tectonic granitoids intruded both the Tsaliet and Tambien Groups and the diamictites age is between~620 and~520 Ma (modified from Beyth, 1972; Alene et al., 2006; Avigad et al., 2007). The names of the units of the Tambien Group are adapted from Beyth (1971) and Alene et al. (2006).

2.3.2.1. Arequa Formation

The Arequa Formation is subdivided into: Werri slate, Assem limestone and Tsedia slate from bottom to top having conformable relationships with each other (Beyth, 1971; Garland, 1980). However, according to Alene et al. (2006), these units are further described as lower slate, lower limestone, upper slate and at the top of these units upper limestone unit which is similar to Mai Kenetal limestone unit.

Werii slate: This unit is the lowest unit contains about 1000 meters thick of interbedded black slate, phyllite and limestone having gradational contact with the underlying Tsaliet Group (Garland, 1980). Also it contains black to blue greenish, well laminated and foliated slate, greenish slate and black greywacke layers (Garland, 1980; Alene et al., 2006).

Assem limestone: It has about 300 meters thick of well-bedded, finely laminated black limestone interbedded with slate (Garland, 1980). It shows stromatolitic lamination, slump structures which indicate the younging direction toward the upper limestone and dark stylolites structures (Alene et al., 2006).

Tsedia slate: It has about 600 meters thick of variegated slate interbedded with limestone, quartzite and dolomite. Green-grey to black slate, graphitic, well laminated and interbedded with fine grained calcareous sandstone and purple slates at the base of the section. These units are intruded by aplitic dikes (Garland, 1980).

2.3.2.2. Mai Kenetal Limestone

The Mai Kenetal limestone is the upper unit of the Tambien Group, which consists of about 800 meters thick limestone. This unit commonly shows karstic topography and has thin interbedded of dolomite and limestone and it is black, massive, finely crystalline and well bedded rock (Garland, 1980). It is occurred in the core of the Mai Kenetal synclinorium and its younging direction is demonstrated by slump structures (Alene et al., 2006).

2.3.3. Didikama Formation

The Didikama Formation consists of more than 1500 meters thick of creamish to white dolomite alternating with gray, black or variegated slates. This formation occurs in Tigrai region and named after its outcrop at a Didikama village in the Shiraro area (Kazmin, 1975; Garland, 1980) and extends northwards into Eritrea. It is conformably overlies the Tambien Group in central and eastern Tigrai region. However, in the west where the Tambien Group is not fully developed or the upper formations of the Tambien Group are missing, it rests unconformably on older formations (Garland, 1980). In the Shiraro area and Negash Syncline, it is unconformably overlain by the Matheos Formation (Kazmin, 1975; Garland, 1980).

2.3.4. Shiraro Formation

This formation was overlies the older rocks with marked angular unconformity (Kazmin, 1975). It consists mainly of sandstone and foliated conglomerate in which slate, phyllite and granite clasts predominate. It is weakly folded as compared to the underlying rocks (Kazmin, 1975). The foliated conglomerate is greenish in color with abundant granite and other rock inclusions, some rounded, mostly angular and well cemented, granite boulders, they are belong to the underlying granite rocks (Tefera et al., 1996).

2.3.5. Matheos Formation

Matheos Formation is a youngest Precambrian formation, occurred only in the Negash syncline (Garland, 1980). It is subdivided into three members at the Negash syncline (Miller et al., 2009). These are; the basal black limestone member, it is partly detrital and well laminated; the transitional member, a transition upward in to a non-calcareous unit/upper slate, and the diamictite member (a pebbly slate).

2.4. Northern Ethiopia regional tectonic setting

The Northern Ethiopia is part of the low grade metavolcano-sedimentary Neoproterozoic basement of the Arabian Nubian Shield (Beyth, 1972; Kazmin et al., 1978; DeWit and Chewaka, 1981; Tadesse et al., 1999; Alene et al., 2006). It was formed during the closure of the Mozambique Ocean and the accretion of several volcanic arcs (900-500Ma), and the intrusion of syn and post- tectonic granitoids at 800, 750 and 500 Ma (Tadesse et al, 1999). The subsequent closure of oceanic basin and final collision of the two Gondwana fragments formed collisional zone (Stern, 1994; Abdelsalam and Stern, 1996) and this gave rise to later phases of deformation, which is recorded in both Tsaliet and Tambien Groups of

northern Ethiopia (Alene, 1998). Likewise, both the Tsaliet and Tambien Group have been subjected to at least two major phases of deformations as a result of N-S and E-W regional compression, respectively (Alene, 1998; Alene and Sacchi, 2000; Sifeta et al., 2005; Alene et al., 2006).

The earlier deformation was N-S compression (D1) accompanied with E-W trending minor recumbent folds (cm to dm scale wave length) (F1), stretching lineation and pervasive regional foliation. However, the later second deformation was E-W directed shortening in association with end-phase collision between East and West Gondwana manifested by upright folding, thrusting and lateral displacements. The later E-W directed phase of ductile deformation refolded and reoriented earlier tectonic structures (D1) along SW trending sub-horizontal fold axis to produce large upright open to tight folds. Tadesse et al. (1999) was demonstrated the presence of accreted intra oceanic arc sequences with varied lithological and geochemical characteristics of the low grade metavolcanic rocks of the west-central Tigrai. The general geological history and sequence of geological events of the region have been summarized as follows; (i) deposition of volcanic and sediment underwater marine condition followed by Pan-African metamorphic event mainly of greenschist regional metamorphism (ii) accretionof Proterozoic metavolcanic and metasediments (iii) intrusions of granitic intrusives of Pan-African age (iv) deposition of Phanerozoic sediments (v) uplift and eruption of basaltic lava.

The present study area is located between the Mai Kenetal and Adwa tectono-stratigraphic blocks of the Axum sheet. The Adwa block has lithologically comprises low grade, intermediate to acidic metavolcanic, volcaniclastics, chert and water reworked volcanoclastic, metasediments. These rocks were formerly mapped as part of the Tsaliet Group rocks (Beyth, 1972; Garland, 1980). The rocks of this block are grouped under one lithostratigraphic name, termed as the Adi Abun Group (Tadesse, 1997). Tadesse et al. (1999) was demonstrated the metavolcanics rocks of the Adwa block have characteristic patterns of subduction related calc-alkaline volcanic arc lavas. The second block is a Mai Kenetal block occupied by variegated slates and weakly metamorphosed limestone units and the bedding of these units dip to the SE. NE to SW trending thrust faults and shear zones are identified within the low-grade metavolcano-sedimentary sequences (Tadesse, 1996; Tadesse et al., 1999). The major NE-SW oriented synclinoria are Mai Kenetal, Tsedia, Chehmit and Negash, which folded the Tambien Group rocks (Beyth, 1972; Alene et al., 2006). Tadesse (1997) has described five deformation phases for the Axum area such as (1) the formation of D1 tight isoclinal folds; (2) steeply to moderately dipping NW and SE verging thrust planes during D2; (3) NNE-SSW narrow shear zones (due to ductile

and brittle ductile deformations) during D3; (4) NE-SW narrow and weak dextral shear zones (brittle ductile deformation) and (5) WNW-ESE fault and joints.

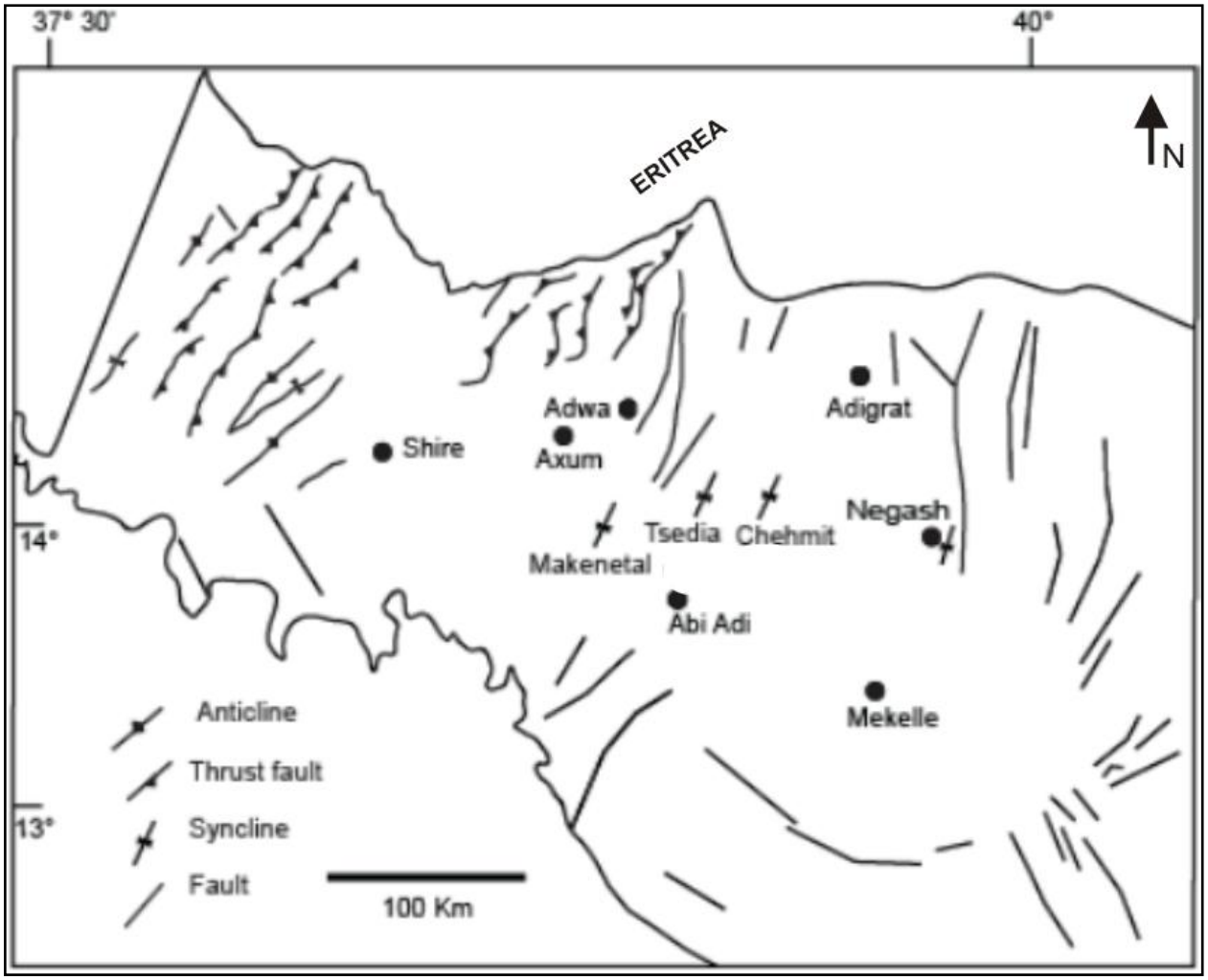

Figure 2.6. Distribution of major tectonic structures of basement rocks of Tigrai region (modified after Tadesse et al., 1996, 1999; Asrat et al., 2001).

CHAPTER THREE

3. Geology and petrography of the study area

3.1. Introduction

The geology of Tahtai Logomti and its surrounding area is part of Neoproterozoic low-grade metamorphic rocks of northern Ethiopia. Based on field observation and pervious data, the study area consists of metavolcanics, metavolcano-clastics, lower slate, lower metalimestone, upper metalimestone and upper slate. In addition to these rocks, there are also small intrusion bodies having intermediate to felsic in composition. Metavolcanics and metavolcano-clastic rocks are covering a large area mainly exposed in the northwestern, central and southwestern part of the study area. The lower slate, lower metalimestone, upper slate and upper metalimestone units are exposed in northeastern, eastern and southeastern part of the study area (Fig.3.1). According to Alene et al. (2006), the metasedimentary rocks (lower slate, lower limestone, upper slate and upper limestone) are part of the Tambien Group, whereas metavolcanic and metavolcano-clastics are parts of the Tsaliet Group. There is also development of different primary sedimentary structures like bedding, lamination, cross lamination/bedding, stromatolitic lamination and slump structures that show the younging direction (Fig.4.2) and also there are secondary structures such as meso-micro folds, faults, foliation, linear (pencil) and styloititic structures (see chapter 4). A detail description for each lithological unit of the study area is given as follows.

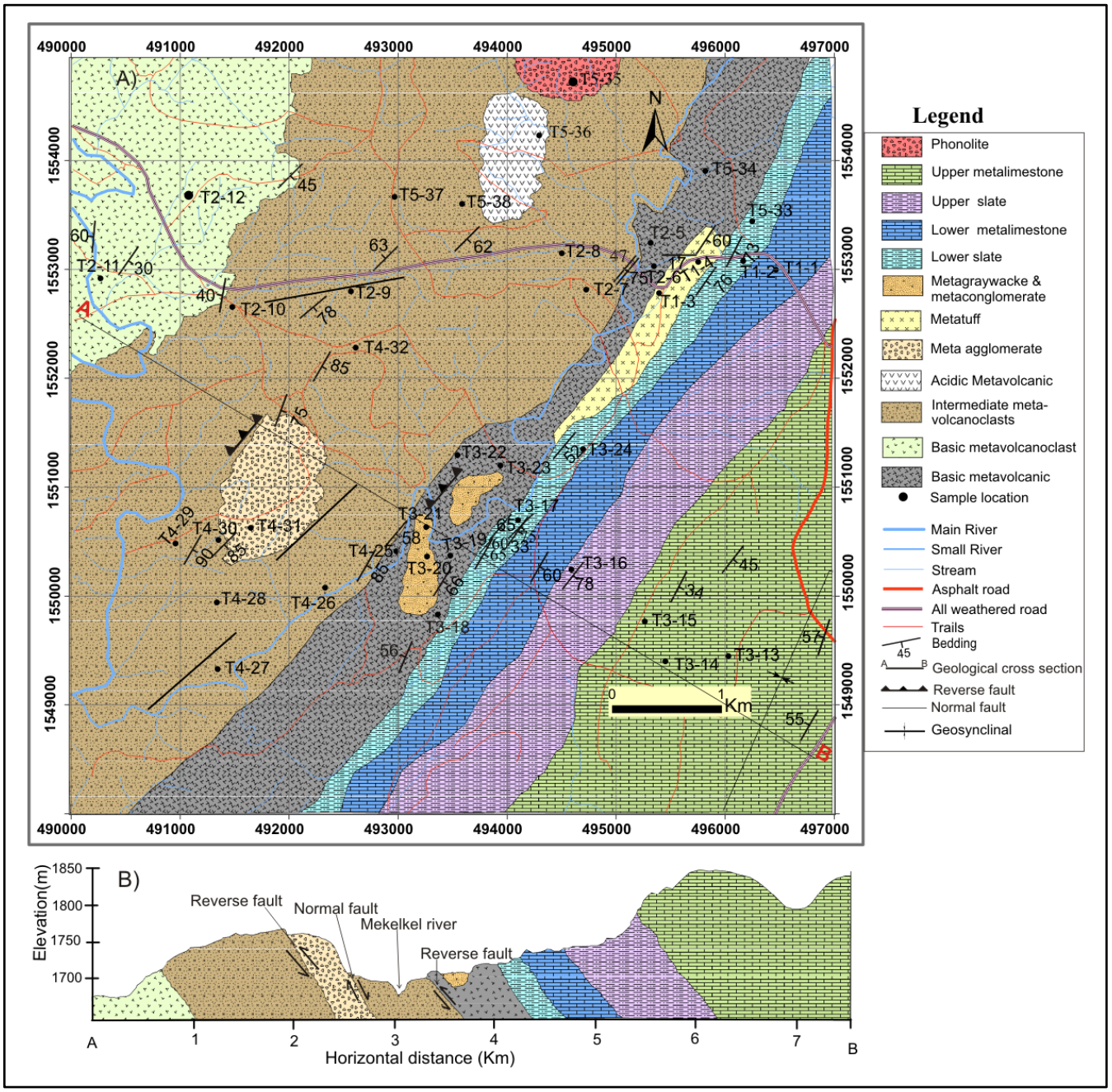

Figure 3.1. A) Geological map and sample location of Tahtai Logomti area. B) Geologic cross section of the study area along the line A-B.

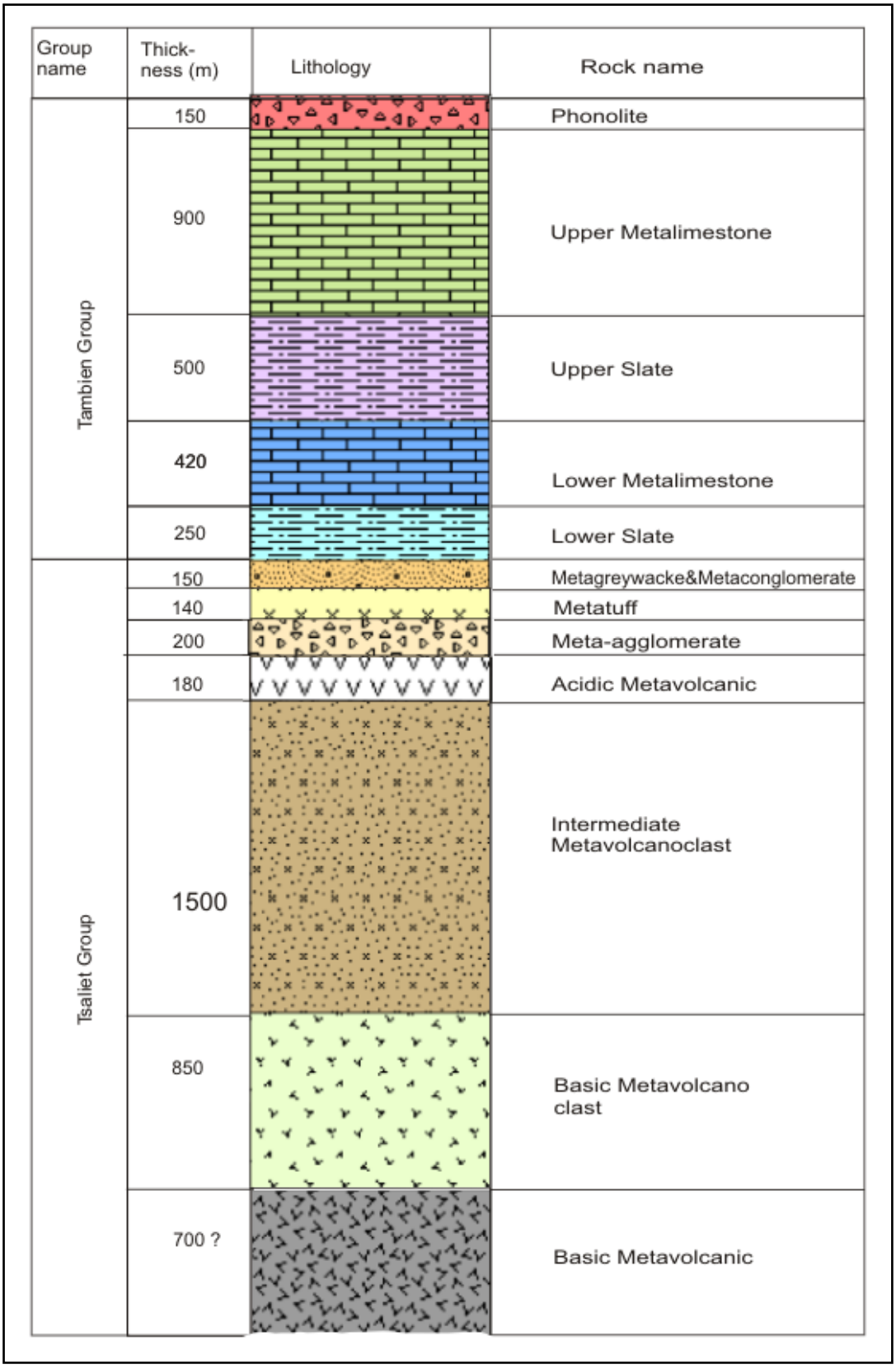

Figure 3.2. Stratigraphic section of different rocks exposed in the study area with respect to their thickness and regional group name.

3.2. Lithological description of the study area

Based on the field observation, there are different lithological units having different age of formation, mineralogy, texture, degree of deformation and metamorphism. Those lithological units are arranged below according to their stratigraphic position from older to younger (Fig.3.2) and accordingly discussed. Those are basic metavolcanic, basic metavolcanoclast, intermediate metavolcanoclast, acidic metavolcanic (meta-rhyolite), meta-agglomerate, metatuff, metaconglomerate and metagreywacke, lower slate, lower metalimestone, upper slate, upper metalimestone and phonolite rocks.

3.2.1. Basic metavolcanic

Basic metavolcanic rock is exposed in southeastern part of the study area with an approximate thickness of ~ 700m forming ridge topography. It is characterized by dark greenish, green brownish, light grey, grey reddish to dark color (Fig.3.3). Going along strike of the bed (from NE to SW part) it changes the foliation from less foliated to moderate foliated. This unit contains pyroxene phenocryst and also has pyrite mineral (dark brownish color) relatively in small amount. In some places the outcrop also shows exfoliation/spherical type of weathering and it is cut by randomly oriented quartz veins. Based on the field observation this rock is a basaltic rock type.

Figure 3.3. Outcrop of basic metavolcanic unit. It is less foliated and photo taken facing to W direction (0495380E:1553101N).

The petrographic description of dark blackish metavolcanic rock shows that it is composed of plagioclase, pyroxene, epidote, chlorite, quartz, and opaque minerals. The percentage of minerals found in sample#T3-19 are 33% calcite, 30% chlorite, 20% plagioclase, 5% muscovite/sericite, 5% quartz, 4% pyroxene, 3% epidote and opaque minerals. This rock unit shows porphyritic texture due to the phenocrysts of plagioclase and pyroxene minerals incorporated with fine grain quartz, calcite, chlorite, and plagioclase minerals. It has development of foliation, which is identified due to chlorite, muscovite/sericite and plagioclase feldspar alignments. This alignment is formed by D1 phase of deformation and indicates M1 metamorphic event (Fig.3.4 A and B). The relict of pyroxene is altered in to epidote, calcite and chlorite minerals everywhere in the section. The quartz grains show undulose extinction and grain recrystallazation.

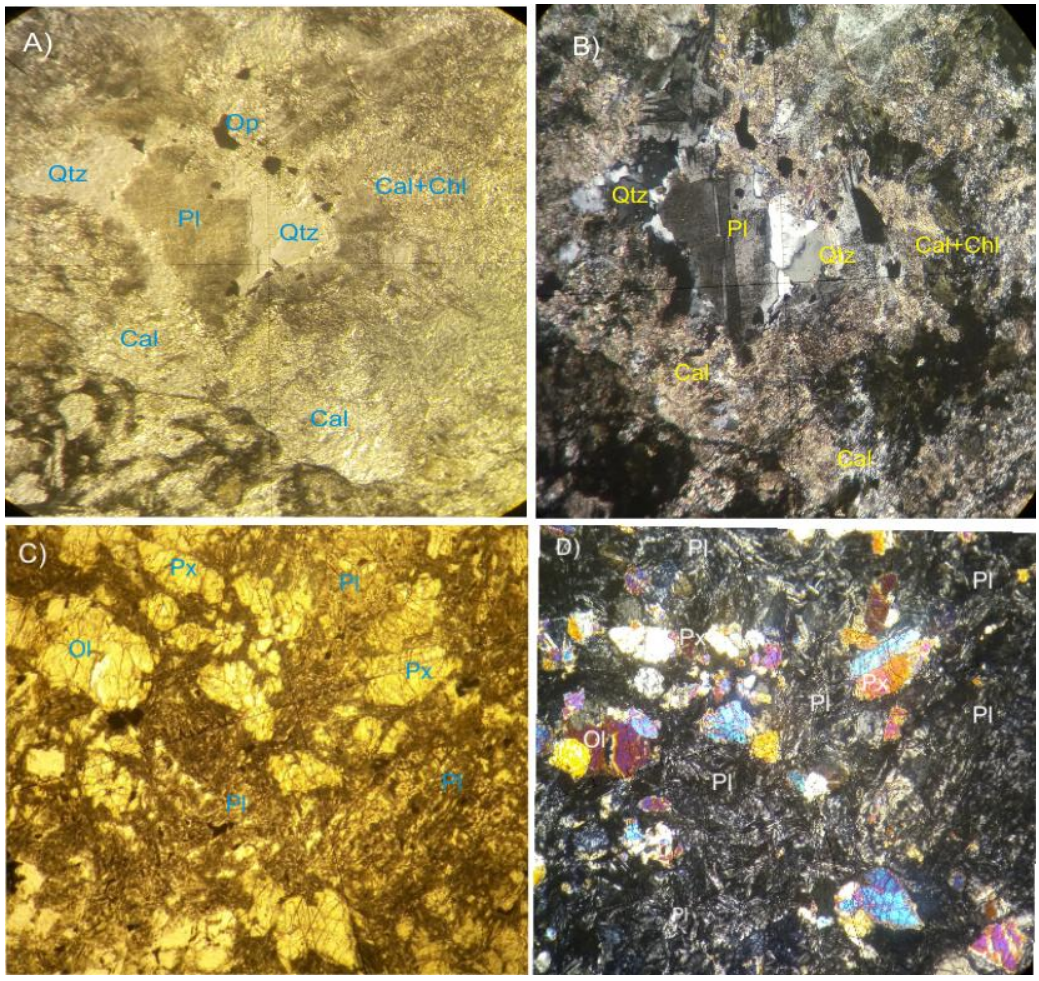

Figure 3.4.Microscopic photo of the basic metavolcanic rock unit. Both plates A and B show sample # T3-19 under PPL and XPL view with 100x magnifications, location (0493495 E: 1550379 N). Plate C and D are photo of sample # T5-34 under PPL and XPL view with 40x magnifications, location (0495802 E: 1553482 N).

The representative sample#T5-34 of metavolcanic rock contains 33% augite, 26% plagioclase, 16% chlorite, 10% olivine, 8% opaque and 7% serpentine minerals. The natrolite mineral is occurring as a cavity filling mineral with these minerals. This rock show porphyritic texture due to the phenocryst of pyroxene and olivine minerals associated with fine grain plagioclase, chlorite, serpentine and opaque minerals. The phenocryst minerals are altered into chlorite and serpentine minerals. The minerals of this section are randomly distributed, but some of the minerals are shown alignments(Fig.3.4 C and D). Based on this petrographic information, both representative samples are derived from basic volcanic rocks.

3.2.2. Basic metavolcanoclastic

Basic metavolcanoclastic rock is exposed in the northwestern part of the study area which has greater than about 850m thickness. It is massive to moderately foliated, epidotized basic to intermediate ground mass, medium grain size, green, dark greenish to greenish color and the clasts have angular to sub angular shapes ranging 1mm-2cm in diameter. This metavolcanoclastic rock unit contains some primary volcanic textures (porphyritic) because of the presence of relict pyroxene minerals. There is also a pyrite mineral near Assem River in these rocks. Generally, this rock is characterized by steep topography, river and hill side exposure and it is dominated by nonsystematically and systematically aligned continuous and discontinuous quartz and epidote veins (Fig.3.5). Some of these veins occur parallel to the general trend and another are perpendicular.

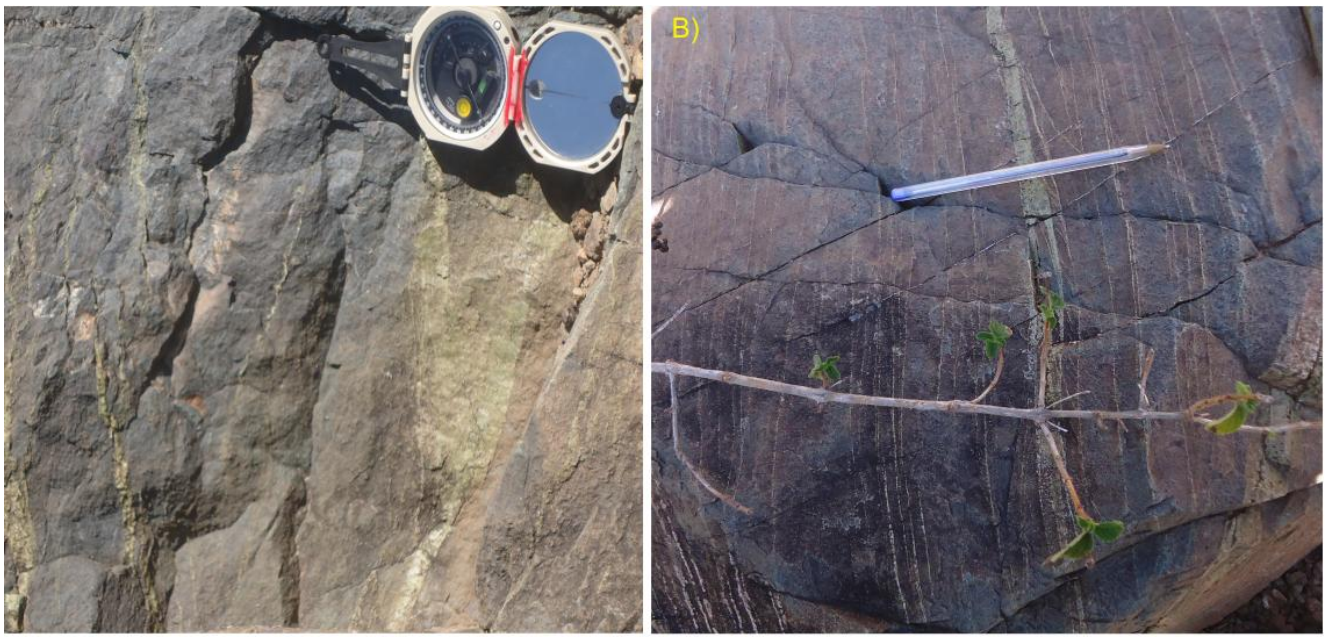

Figure 3.5. Outcrop photo of basic metavolcanoclast rock unit. A) This unit shows epidotized veins that are discordant to the bed of the unit having a relatively larger thickness and photo is taken facing to NE direction

(0490928 E: 1552727N). B) This rock shows systematically aligned epidotized veins. These veins have small thickness, light greenish color and photo is taken facing to NE direction (0490197 E: 1552975N).

The petrographic analysis of a representative sample of basic metavolcanoclastic rock is composed of 25% calcite, 20% plagioclase, 14% quartz, 13% actinolite, 12% chlorite, 5% pyroxene, 4% opaque, 3% muscovite/sericite, epidote 3% and 1% K-feldspar minerals. The rock unit exhibit porphyritic texture due to the presence of relict or phenocryst of plagioclase and pyroxene minerals in the fine grained matrix of calcite, quartz, plagioclase and epidote minerals (Fig. 3.6 A and B).

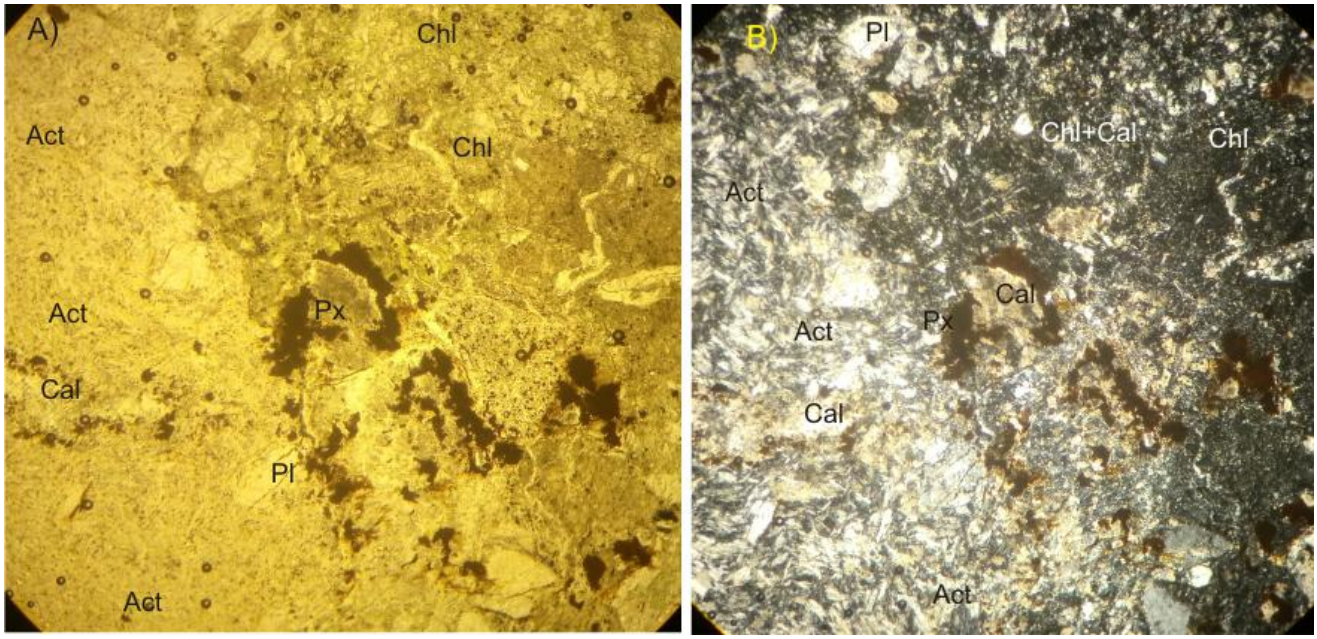

Figure 3.6.A and B are microscopic pictures of the basic metavolcanoclastic rock unit under PPL and XPL view for sample # T2-12 with magnification 100x (0491144 E: 1553564 N).

The phenocryst minerals are altered into secondary mineral such as sericite, calcite, epidote, actinolite and chlorite. In this plate there are large size sub angular clasts consisting of elongate plagioclase, chlorite, opaque/mafic and sub rounded quartz matrix minerals. The cleavage of this rock is defined by the alignment of muscovite/sericite, actinolite and chlorite minerals. The quartz grain shows undulose extinctions because of recrystallization and its shape is angular to sub angular. This unit is affected by different sizes of quartz microvein structure in elsewhere of the thin section. The abundance of relict pyroxene, plagioclase, their alteration result of the minerals and their porphyritic texture indicate that basic volcanic rocks as its protolith.

3.2.3. Intermediate metavolcano-clastics

Intermediate metavolcanoclastic unit is exposed in northern, northwestern and southwestern part of the study area forming ridge topography with an approximate thickness of~ 1500m. This rock unit cut by

quartz veins, intermediate composition of dike, joints and affected by small scale folds of different wavelengths. In the central and northwestern parts, the exposures have heterogeneous rock associations. They comprise metatuff, basic metavolcani/clastic, acidic metavolcanic, meta-agglomerate and also there is metasediment (metaconglomerate) lihological unit occur with these units. These all lithological units are not mappable individually and they occur sparsely in different places of the area. The intermediate metavolcanoclastic rocks are characterized as light dark pinkish/reddish to light dark, light dark to light grey color; sub rounded to angular shape of clasts (2mm to 35mm its size), fine grain size and show porphyritic textures (with relicts of pyroxene). In northwestern part, this rock show elongated white color clasts.

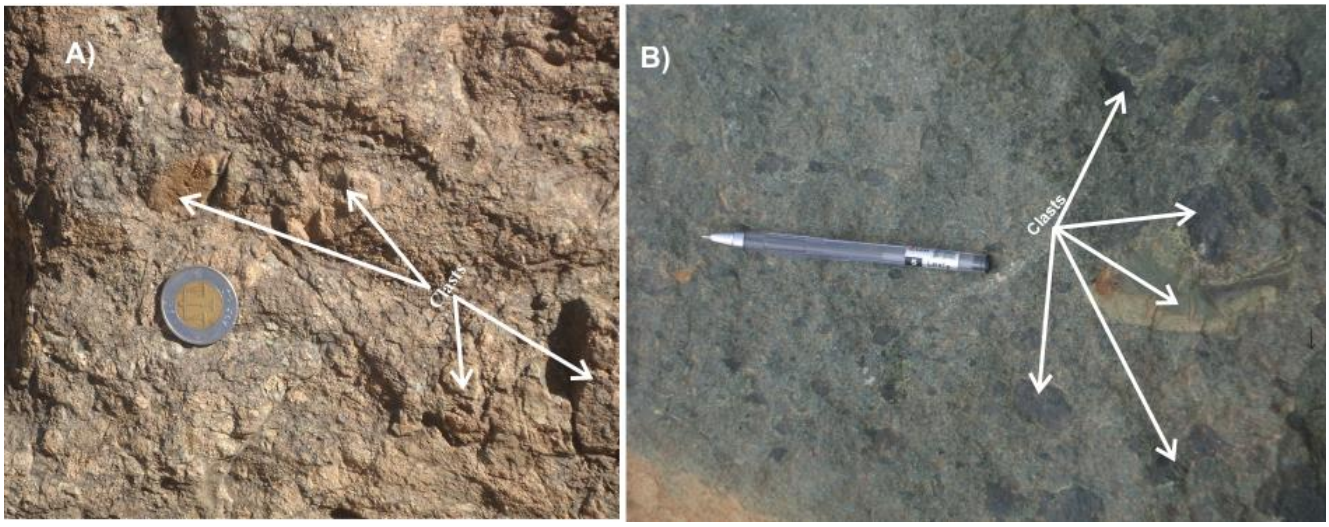

Figure 3.7.Outcrop photo of intermediate metavolcanoclastic rock. A) The clast of this unit has light pinkish to reddish color; sub rounded to angular shape and it has fine grain size and light grey ground mass (049489 E: 1552929 N). B) This unit is fine grain size and it has light darkish color of groundmass with black to greenish color clasts (0493277E: 1552544N).

The petrographic analysis of representative sample intermediate metavolcanoclastic rock indicates that it is composed of calcite, plagioclase, quartz, pyroxene, epidote, opaque, actinolite, chlorite, and sericite minerals (Fig.3.8-3.11).

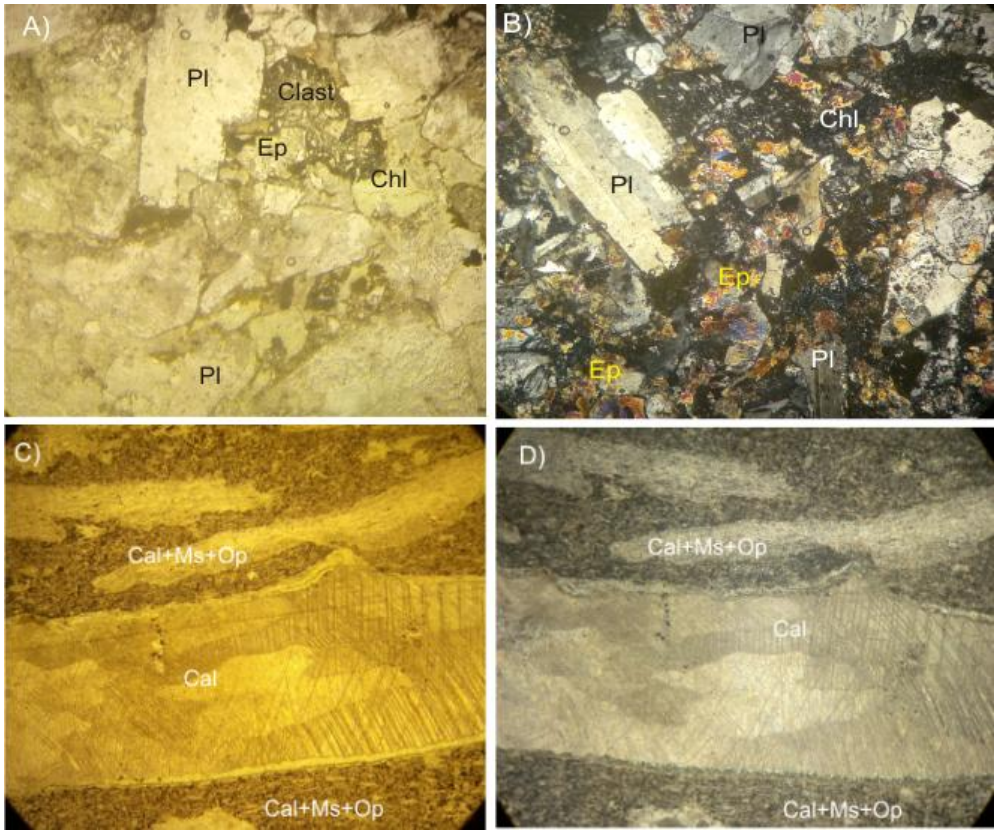

Figure 3.8.Microscopic pictures of intermediate metavolcanoclastic units. Plate A and B are photo of sample # T2-7 under PPL and XPL view with magnification 100x and location (0494893 E: 1552929N). Plate C and D are also microscopic photo of sample # T2-10 under PPL and XPL view with magnification 40x and location (0491497 E: 1552667 N).

Sample# T2-7 contains 33% chlorite, 25% plagioclase (albite), 15% calcite, 14% quartz, 6% opaque 4% epidote and 3% pyroxene minerals. It exhibits porphyritic texture due to the presence of large grain/phenocryst of plagioclase mineral incorporated in the fine grain matrix of calcite, chlorite, quartz, plagioclase and epidote minerals and it shows zoning structure. The phenocrysts and mafic minerals are altered in to secondary minerals such sericite, epidote, calcite, and chlorite throughout the section. There are also other associated sub angular to sub rounded clasts which are composed of pyroxene/mafic, chlorite and quartz minerals (Fig.3.8 A and B). In addition to this, the rock of this section shows three types of micro veins. The first one is quartz microvein which shows refolded micro folds and it is cut by epidotized microvein whereas the epidotized vein has greenish color with small micro folds and the opaque mineral is aligned parallel to the microfolds. The third one is calcite microvein which shows microfold similar to the others veins. The cleavage of this unit is defined by the alignment of chlorite and plagioclase minerals. Therefore, the slaty cleavage and micro folds in this rock thin section represent the D1 and D2 phase of deformations.

From petrographic description sample#T2-10 contains 32% calcite, 20% muscovite/sericite, 13% plagioclase, 12% opaque, 10% chlorite, 10% quartz, and 3% pyroxene. It is dominated by porphyritic texture because of the calcite and relicts of pyroxene minerals (calcite mineral occurred as phenocryst and microvein filling fractures) with relatively small amounts of fine grain calcite, muscovite/sericite and opaque minerals (Fig. 3.8 C and D). In the thin section, there is sub rounded clast consist of calcite and opaque/mafic minerals and also there is relict of pyroxene mineral which is altered into calcite and opaque. The alignment of chlorite, muscovite/sericite, calcite, stretched clasts and opaque minerals are defined the slaty cleavage. This is cleavage crenulated in some part of the thin section. Both representative sample#T2-7 and T2-10 metavolcanoclastic units are derived from basaltic protolith.

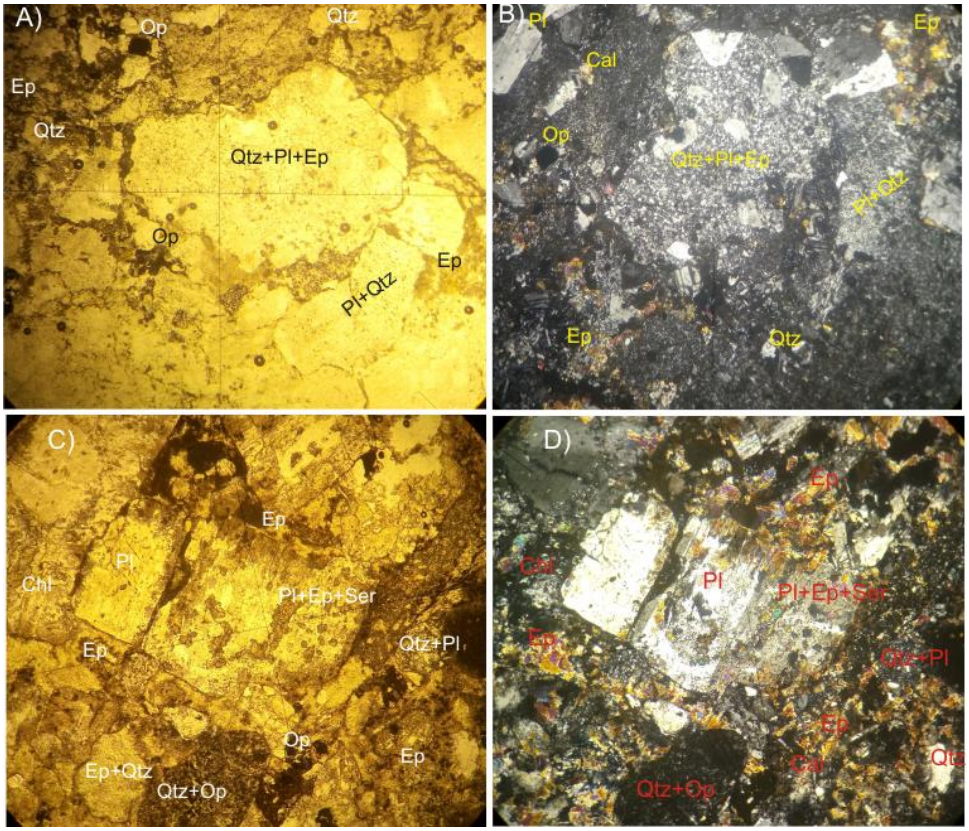

Figure 3.9.Microscopic photo of representative sample of intermediate metavolcanoclast rock. Plate A and B are photo of sample# T4-26 under PPL and XPL view with 40x magnification, location (0492494 E: 1550034 N). Plate C and D are microscopic pictures of representative sample # T4-27 units. It shows under PPL and XPL view with 40x magnifications, location (0491745 E: 1549917 N).

Sample#T4-26 contains 48% plagioclase, 18% quartz, 10% epidote, 5% calcite, 5% chlorite, 5% muscovite/sericite, 4% pyroxene, 3% opaque and 2% k-feldspar. It exhibits porphyritic texture due to the presence of a large grain/phenocryst of plagioclase and pyroxene minerals associated with a fine grain matrix of calcite, quartz, chlorite, plagioclase and epidote minerals. The phenocryst minerals are

altered into secondary minerals of epidote, sericite and chlorite (Fig.3.9A and B). The clasts of this rock in this thin section are composed of different minerals (e.g. quartz, plagioclase, opaque). Generally, the minerals of this rock show trachytic texture due to the aligned fine grained plagioclase minerals. The alignment of chlorite and muscovite/sericite minerals defined the slaty cleavage.

Sample# T4-27 is composed of 35% epidote, 30% plagioclase, 15% quartz, 8% chlorite, 5% muscovite/sericite, 3% calcite, 3% opaque and 1% k- feldspar. It has a porphyritic texture due to the presence of large grains of plagioclase minerals incorporated in fine grain epidote, quartz, chlorite and plagioclase minerals. The mafic mineral and phenocryst of plagioclase minerals are altered in to epidote, chlorite, calcite and sericite minerals. The rock section contains sub rounded clasts composed of plagioclase, opaque/mafic and quartz matrix and has well developed of foliation which is identified due to the alignment of sericite, epidote and chlorite minerals. The quartz grain shows undulose extinctions and recrystallization, whereas epidote and sericite minerals are overgrowing on the plagioclase mineral as inclusion (Fig.3.9 C and D). Based on petrographic information the representative sample# T4-26 and T4-27 are derived from intermediate composition of volcanic rocks.

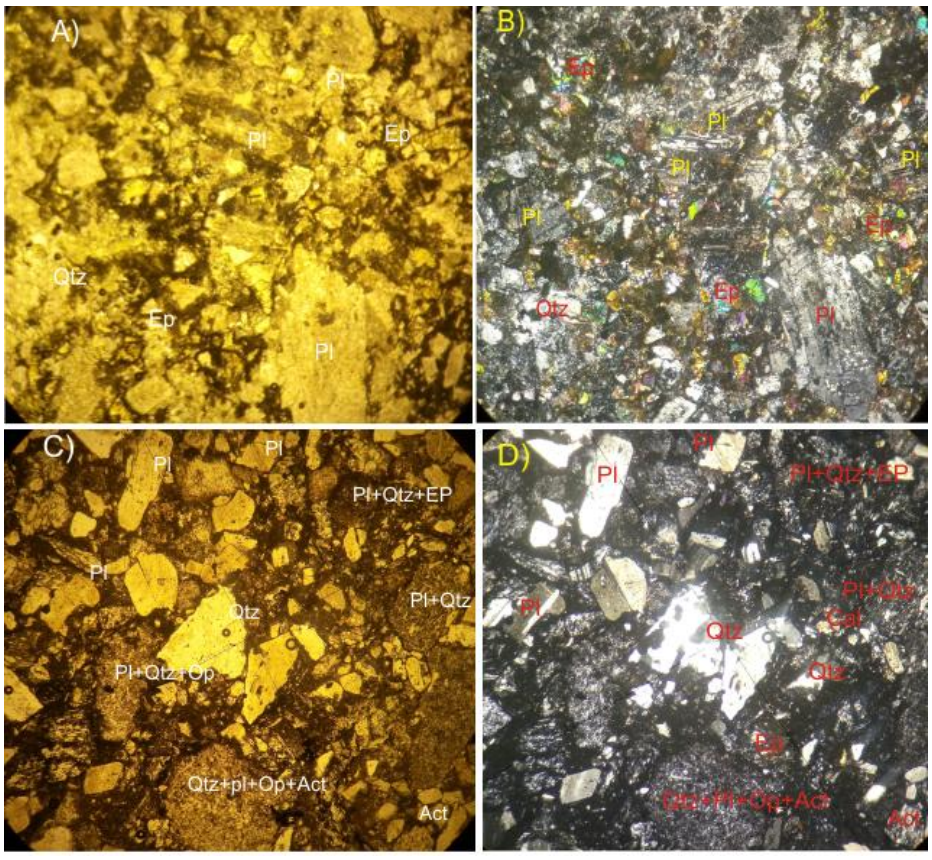

Figure 3.10.Microscopic pictures of intermediate metavolcanoclastic rock. Plate A and B are photo of sample# T4-28 under PPL and XPL view with 40 x magnifications, location (0491355 E: 1549948 N). Plate C and D are also photo of sample # T4-29 under PPL and XPL view with 40 x magnifications, location (0490974 E: 1550493 N).

From the petrographic description sample#T4-28 contains 38% plagioclase, 26% epidote, 17% quartz, 7% chlorite, 5% calcite, 4% muscovite/sericite and the remaining 3% is pyroxene and opaque minerals. This rock unit has a porphyritic texture due to the presence of large grain/phenocryst of plagioclase and pyroxene minerals in the fine grain matrix of epidote, quartz, chlorite, calcite and plagioclase minerals. This thin section shows development of secondary minerals (e.g. epidote, chlorite and sericite) due to the alteration of mafic mineral/pyroxene and plagioclase minerals. It also contains nearly aligned sub rounded clasts composed of plagioclase, opaque/mafic, chlorite and quartz matrix minerals (Fig.3.10 A and B). The quartz grain shows undulose extinction and grain boundary migration, whereas the phenocryst of plagioclase mineral is consist of later coming minerals such as chlorite, epidote and sericite minerals.

The mineral content of sample # T4-29 is 35% Plagioclase, 26% quartz, 10% chlorite, 5% actinolite 7% epidote, 5% calcite, 3% muscovite/sericite, 3% opaque, 3% k-feldspar, 2% pyroxene and 1% sphene minerals. The phenocryst of relict plagioclase and pyroxene minerals show porphyritic texture and altered into calcite, epidote and sericite minerals. The plagioclase feldspar mineral occurred as fine grain size and phenocryst which shows trachytic texture and contains sericite and opaque minerals as inclusions. These inclusions indicate that the plagioclase mineral is formed before the growth of the minerals. This section also consists of sub rounded clasts rich in plagioclase, opaque/mafic, chlorite, actinolite and quartz minerals. The plagioclase, actinolite, sericite and chlorite minerals show slaty cleavage, however the other minerals are nearly aligned. The quartz grain shows undulose extinction and grain boundary migration because of deformation (Fig.3.10 C and D). The dominance of plagioclase and quartz minerals in both samples indicates that the rocks have felsic to intermediate volcanic protolith.

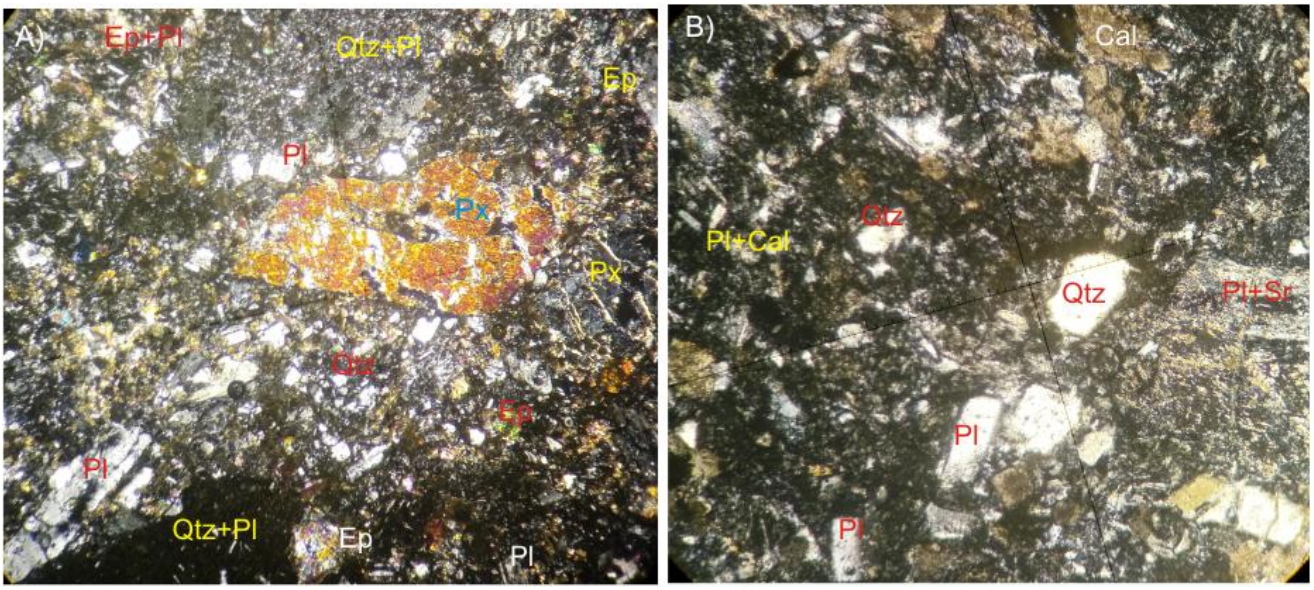

Figure 3.11.Microscopic photo for representative samples (T4-32 and T5-37) of intermediate metavolcanoclast rocks. A) This plate observed under XPL view with 100 x magnifications, location (0492628E: 1552289N), whereas plate B for sample # T5-37 under XPL view with 100 x magnifications, location (04922985E: 1552679 N).

The petrographic description of representative sample#T4-32 contains 36% epidote, 25% plagioclase, 15% quartz, 8% actinolite, 5% chlorite, 5% pyroxene, 5% calcite and 1% opaque minerals. It has a porphyritic texture due to the presence of large grain of pyroxene and plagioclase minerals associated with the fine grain matrix of epidote, quartz, chlorite, calcite and plagioclase minerals. It also contains secondary minerals (e.g. epidote, chlorite and sericite) which are formed due to the alteration of mafic mineral/pyroxene and plagioclase (Fig.3.11 A). There are also minerals over growing on plagioclase minerals as inclusion. The rounded clasts are composed of plagioclase, opaque/mafic and quartz matrix minerals. Generally, the minerals of this rock unit are less foliated and almost they are nearly aligned.

The representative sample# T4-37 is composed of 34% calcite, 26% plagioclase, 21% quartz, 5% muscovite/sericite, 5% chlorite, 3% K-feldspar, 4% opaque and 2% pyroxene minerals. The rock unit of this section shows porphyritic texture due to the presence of plagioclase phenocryst in the fine grained matrix of quartz, chlorite and calcite minerals. The phenocrysts and mafic minerals are altered into secondary minerals such as chlorite, calcite, opaque and sericite. The clasts are rounded in shape and they are composed of plagioclase, opaque/mafic and quartz. This rock unit shows well developed of foliation, which is identified by the alignment of muscovite/sericite, chlorite and plagioclase minerals (Fig.3.11 B). Based on the mineralogical information, it is derived from felsic volcanic rock, but sample#T4-32 is derived from basaltic rocks.

3.2.4. Acidic metavolcanic (meta-rhyolite)

This rock unit is mainly exposed in the northern part of the study area forming nearly steep topography with an estimated thickness of~180m. It is characterized by primary layering or banded structure, light grey to grey, light pinkish/reddish, light greenish, whitish color, fine to medium grain size and moderately foliated. It is also dominated by different types of joints and quartz veins which show cross cutting relationships. The petrographic description of the representative sample # T5-36 of acidic metavolcanic rock indicates that it is composed of quartz, plagioclase, K-feldspar, chlorite, opaque and muscovite/sericite minerals (Fig.3.12).

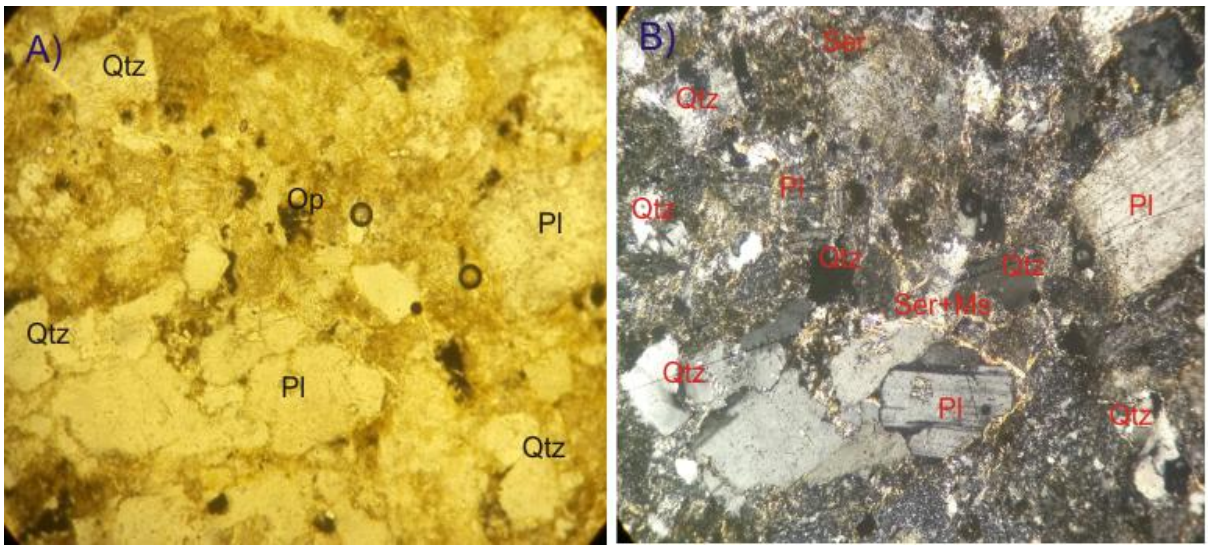

Figure 3.12. Microscopic photo of acidic metavolcanic rock sample # T5-36 under PPL and XPL view with 100x magnifications, location (0494311 E: 1554245 N).

It consists of 50% quartz, 20% plagioclase, 15% muscovite/sericite, 5% K-feldspar, 5% chlorite, and 5% opaque minerals. This rock exhibit porphyritic texture due to the phenocryst of plagioclase mineral incorporated in fine grain plagioclase, quartz, sericite, chlorite and opaque minerals (Fig.3.12). Some of the minerals are randomly distributed while others are aligned parallel specially, the plagioclase and sericite minerals. The sericite mineral is growing over the feldspar grains and along the grain boundaries. This indicates that the sericite mineral is formed after the formation of the feldspar minerals. The presence of dominant quartz and plagioclase minerals indicates that the protolith is felsic volcanic rocks.

3.2.5. Meta-agglomerate

This rock is exposed in the southwestern part of the study area with an approximate thickness of~200m. It is characterized by fine grain size, light greenish to whitish and light grey greenish color, angular to sub angular and sub rounded clasts (1mm-10 cm), massive to moderately foliated unit. The outcrop is mostly whitish in color in most parts may be it is felsic rock (Fig.3.13). It has intermediate groundmass and shows light greenish and dark to light grey color due to alteration effect in some places. It also contains some primary volcanic textures (porphyritic) due to the presence of relict pyroxene minerals.

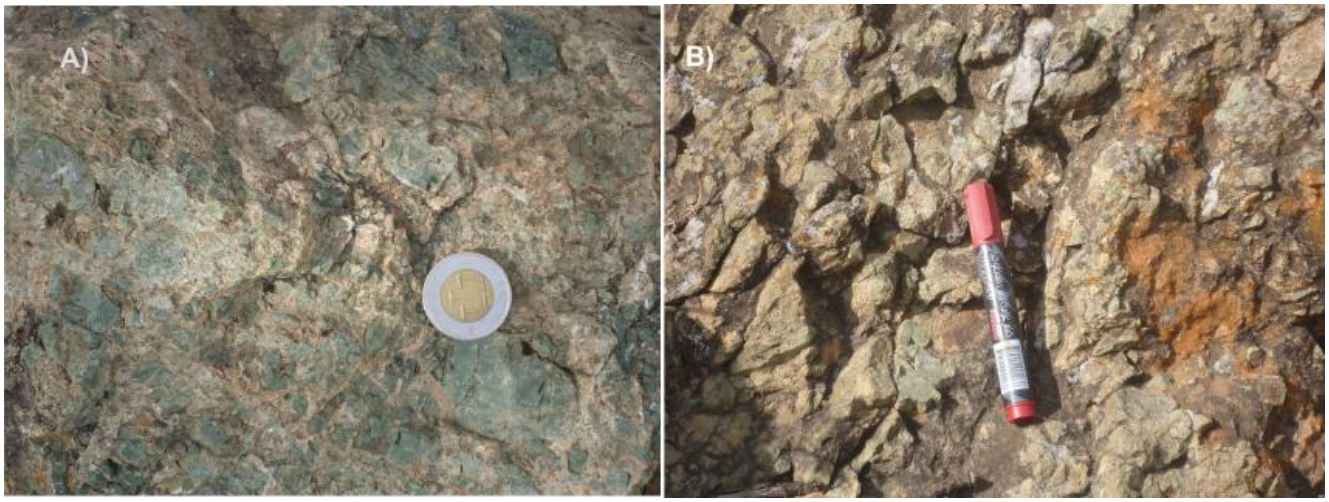

Figure 3.13.Outcrop photo of meta-agglomerate unit. A) It has light grey to greenish color and it is less foliated unit (0491665E: 1550631N). B) This lithiological unit is weathered, show angular to sub angular clasts and it is less foliated (0491664 E: 1550630 N).

From the petrographic description, this rock unit is composed of 39% epidote, 31% quartz, 18% plagioclase, 7% K- feldspar, 3% sphene and 2% opaque minerals(Fig.3.14). The natrolite mineral is occurred as cavity filling mineral.

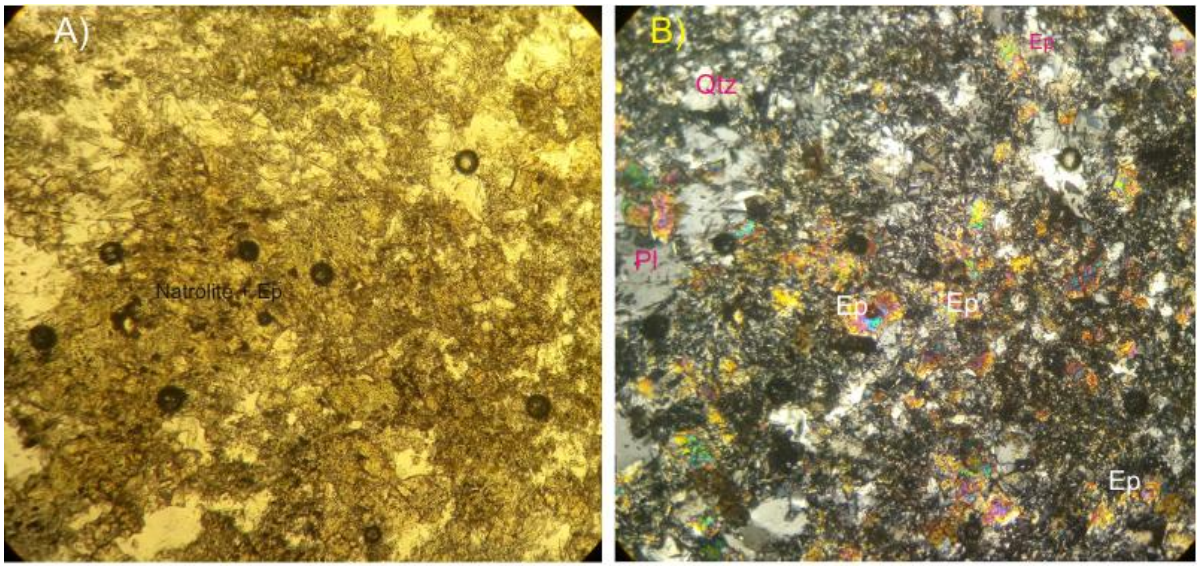

Figure 3.14. Plate A and B are microscopic photo of a representative sample # T4-31of meta-agglomerate rock unit under PPL and XPL view with magnification 40x, locations (0491664 E: 1550631N)

The feldspar minerals are altered into epidote minerals. In the thin section, the quartz grains are larger in size, deformed and recrystallized, having angular to sub angular shape and shows undulose extinction. The clasts are composed of epidote, opaque/mafic? and fine grain quartz minerals (Fig.3.14). The weak alignment of epidote and feldspar minerals indicates development of cleavage. The abundance of plagioclase, quartz mineral and rock fragments indicates that its protolith is felsic volcanic rock.

3.2.6. Metatuff

This rock is mainly exposed in the northeastern part of the study area and it has an estimated thickness of ~150m. It shows primary layering structure. The grain size of the clasts are ash size (< 2mm sizes) with light grey to grey and light greenish color (Fig.3.15).This unit shows variation in degree of compactness from welded to unwelded tuff of moderately foliated.

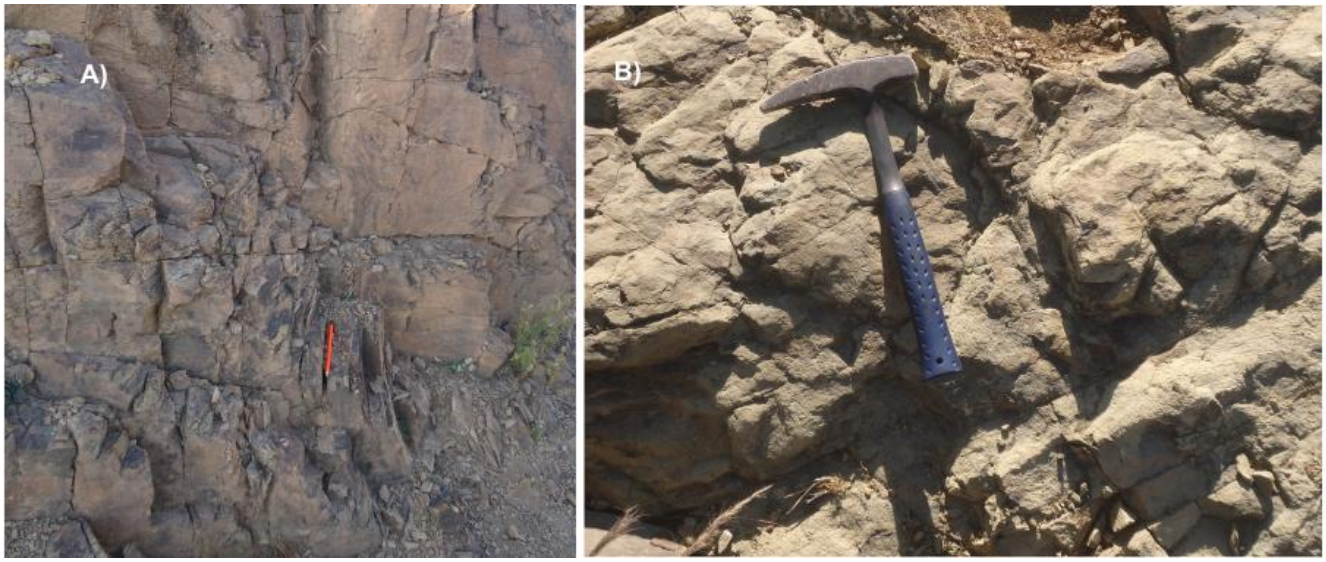

Figure 3.15. Outcrp photo of metatuff unit. A) It is foliated, moderately compacted and cross cut by a systematically aligned joint and this photo is taken facing to NW (0495770 E:1553076 N). B) This unit is more compacted having light grey color and the photo is taken facing to N direction (0495367E:1553060N).

3.2.7. Metaconglomerate and metagreywacke

These rock units are mainly exposed in the central part of the study area with an estimated thickness of~140m. Both have light grey to dark, white reddish, light greenish and dark brown color respectively (Fig.3.16) and show less development of foliation. The metaconglomerate contains fragments of quartz and feldspars (K-feldspars?) minerals. The rock fragments of the metaconglomerate unit are sub angular to sub rounded in shapes, which indicates may be the distance of transportations during sedimentation processes.

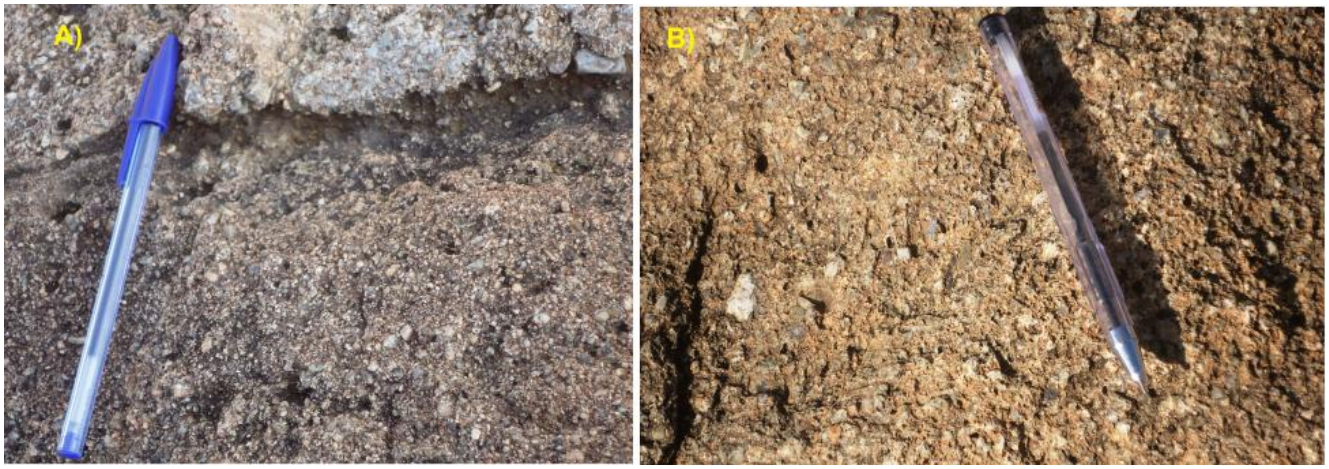

Figure 3.16.Outcrop photo of metaconglomerate rock unit. A) It has sub rounded to rounded shape of clasts and it is less foliated unit (0493274E: 1550645 N). B) It is less foliated and has sub angular to sub rounded shape of clasts and photo taken facing to southeastern direction both photo of A and B (0493270E:1550641N).

The metagreywacke is composed of plagioclase, K-feldspar, quartz, mica/sericite, opaque, and lithic fragments. The lithic fragment/clasts are containing very fine grained of different minerals (Fig.3.17).

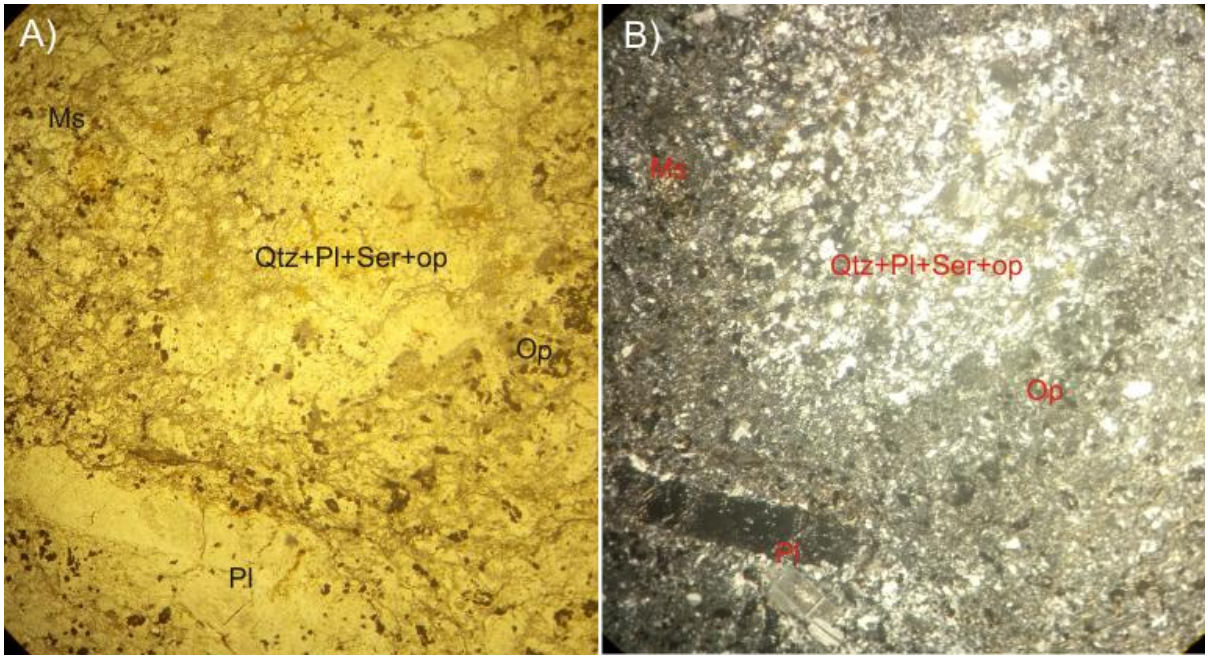

Figure 3.17. Microscopic pictures of the metagreywacke rock unit, sample#T3-20 under PPL and XPL view with 40x magnifications, location (0493283 E: 1550371N).

Mineral content of this rock is 40% quartz, 23% plagioclase, 20% opaque, 10% K-feldspar, 4% mica/sericite, 3% pyroxene and rutile minerals. These minerals are occurring as fine grain size and they are nearly aligned. There are also clasts that have sub angular shape rich in plagioclase, quartz, opaque and mica/sericite minerals (Fig.3.17). Based on the petrographic information this unit is dominated by quartz and plagioclase minerals. Therefore, this indicates that, it is derived from felsic volcanic rocks by sedimentation processes.

3.2.8. Lower slate

This rock unit is mainly exposed in the southeastern part of the study area with an estimated thickness of~250m and it is characterized by variegated color from light grey to grey, light brownish to brownish, light pinkish and reddish color respectively(Fig.3.18). It is underlying the basic metavolcanic and metatuff unit in the central, northeastern and southwestern part of the study area, however it overlying the lower metalimestone unit. In this unit, bedding and thin laminations of primary sedimentary structures are well preserved, which indicates that it is relatively less deformed in some places. However, in the other places it is highly foliated, lineated (shows pencil like structures), shows minor sub-horizontal fold axis, kink band fold and it is closely jointed/fractured. The strike orientation of the

foliation is ranging from N25^{0}E-N55^{0}E and dips 30-90^{0}SE. It also shows composite fabric such as primary and secondary foliation. The primary foliations are recognized by variation of thickness, composition and color of the layers, but the secondary structures are slaty cleavage and pencil (linear) structures.

Figure 3.18. Outcrop of the lower slate unit. A) The slate shows kink band structure (0494702E:1551367 N). B) It shows pencil structures and has light greenish to reddish color (0494134 E: 1550618 N).

Petrographic analysis of the representative samples of slate (Fig.3.19 A-D) indicates that they are composed of quartz, feldspar, muscovite/sericite, chlorite, and opaque minerals. Further detail description is done as follows.Sample#T3-24 is composed of 30% quartz, 25% feldspar, 18% muscovite/sericite, 10% clay mineral/organic matter?, 9% chlorite, 5% opaque and 3% biotite minerals. It shows foliation which is identified due to the weak alignments of chlorite and muscovite/sericite minerals that represent the M1 event of metamorphism (Fig.3.19A and B).This cleavage is less deflected by the porphyroclast mineral. The porphyroclast is altered into muscovite and quartz minerals, but it preserved its tabular shape therefore; the original mineral of this porphyroclast may be feldspar. It is formed before the weakly developed slaty cleavage, indicates that the relation between metamorphism and deformation is pre-tectonic.

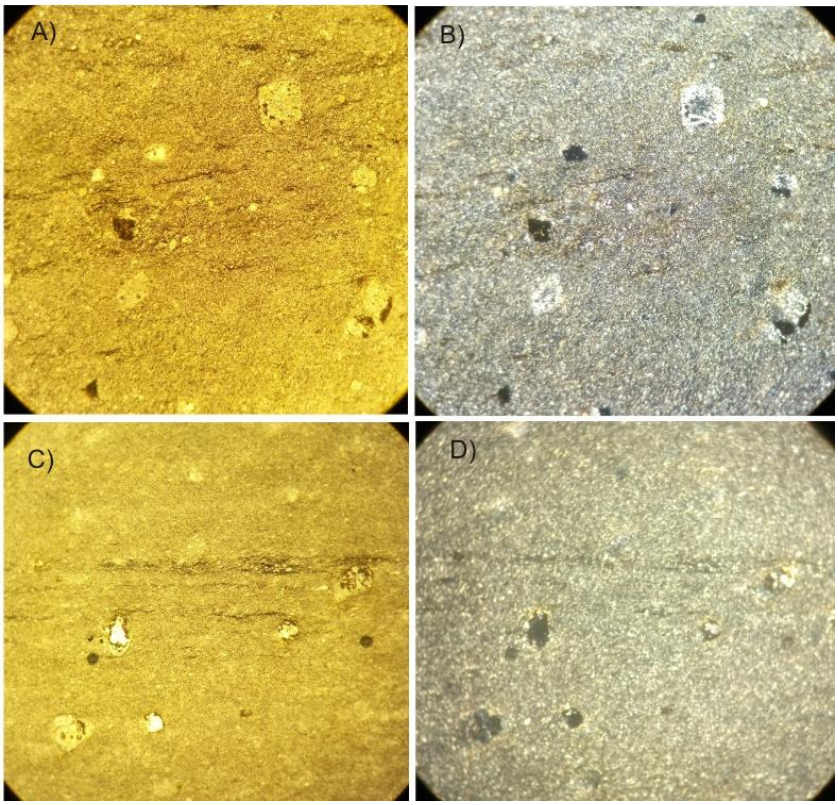

Figure 3.19.Microscopic pictures of the different types of lower slate rock unit. Plate A and B are photo of sample # T3-24 under PPL and XPL view, with 40x magnification and location (0494712 E: 1551363N). Plate C and D are photo of sample # T1-2 under PPL and XPL view, with 40x magnifications and locations (0496183 E: 1553087 N).

The mineral content of slate rock sample#T1-2 is 26% calcite, 22% quartz, 14% Fe-rich mineral, 12% muscovite/sericite, 10% clay mineral/organic matter?, 8% plagioclase, 6% opaque and 2% biotite minerals. This rock unit shows slaty cleavage because of the D1 deformation event (Fig.3.19 C and D). The M1 (first metamorphic event) minerals are muscovite/sericite and plagioclase. The slaty cleavage is less curved by the porphyroclast minerals. This mineral is replaced by calcite and quartz, but there is a relict of Fe-rich brown color mineral and it represents pre-tectonic with respect to the weakly developed cleavage in some part of the section. Therefore, this unit is derived from Fe-rich carbonate rock, however sample #T3-24 is from felsic volcanic rock.

3. 2.9. Lower Metalimestone

Lower metalimestone is overlaying the lower slate and underlying the upper slate unit. It is characterized by stromatolitic lamination, cross bedding and stylolitic structures. These structures are cross-cut by en echelon types of calcite veins and it indicates the younging direction towards the upper metalimestone unit. It is fine grained and weak karstified structure occurring locally in these rocks. This

unit shows highly variegated color from light grey to dark and black, brownish to light brownish color (Fig.3.20) and has an estimated thickness of~420m.

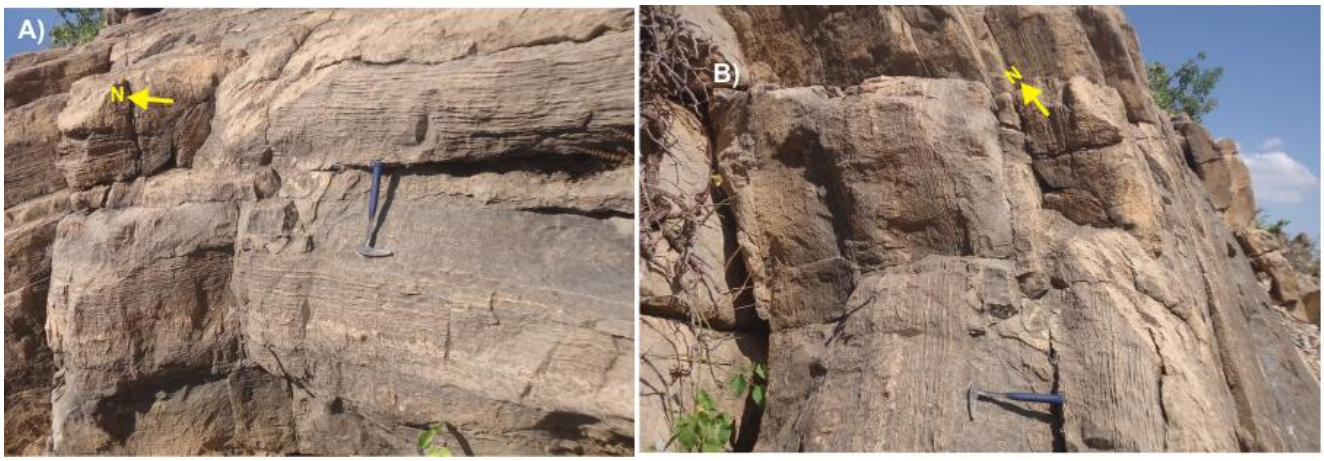

Figure 3.20.Outcrop photo of lower metalimestone unit. A) The fine grained metalimestone rock shows stromatolitic laminations trends N-S direction (0494490 E: 1550289 N). B) The stromatolitic lamination trends NE-SW directions in the metalimestone rock units (0494493E: 1550292N).

The petrographic description of a representative sample of metalimestone rock is composed of calcite, opaque and quartz minerals (Fig.3.21).

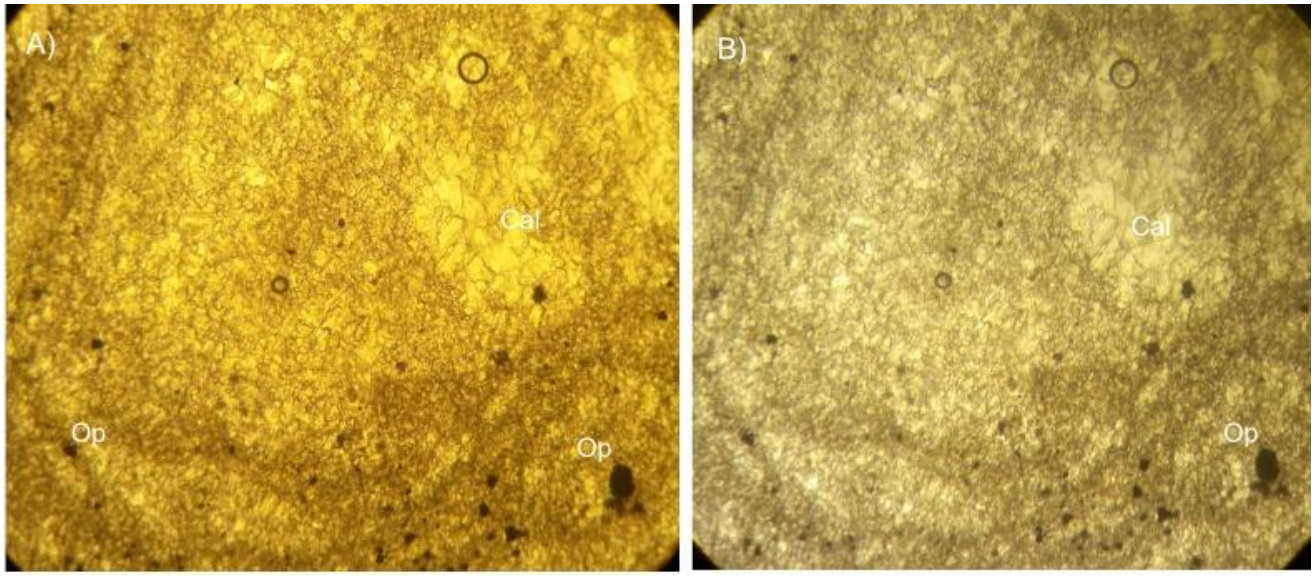

Figure 3.21. Microscopic photo of lower metalimestone unit. Plate A and B are photo of sample#T1-1 under PPL and XPL view, with 40x magnification and locations (0496483 E: 1553011 N).

It contains 92% calcite, 6% opaque and 2% quartz and these minerals shows less alignment and shows stromatolitic lamination and micro stylolitic structures. Based on the petrographic description, this rock is derived from carbonate sedimentary rock.

3.2.10. Upper slate

This rock unit is exposed near the core of the syncline having light grey, light greenish and light grey reddish color (Fig. 3.22) with an estimated thickness of~500m. It is underlying and intercalated with the upper metalimestone. The strike orientation of the slaty cleavage is 035^0 and dipping 51^0 towards southeast directions and shows less developed linear/pencil structures.

Figure 3.22.Moderately foliated, less lineated, folded and has a light grey to greenish color of the upper slate unit. Outcrop photo taken facing to SE direction (0494607 E: 1550255N).

From the petrographic description, the modal composition of this unit contains 20% opaque, 18% plagioclase, 16% quartz, 14% chlorite, 12% muscovite/sericite, 11% clay minerals and 9% biotite. The minerals of this section show primary lamination structure (Fig.3.23) due to the alignments of platy minerals during deposition. Based on the mineralogical information, this rock is derived from mafic rich rocks.

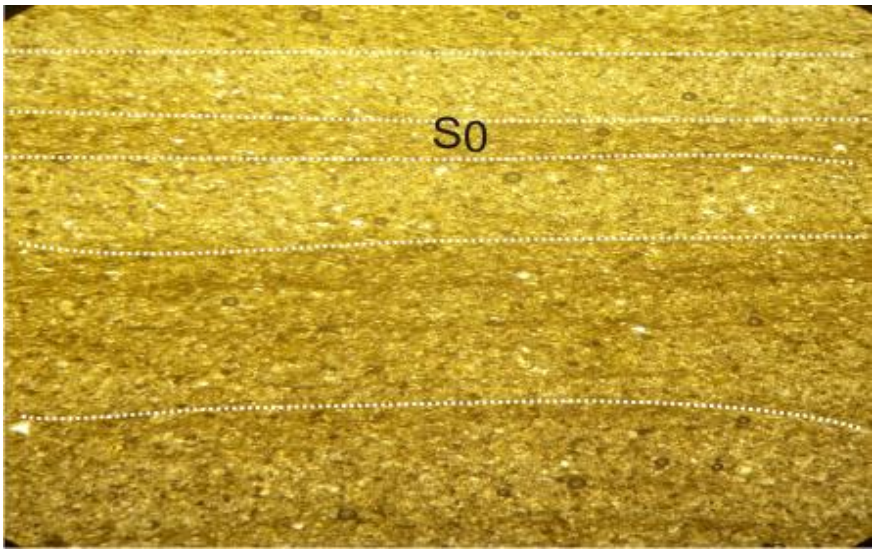

Figure 3.23.Microscopic picture of upper slate unit. Sample # T3-16 in PPL view, with 40x magnifications and locations (0494607 E: 1550255N).

3.2.11. Upper metalimestone

This rock is exposed in the core of the syncline having an estimated thickness about~ 900m and it is characterized by light gray to dark gray and black color and shows stylolitic structure. This unit shows primary bedding, less developed secondary foliations, variation of layering/bedding thickness, color and it is highly dominated by cross cutting, en echelon type and other systematically aligned and discontinuous calcite veins (Fig.3.24). It shows elephant skin types of weathering with tabular dark color carbonate material that is re-deposited calcareous fragments. In addition to that, there is development of minor sub vertical to sub horizontal fold axis. In few localities there is also grey to whitish color travertine formed due to the dissolution of metalimestone as the result of the rain water.

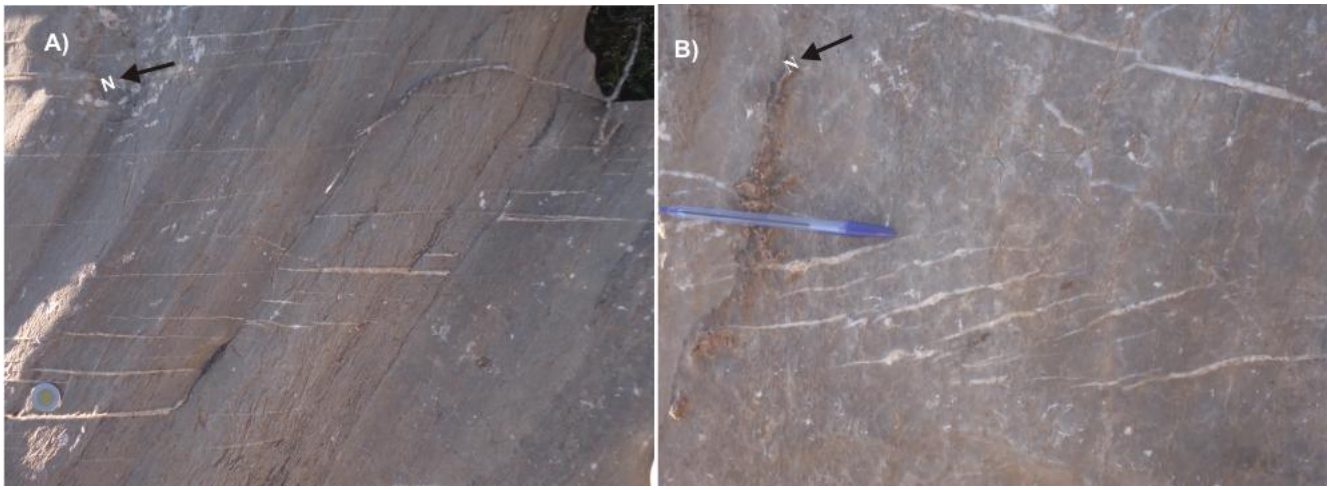

Figure 3.24.Outcrop photo of upper metalimestone unit: A) Fine grained unit shows dextral movement of en echelon calcite veins (0496355 E: 1553072 N). B) Show dextral movement of en echelon calcite vein structures in the metalimestone lithological units (0496352 E: 1553069 N).

The petrographic description of metalimestone rock is composed of calcite, opaque and quartz minerals (Fig.3.25).

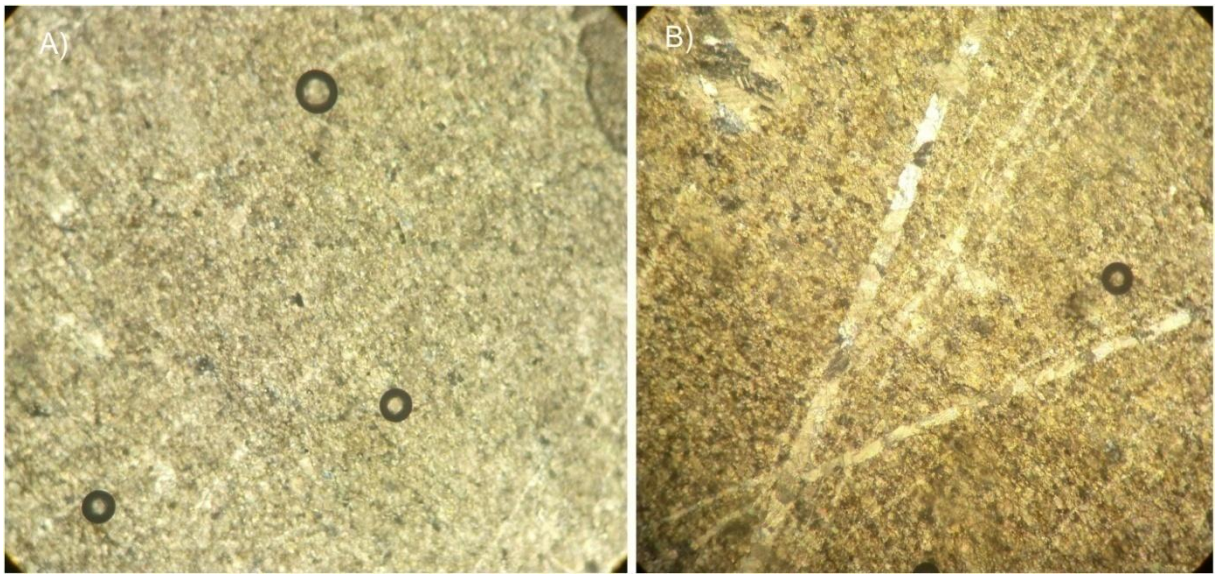

Figure 3.25.Microscopic photo of upper metalimestone unit. Plate A and B are photo of sample #T3-13 under PPL and XPL view with 40x magnification and locations (0496044 E: 1549458N).

The representative sample of metalimestone rock contains 95% calcite, 3 opaque and 2% quartz minerals. The calcite mineral shows equigranular textures (fine grain size and have same shapes) in some parts of the section, but in another part of the section the minerals are form preferred alignments. The calcite microveins show crosscutting relationships, they are folded and occur as sets. There is also less development of microstylolitic structure and also altered dark brown color carbonate mineral in the section. The parent rock of this slate unit is carbonate sedimentary rock.

3.2.12. Phonolite

Phonolite is exposed in the northern part of the area with an estimated thickness of~ 150m having uniform grain size distribution, light grey and light greenish fresh color and light grey reddish weathered color (Fig.3.26). It is unmetamorphosed, younger lithological unit forming steep sloped ridges. According to Tadesse (1997), this unit is a volcanic plug and occurs as sub circular or elliptical bodies at the center of pyroclastic falls and flows.

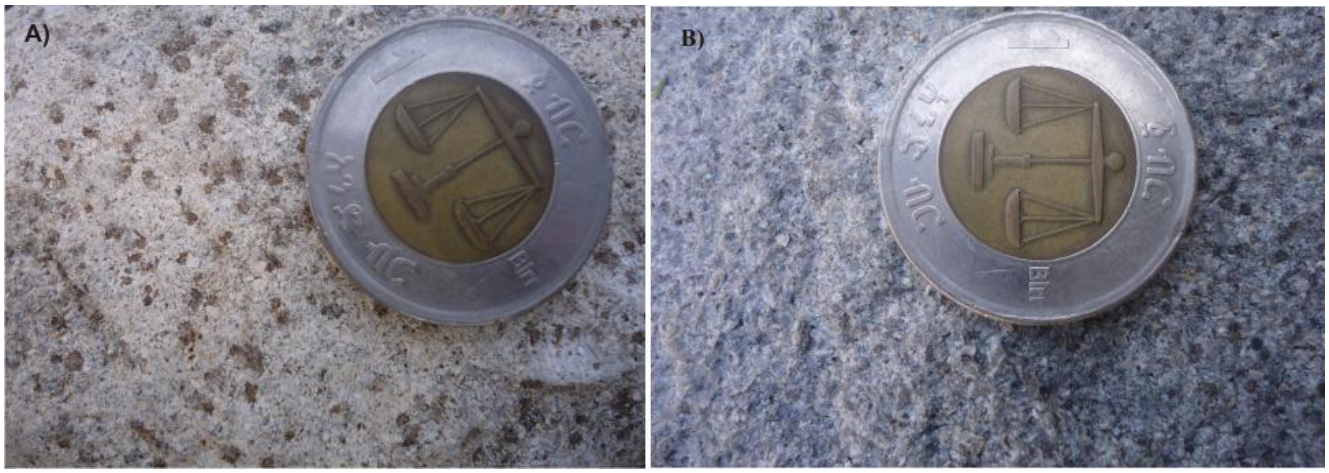

Figure 3.26. Outcrop photo of phonolite rock unit. A) It is moderately weathered unit and it shows medium grain size,light grey to dark color (0494605 E: 1554719 N). B) This photo shows less weathered and taken from location (0494606 E: 1554720 N).

3.3. Metamorphism

All the exposed lithiological units of the study area are mostly metamorphosed and show a variable degree of metamorphism and deformations. Some minerals show relict texture (porphyritic texture) and recrystallization in most rocks. For example, quartz mineral is recrystallized, show undulose extinction and grain boundary migration in most sections of the metavolcanic and metavolcanoclast rocks. The relict texture is preserved by the augite and plagioclase minerals. In most of the section, these minerals are altered into chlorite, epidote, calcite, actinolite and sericite minerals. However, the slate unit shows primary lamination structure. The mineral assemblages of these rocks are important for the determination of the metamorphic grade of rocks. Most of the mineral assemblages are given information of volcanic origin. These minerals of the various rock units are shown below. The bold are critical minerals that are important to determine the grade of metamorphism.

1. Basic Metavolcanic
    a. Calcite+ **chlorite**+ plagioclase+ **muscovite/sericite**+ quartz+ **epidote** + opaque +pyroxene
    b. Pyroxene + plagioclase+ **chlorite**+ olivine+ opaque+ **serpentine**
2. Basic metavolcanoclastic
    a. Calcite + plagioclase + **actinolite** + **chlorite** + quartz + **muscovite/sericite** + **epidote** + opaque + K-feldspar
3. Intermediate metavolcanoclastic
    a. **Chlorite +** plagioclase **(albite)** + calcite <u>+</u>**muscovite/sericite** <u>+</u> **epidote** + quartz + opaque + pyroxene

   b. Plagioclase**(albite) + epidote +chlorite +muscovite/sericite** + quartz+ calcite + opaque ± k-feldspar ±**actinolite**± pyroxene ± sphene
   c. Calcite + plagioclase+ quartz + **muscovite/sericite + chlorite** + K-feldspar + opaque
4. Acidic Metavolcanic
   a. Quartz + plagioclase+ **muscovite/sericite** + k-feldspar + **chlorite**+ opaque
5. Meta-agglomerate
   a. **Epidote**+ quartz **+** plagioclase + k-feldspar + sphene + opaque
6. Metagreywacke
   a. Quartz+ plagioclase + opaque+ K-feldspar + **mica/sericite**+ rutile + pyroxene
7. Slate Unit
   a. Quartz + **muscovite/sericite +chlorite** + plagioclase ±**biotite +** opaque
   b. Calcite +quartz +Fe-rich mineral+ **muscovite/sericite** + plagioclase ±**biotite** + opaque
8. Metalimestone
   a. Calcite + opaque ± quartz

CHAPTER FOUR

4. Deformation and geological structures

4.1. Introduction

The geological structures developed on the basement rocks of Tahtai Logomti area are determined on a scale of microscopic to macroscopic. These structures are recognized as brittle and ductile deformations and have experienced different phases of deformation. The field observation (Fig.4.1), petrographic study, deformation and micro-structural analysis indicates the presence of at least three phases of deformations (D1, D2 and D3) in different parts of the study area. The D1 (first phase of deformation) is determined by the existence of a prevalent foliation (S1) and pencil structure, the D2phase of deformation is shown by plunging folds, kink band folds and en echelon array veins, and D3 is represented by younger brittle structures. These are faults and different type of joints. The exposed basement rocks have also preserved primary structures (Fig.4.2). The deformational structures are classified into ductile, brittle-ductile, brittle, and structures associated with diffusion mass transfer processes. The general orientation of the various structures has been determined by using stereographic projections as illustrated in the following diagrams. Here the various primary and deformational structures are described as follows.

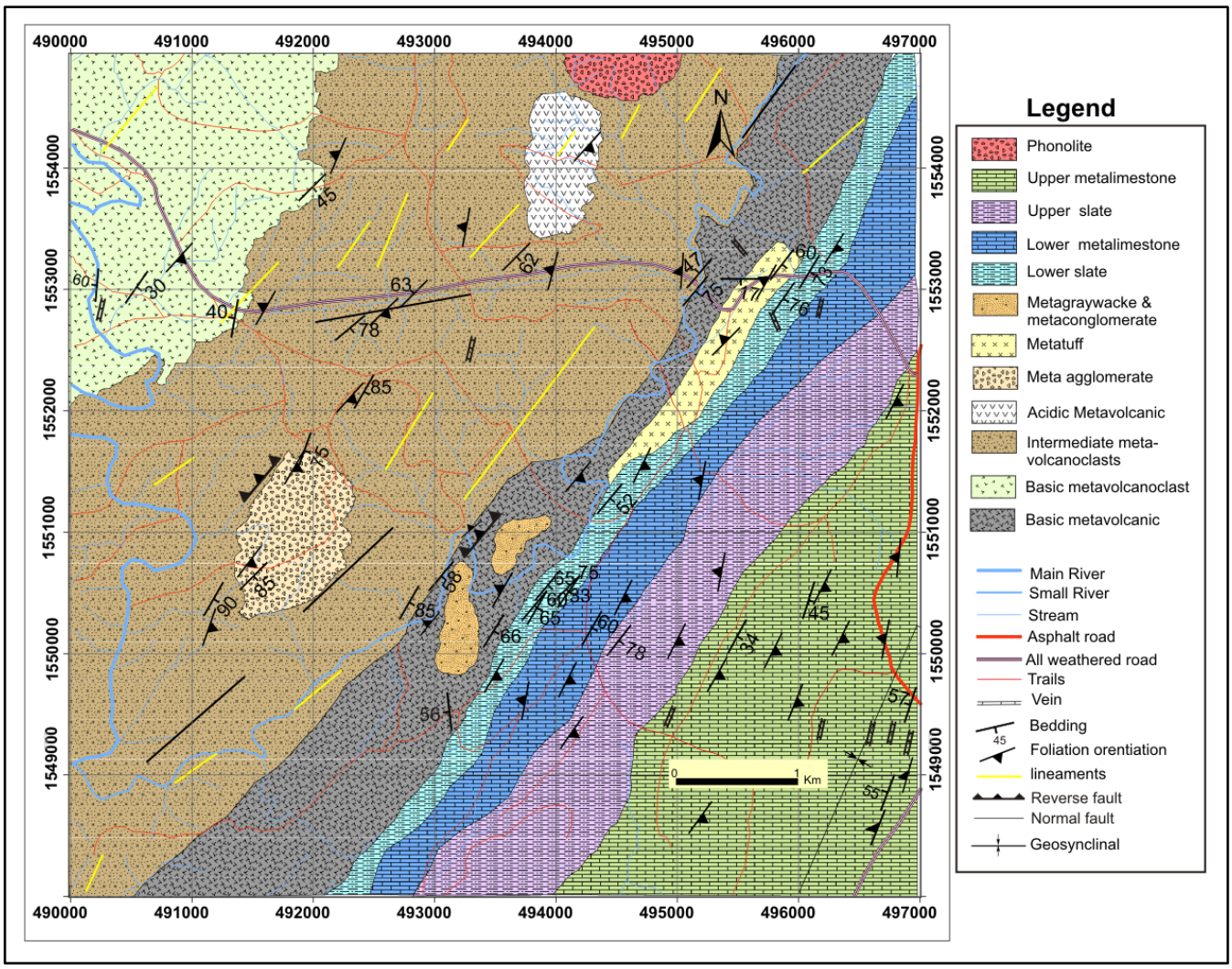

Figure 4.1. Structural map of the study area.

4.2. Primary structures

The primary structures identified in the study area are bedding, lamination, cross bedding, tuffaceouse layer, slump structure and stromatolitic lamination. These structures are preserved as primary structures in some lithological units (Fig. 4.2) with various color, composition and thicknesses. Slump structure is synsedimentary structure that is warped or folded due to the overload of the sediments during depositional processes (Fig.4.2A) however; the stromatolitic lamination shows alternation of laminea as white and grey color and warped upwards where convex side is on the younging directions (Fig.4.2 D). Tuffaceouse layer displays variable thicknesses of layering with light grey to light greenish color and weakly foliated (Fig.4.2B), whereas the bedding and thin lamination of the metalimestone show black to light grey color variations (Fig.4.2 C). The bedding structure of the slate rock unit mostly shows variable thickness of beds with striking NE and dipping towards southeast directions.

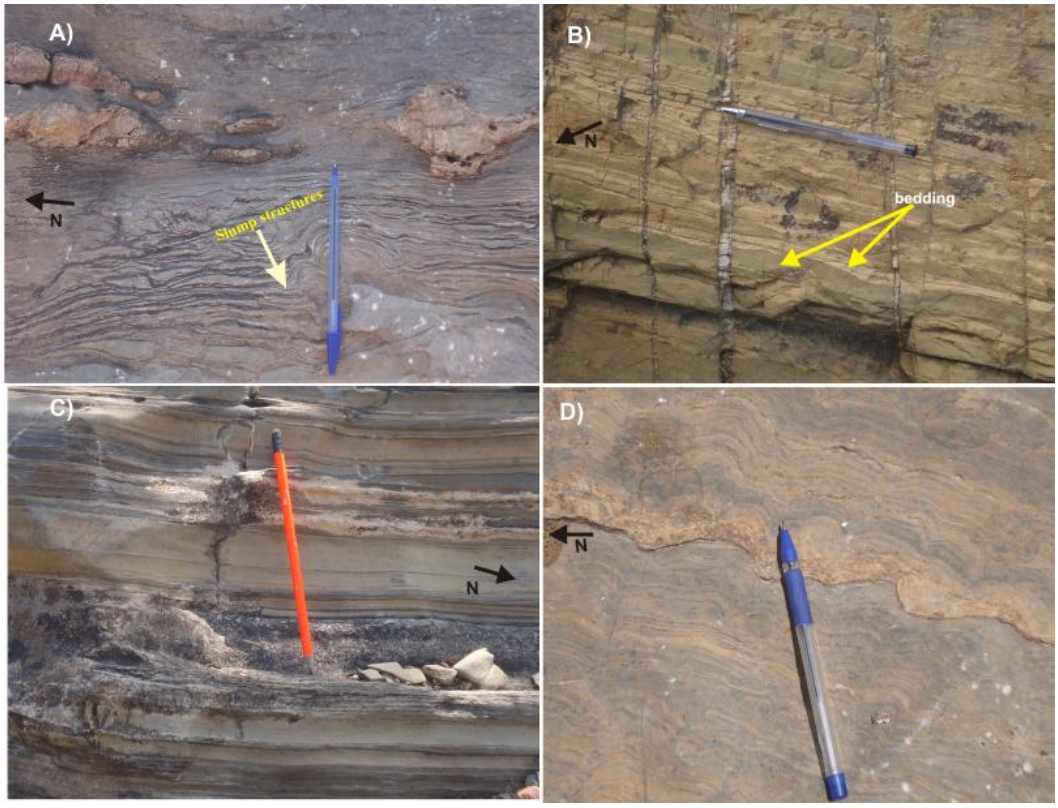

Figure 4.2.Field photo of primary structures. A) Slump structures in the lower metalimestone, it is synsedimentary folded (0496307 E: 1549401 N). B) Tuffaceouse layer shows different colors and cross cut by quartz vein (0493277 E: 1552544 N). C) Bedding and thin lamination in the upper metalimestone shows different thicknesses (0495280 E: 1549778 N). D) Stromatolitic horizon shows sub laterally linked small size domes and stratiform that displaying the characteristics laminations of the medium grain stromatolite in the lower metalimestone rock units (0496483 E: 1553011 N).

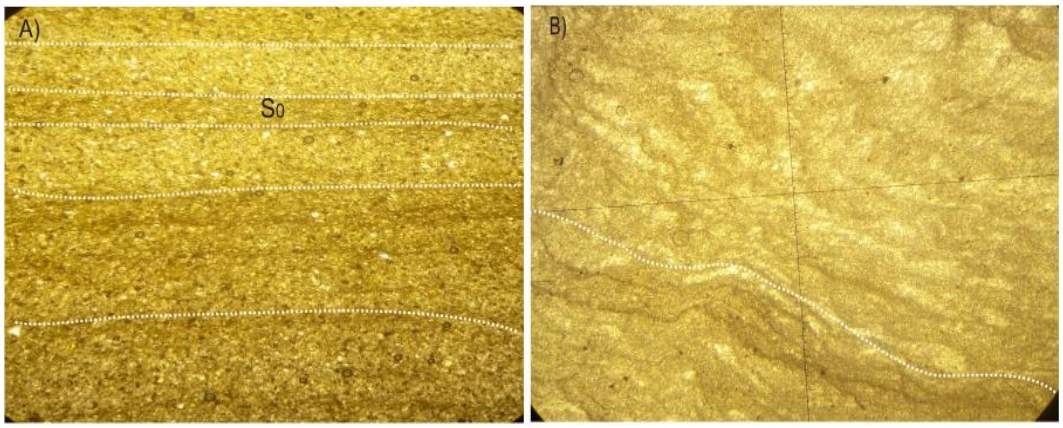

Figure4.3.Microscopic photo of the upper slate and lower metalimestone units under PPL view. A) This unit shows a primary lamination (S0). This S0 cleavage is formed due to alignment of platy minerals that show a compositional layering of mica minerals. A representative sample (T3-16) of slate rock under PPL view with 40x magnifications, locations (0494607 E: 1550255 N). B) Representative sample#T1-1 contains stromatolitic laminations in metalimestone unit, the whitish broken line indicates the orientation of thin lamination. The difference in lamina color dominantly related to change in micro fabric compositions and show alternating lamination. It is identified with 40x magnification, locations (0496483 E: 1553011N).

The cross bedding structures are dominantly identified in metalimestone units, which tells the younging directions (Fig 4.4).

Figure 4.4.Cross bedding in the lower metalimestone unit (0496254 E: 1553070 N).

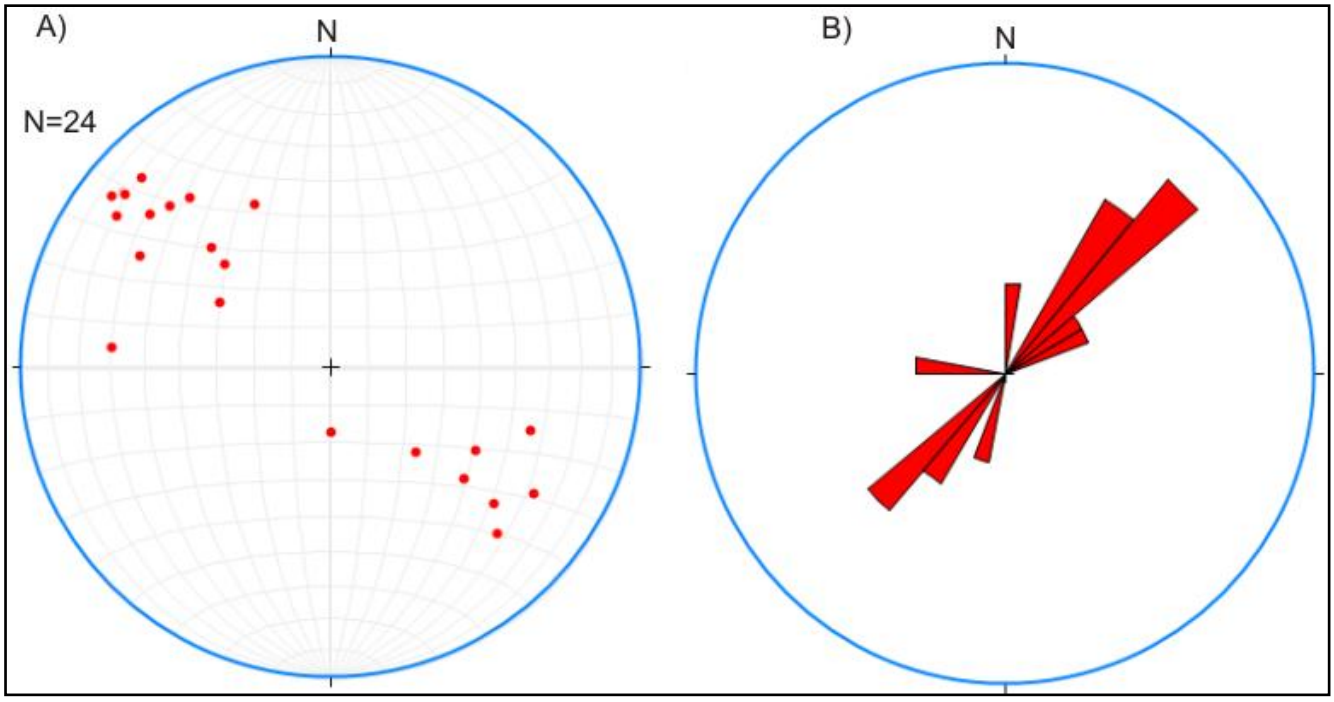

Figure 4.5. Primary structure (S0) data plotted as: A) The poles to the S0 foliation is dominantly occurring in the NW than SE quadrant of the stereonet, whereas the poles are dominated on the NW quadrant dipping towards to the SE quadrant. B) The rose diagram of the S0 foliation represents the strike direction of the bedding of the rocks by the longest wedge of the rose diagram. The mean value of the strike direction is $N33^0$- 40^0E value of the S0 foliation of the area.

4.3. Deformational structures

4.3.1. Ductile structure

Ductile structures are formed by bending or stretching of rocks. These structures are fabrics and folds.

4.3.1.1. Foliation (S1)

The most prevalent structural feature of the area is S1 foliation and it is striking NE and dipping SE or NW. It is predominantly developed on the slate rock units and represented by slaty cleavages (Fig.4.6). However, a weak S1 foliation is also common in all lithiological units (e.g. basic metavolcanic, metatuff and meta-agglomerate units.

Figure 4.6.Outcrop photo of slaty cleavage in rocks of the area. A) Cleavage in lower slate is consisting of closely spaced vertical fractures dipping toward SE (45^0)similar to the bedding direction (0496175 E: 1553081 N). B) Cleavages in metatuff at some angle to the bedding and discordant by joints (0495770 E: 1553076N).C) S1 foliation is weakly developed in the intermediate metavolcanoclastic units (0494516 E: 1553158N). D) S1 foliation in the lower slate unit (0494712 E: 1551363 N).

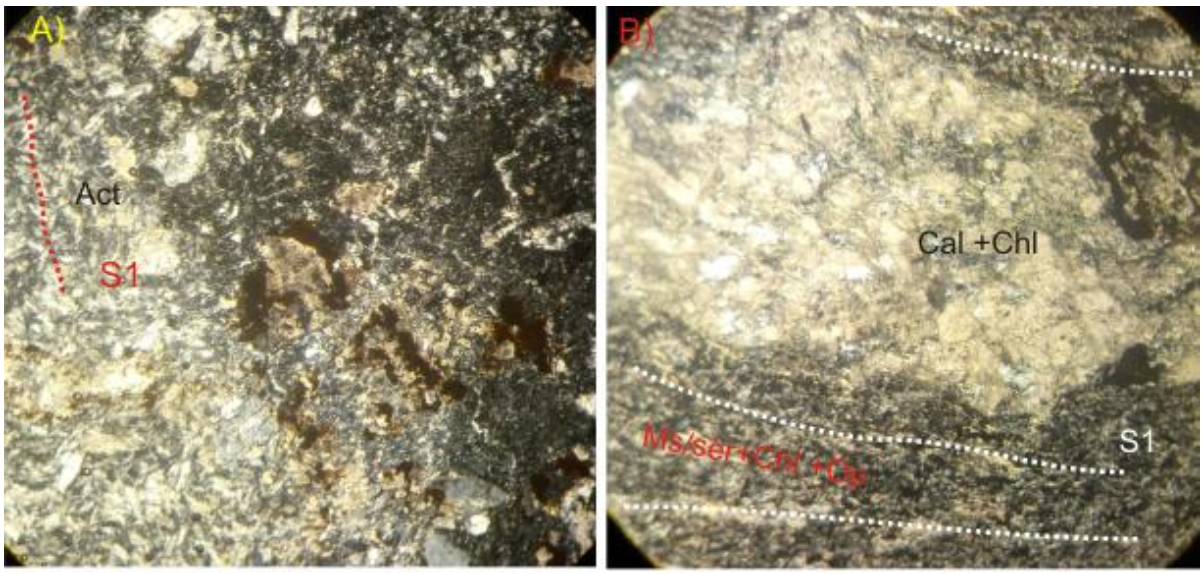

Figure 4.7.Microscopic photo of S1 foliation in the metavolcanoclastic units: A) The slaty cleavage is formed by the preferred orientation of actinolite and fine grain chlorite minerals in the basic metavolcanoclastic rock. Sample #T2-12 under XPL view, with 40x magnifications and locations (0491144E: 1553564 N). B) This thin

section shows also S1 foliation is defined by the preferred alignment of muscovite/sericite, chlorite, calcite, and elongates opaque minerals of intermediate metavolcanoclast. This sample # T2-10 photo is under PPL view with 40X magnifications, locations (0491497 E: 1552667N).

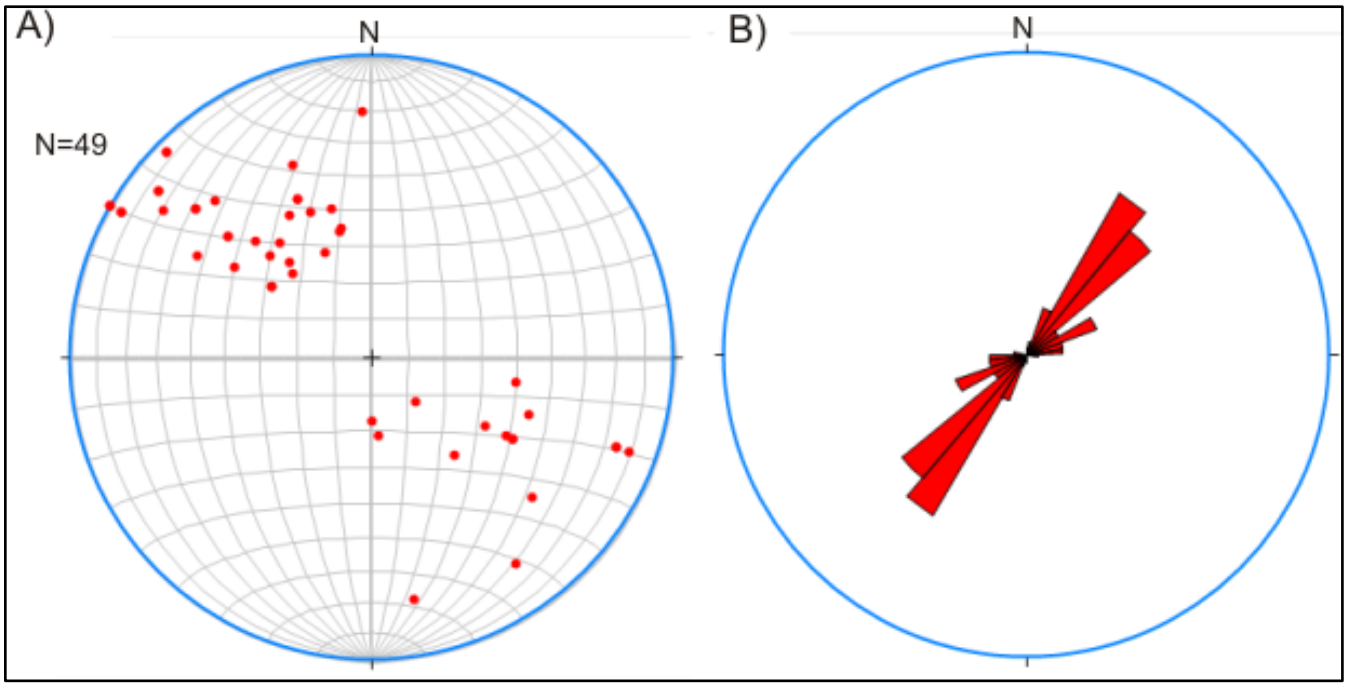

Figure 4.8 The S1 foliation data is plotted as: A) Poles of the S1 foliation plot more dominantly on the NW quadrant. Based on the dominant poles the S1 foliation dips towards SE quadrant. B) The rose diagram represents the strike direction of the S1 foliations is $N31^0$-42^0E.

4.3.1.2. Linear structures

4.3.1.2.1. Pencil structures

Pencil lineation (L1) is mostly identified in the lower slate noted by the intersection between bedding and cleavage (Fig.4.9).This linear structure is aligned parallel to the original bedding and they are formed by the D1 deformation event.

Figure 4.9.Pencil structure in the lower slate rock unit, it is defined by the intersection of bedding and slaty cleavage (Location: 0494055 E: 1550509 N and 0494134 E: 1550618 N).

4.3.1.3. Kink bands

Kink band fold is occurring in lower slate rock unit (Fig.4.11). It is characterized by nearly straight limbs and sharp hinges and occurred in highly lineated/deformed lithological units. The lithological unit that has this structure shows different color and layering structure. It is formed by the second phase of deformation (D2).

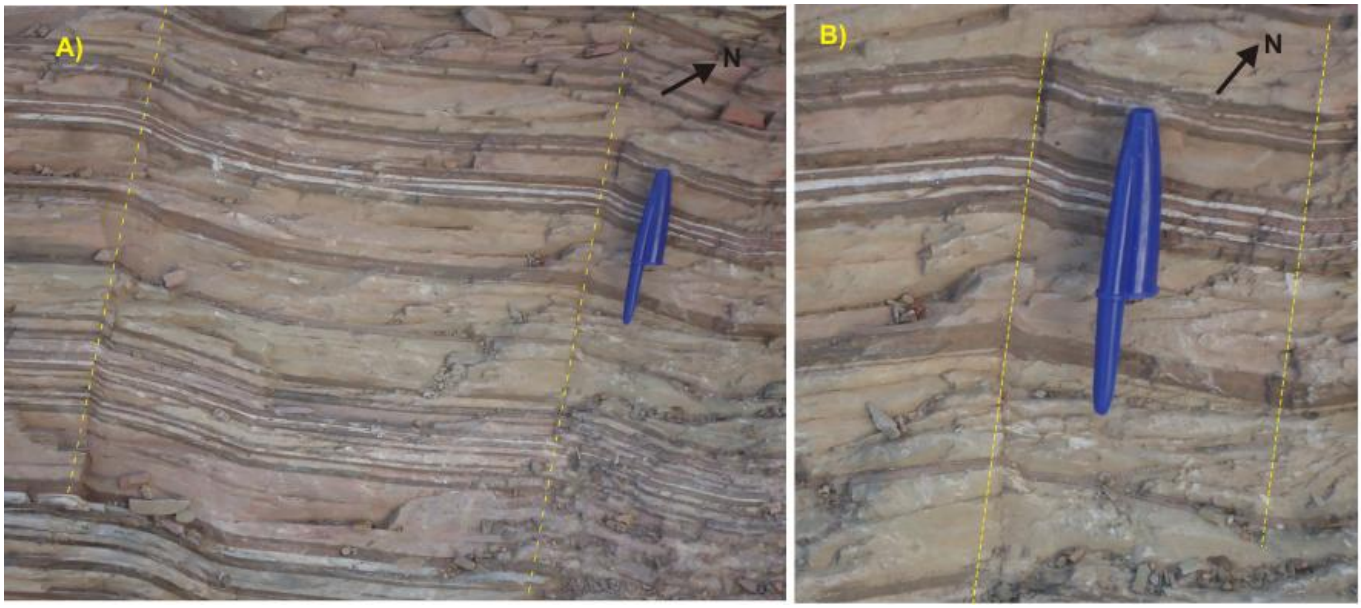

Figure 4.10.Field photo of lower slate outcrop that shows kink band fold in both A and B photos (Location: 0494700 E: 1551365 N).

4.3.1.4. Fold

Folds are observed in the field and they are formed due to the second phase of deformation (D2).These folds are small scale minor folds, observed on lower slate, upper metalimestone and intermediate metavolcanoclast rocks in the central, southeastern and northwestern part of the study area. These types of folds are sub-horizontal to moderately plunging folds (Fig.4.12). In the lower slate rock unit and upper metalimestone the folds occur in a scale of centimeter to meter antiforms and synforms.

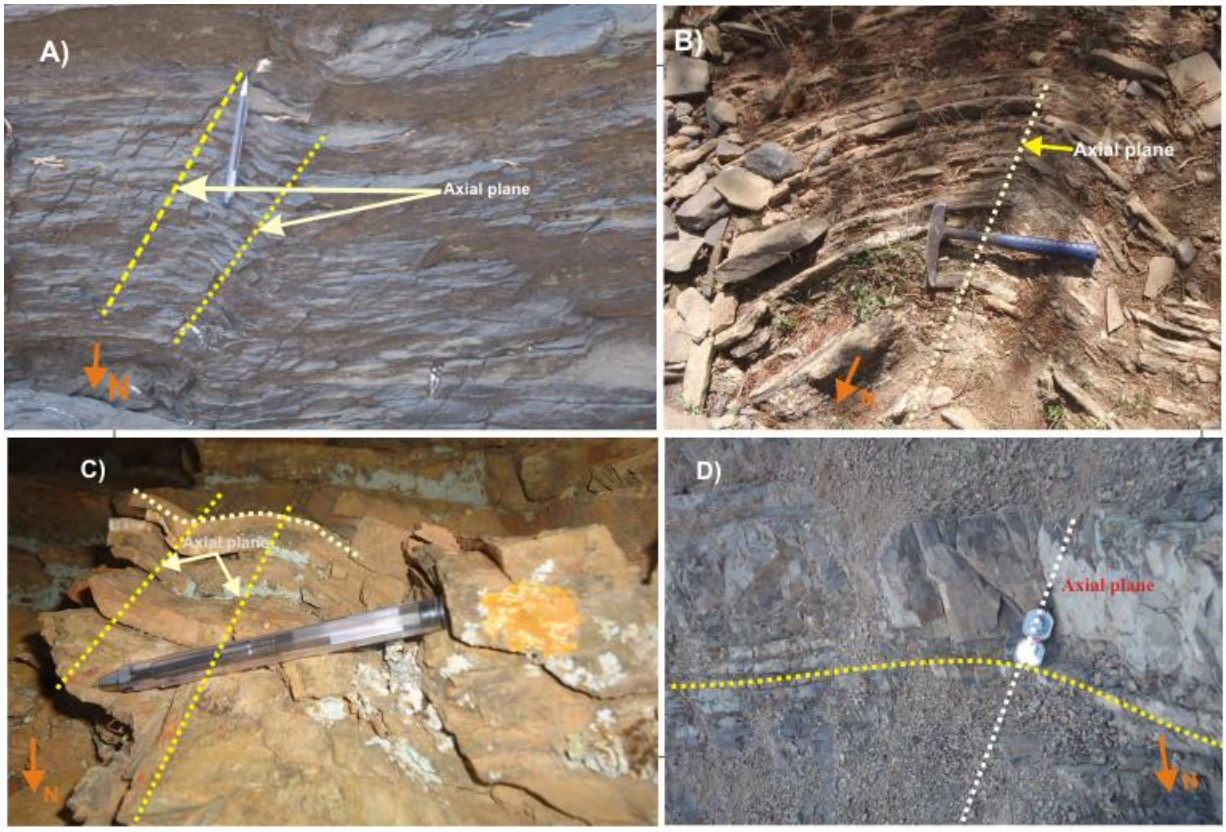

Figure 4.11. Field photograph of outcrops that show minor folds. A) Gentle to open folds in upper metalimestone (0495868 E: 1549478 N). B) Thin upper metalimestone layers showing minor folds. (0495429 E: 1549629 N). C) Minor folds in the lower slate (0496098 E: 1553049 N). D) Monocline fold in the intermediate metavolcaniclasts rock (0493603 E: 1553611 N).

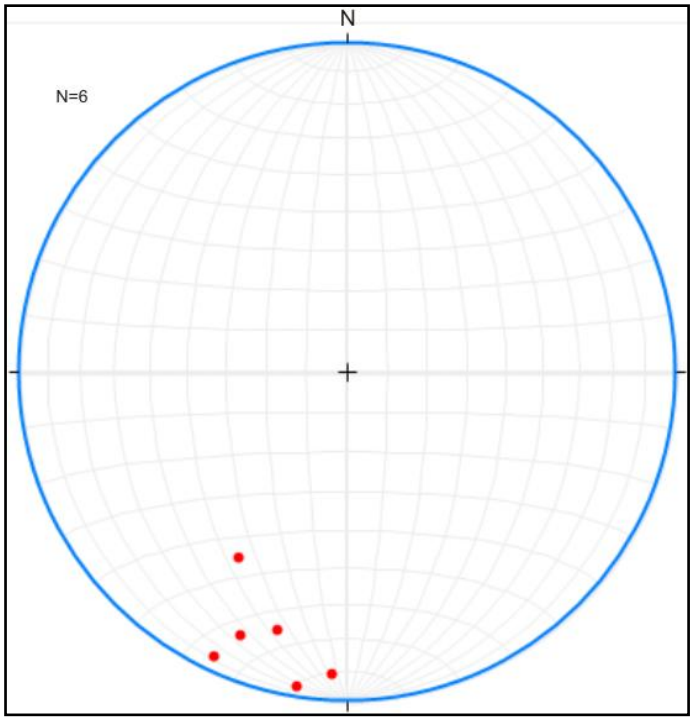

Figure 4.12.The fold axis data are plotted as poles and they are gently dip SW direction.

4.3.2. Diffusion mass transfer by solution

4.3.2.1. Stylolitic structure

The stylolitic structures are observed in the metalimestone rocks. These structures are formed due to pressure solution process (Fig.4.14). They are formed at some angle to the bedding and they are dark in color containing residues of insoluble materials. The saw-tooth of the stylolities structure determines the direction of movements, because the maximum compressive stress is normal to the stylolite plane (Barker, 1998**)**.According to Jamicic (2002), stylolitic structures are oriented at an angle and parallel relative to the bedding, have been formed under tectonic processes and during sediment compaction processes. Therefore, the stylolitic structure of this unit (Fig. 4.13) could be formed during sediment compaction process, because the stylolitic structure is parallel to the lamination structure.

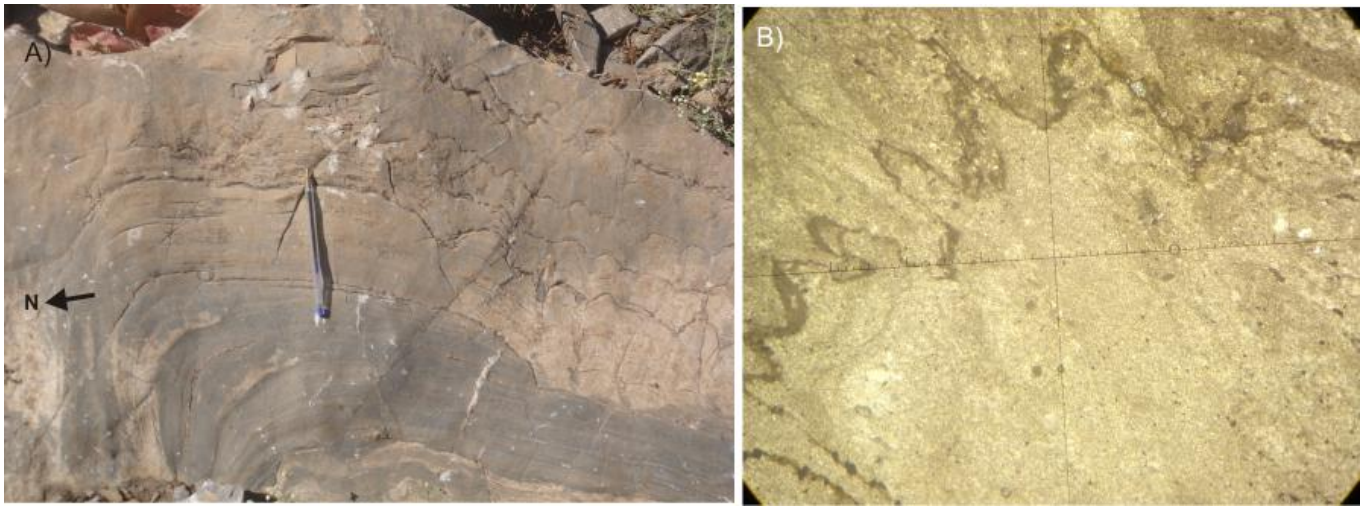

Figure 4.13. Outcrop photo and microscopic photo of stylolitic structure in lower metalimestone. A) Stylolitic structures in the outcrop of lower metalimestone units (Location: 0496483 E: 1553011 N). B) Microscopic photo of the microstylolitic structure in the metalimestone unit. Sample#T1-1 with 40x magnification, location (0496483 E: 1553011N).

4.3.3. Brittle-ductile and brittle structures

The brittle-ductile and brittle structures are formed due to the D2 phase of deformation and D3 phase of deformation. These structures are fault, vein, and joint as D3 deformations, whereas en echelon vein is as D2 deformation.

4.3.3.1. Fault

Some of the faults occurred in the study area are normal and thrust faults. These faults are found in the southwestern and the central part of the study area. These late brittle faults are crosscut the preexisting structural elements; therefore they are generalized under this phase of deformations. Lineaments are exposed, but undifferentiated linear features that show NE-SW trending and identified from the satellite image of the area (Fig. 4.1).

4.3.3.2. Joint

Joints are common brittle structural features which are identified in all the lithological units of the study area (Fig. 4.14). There is one major set of joint trend in NW-SE direction in the rocks of the area. This is followed by approximately E-W trending minor joints. In all rock units the joints are mostly sub vertical to vertical and cut the lithologies.

Figure 4.14.Systematic joint sets crosscutting the compacted metatuff units (0495770 E: 1553076 N).

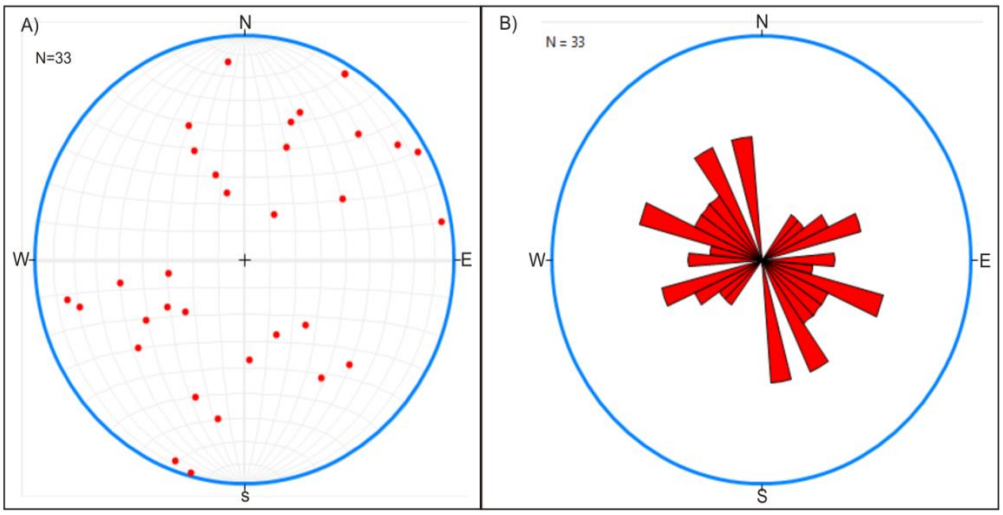

Figure 4.15.The joint data are plotted as: A). Poles of the joint is occurring on the NE and SW quadrant. B).The rose diagram represent the strike direction of the joint is S 25^0- 45^0E.

4.3.3.3. Vein

In the study area, two types of veins (quartz and calcite veins/vein lets) were recognized. The calcite vein has an estimated thickness ranging from 1mm-10cm and light grey to whitish color(Fig.4.17), whereas quartz vein occur as a large and a thin stringers (vein lets and <1cm) and larger than 10 meters associated with fractures (joints) and mostly crosscut the regional trend of foliation. These structures are formed by brittle deformation (4.17B). However, there is en echelon array of calcite vein which is

formed due to brittle deformation (which forms fractures) and also ductile deformation which rotate the mineral filled fractures. This structure is occurred mostly in the metalimestone lithological units (Fig. 4.17). It shows dextral and sinistral sense of movement (Fig.4.17 A and C).In addition to, microveins of quartz, epidote and calcite were identified in most of the lithiological units under thin section, but dominantly occurred in the metavolcanoclastic and metalimestone rocks. Most of these microveins show crosscutting relationship, but the quartz microvein shows en echelon array in the metavolcanoclastic rock in thin section parts.

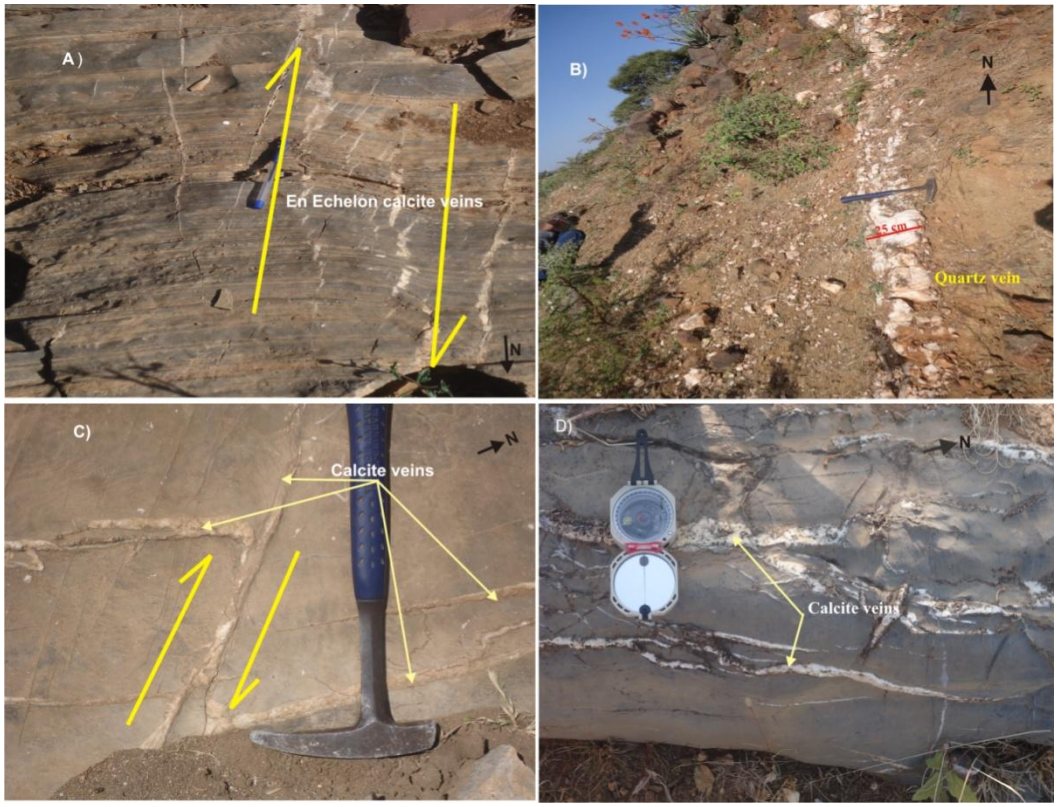

Figure 4.16.Outcrop photo of veins in different lithological units. A) Dextral en echelon type of calcite vein in the lower metalimestone lithological rock units, they are parallel five sets of en echelon type of calcite veins (0496355 E: 1553072 N). B) Discordant large size quartz vein crosscutting at an angle to the basic metavolcanic units (0495792 E: 1553472 N). C) This calcite vein shows shear displacement (dextral reverse displacement) in the upper metalimestone lithological units (0494318 E: 1550624 N). D) Shows irregular arrangement of calcite veins in the upper metalimestone rock units (0496856 E: 1549413 N).

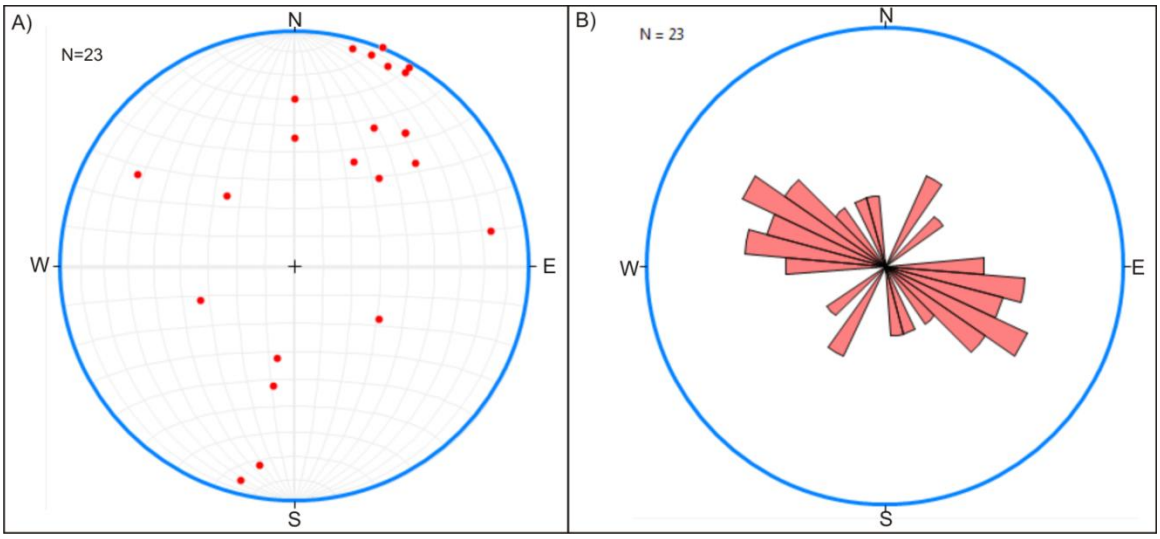

Figure 4.17.The vein data is plotted as: A) Poles of the veins occur mostly on the NE and SW quadrant. B) The rose diagram represents the strike direction of the veins.

4.3.3.4. Acidic dike

The dykes are found within the intermediate metavolcanoclasts unit. The width of the dyke varies from centimeters to over a meter with strike direction of 190^0(SW), having light reddish to light grey color, massive and fine grained.

Figure 4.18.This dike developed in the intermediate metavolcanoclastic rocks, trends NE-SW direction (0494518 E: 1553160 N).

4.4. The time relationship between metamorphism and deformation

The time relationship between metamorphism and deformation events can be determined by using the microstructures that are observed in the petrographic part. The lithological units of the area show two types of structures. These are S0 (primary lamination) and S1 (slaty cleavages) foliations. The S1 foliation is formed during the D1 deformational event and due to preferred alignment of the M1 phase of minerals such as muscovite, chlorite, biotite, sericite, epidote, calcite, plagioclase, actinolite and recrystallized quartz minerals mostly in the metavolcani/clastic and slate units. In the slate unit thin sections, the foliation is less deflected by the porphyroclast mineral (Fig.3.19). Therefore, the porphyroclast relative to the S1 foliation is pre-tectonic. The D2 deformation is form small scale minor folds with sub-horizontal to sub vertical fold axis in the rocks of the area.

CHAPTER FIVE

5. Geochemistry of the metavolcanic rock

5.1. Introduction

Ten samples of metavolcanic rocks were prepared for whole rock geochemical analysis to determine the concentration of elements. Analysis was made to evaluate and determine magma characteristics in terms of composition and paleo-tectonic setting. More care has been taken during sample selection to obtain least deformed and least altered samples.

5.2 Analytical Methods

The samples were first dried in a dry oven and then spilt into different sizes, then crushed and milled to very small sizes. Later they were homogenized, split and pulverized to minus 200 mesh size, which resulted in 100 gram representative powder these all procedures were conducted Nifas Slik, wereda 09 milling room in the Addis Ababa city. The samples were packed in a plastic bag and submitted to Australia laboratory Science (ALS) for whole rock geochemical analysis of major, trace and rare elements. The techniques used for elements were carried by inductively coupled plasma-atomic emission spectroscopy (ICP-AES) and inductively coupled plasma mass spectrometry (ICP-MS) techniques. The major element and LOI (loss on ignition) were analyzed by multi element Inductive coupled Plasma 06, whereas the trace and rare elements were analyzed by multi element Mass Spectrometry 81 in Ireland by Australian Laboratory Science. The website www.alsglobal.com gives more information about ME-ICP06 and ME-MS81 analytical methods based on their precision, analytical procedure, accuracy and detection limits.

According to Rollinson (1993), LOI is the total volatile content of the rock obtained after igniting it with a temperature of 1000^0C.The geochemical analysis of different basement rocks of Tahtai Logomti area is important for understanding tectonic setting and petrogenetic evolution. These things are interpreted by using geochemical properties of the elements.

Table5.1. Geochemical data of major elements (wt%), trace and rare earth elements (ppm) of the metavolcanic rock samples from the Tahtai Logomti area.

	Basic metavolcani/clast			Intermediate metavolcanic clast					Acidic metavolcani /clast	
Sample	T2-12	T3-19	T5-34	T4-27	T4-28	T4-29	T4-32	T5-37	T5-36	T4-31
SiO_2	50.5	41.2	47.4	58.7	51.9	60.4	48.8	62.2	71.7	66.9
Al_2O_3	17.75	13.05	13.6	16.5	16.85	15.35	17.3	14.5	15.25	12.2
Fe_2O_3	7.73	9.6	10.45	5.72	10.4	8.76	10.7	6.42	3.04	4.85
CaO	3.68	10.95	10.45	9.89	8.31	2.9	8.6	2.99	0.93	10.65
MgO	3.9	7.96	9.38	1.54	4.18	2.76	5.3	1.72	0.57	1.29
Na_2O	5.05	0.75	2.72	3.25	2.84	5.93	3.77	5.89	5.41	0.16
K_2O	3.94	1.17	1.09	0.23	0.32	0.7	0.33	0.87	1.6	0.15
Cr_2O_3	0.01	0.04	0.08	0.01	0.01	<0.01	0.01	<0.01	<0.01	0.01
TiO_2	1.17	0.73	0.84	0.56	0.78	0.88	0.96	0.92	0.72	0.28
MnO	0.2	0.17	0.18	0.11	0.2	0.18	0.18	0.15	0.05	0.08
P_2O_5	0.58	0.14	0.19	0.18	0.23	0.24	0.23	0.31	0.19	0.09
SrO	0.05	0.04	0.03	0.03	0.05	0.03	0.05	0.04	0.03	0.13
BaO	0.1	0.05	0.04	0.01	0.02	0.02	0.04	0.06	0.06	0.01
LOI	4.49	13	3.27	3.03	3.26	2.39	3.43	4.6	2.11	2.92
Total	99.15	98.85	99.72	99.76	99.35	100.54	99.7	100.6	101.66	99.72
Sc	8	34	43	19	23	24	28	17	8	9
V	6	270	308	161	224	217	277	121	70	134
Cr	80	250	470	40	40	30	80	20	20	50
Co	18	42	42	13	25	18	31	12	6	9
Ni	6	79	86	9	7	4	27	2	2	9
Cu	180	89	49	37	70	112	96	34	15	7
Zn	111	78	77	54	109	99	94	102	58	36
Ga	17.5	11.9	14.9	14.9	17.2	14.6	16.7	13.7	13	16.9
As	<5	99	<5	<5	8	7	<5	10	8	<5
Rb	45.4	21.1	12.8	4.5	6.5	7.5	4	17.8	28.9	2.7
Sr	370	376	176.5	220	424	222	434	334	230	1020
Y	25.2	14.1	15.3	14.4	14.3	18.9	18.5	25.5	23.2	7.4
Zr	163	27	36	39	56	79	60	130	175	35
Nb	7.7	1	2.2	1.6	1.8	3	2.7	4.4	6	1.3
Mo	1	1	1	<1	1	1	<1	1	1	<1
Cd	<0.5	<0.5	<0.5	<0.5	<0.5	<0.5	<0.5	<0.5	<0.5	<0.5
Cs	0.18	1.43	0.48	0.23	0.27	0.14	0.21	0.3	0.44	0.16

Ba	863	419	381	97.4	157	206	357	514	536	49.2
La	25.5	4.8	5.6	5.9	8	11.4	8.5	15.1	20.3	3.8
Hf	3.9	0.8	1.1	0.9	1.3	2	1.6	3.6	4.8	1
Ta	0.4	<0.1	0.1	0.1	0.1	0.1	0.1	0.2	0.4	0.1
W	<1	1	1	<1	<1	<1	1	1	1	<1
Sn	1	1	<1	<1	1	1	1	1	1	<1
Pb	7	5	3	<2	7	5	<2	6	8	4
Ce	58.6	11.1	13.5	12.6	17	24.2	19.5	32.8	37.8	8.4
Pr	7.1	1.67	1.81	1.75	2.25	3.01	2.58	4.15	4.67	1.07
Nd	34.1	9	9.9	8.9	10.5	14	13.2	20.7	21.7	5.3
Sm	7.23	2.62	2.48	1.98	2.76	3.52	3.38	4.7	4.61	1.68
Eu	1.85	0.89	0.95	0.9	0.94	1.14	1.06	1.26	1.27	0.47
Gd	5.26	2.49	2.27	2.11	2.57	3.12	3.67	4.15	3.97	1.31
Tb	0.82	0.44	0.42	0.35	0.47	0.51	0.57	0.71	0.7	0.22
Dy	4.86	2.63	2.57	2.58	2.57	2.57	2.57	2.57	2.57	2.57
Ho	1	0.57	0.54	0.55	0.58	0.68	0.71	0.82	0.81	0.29
Er	2.63	1.41	1.73	1.5	1.62	1.93	2	2.61	1.98	0.775
Tm	0.35	0.23	0.26	0.18	0.21	0.32	0.28	0.45	0.33	0.1
Yb	2.64	1.51	1.41	1.49	1.4	2.07	2.09	2.91	2.53	0.87
Lu	0.36	0.24	0.2	0.25	0.22	0.3	0.29	0.47	0.43	0.11
Th	3.34	0.53	0.56	0.59	0.84	1.69	0.97	2.2	4.99	0.38
U	1.3	0.22	0.26	0.33	0.42	0.7	0.45	0.84	1.86	0.17
Y/Nb	3.27	14.1	6.95	9	7.95	6.3	6.85	5.79	3.87	5.69

The analyzed geochemical data (Table 5.1) is interpreted using integrated different software packages such as Microsoft office excels 2007, GCDKit 3.00 version, Petrograph version 2beta, and Corel draw 4.5 version. The GCDKit 3.00 version and Petrograph version 2beta software packages are used to produce different geochemical variation diagrams, whereas Corel draw 4.5 version is used to increase the resolution of the different variation diagrams.

5.2. Rock geochemistry

5.2.1. Major element characteristics

The metavolcanic rocks of the Tahtai Logomti area are subjected to extensive degree of deformations which are parts of lower greenschist facies metamorphism. According to Tadesse et al. (1999) and Alene et al. (2000), major elements data are important for rock classification, but less for understanding of petrogenesis evolution because they are less resistant to weathering, metamorphism and hydrothermal activities. The major elements consist Mg, Ca, Fe, Al, Na, K, Mn, Ti and P as oxides.

These major oxides are listed (Table5.1) with volatiles. Then, before using, they are normalized to get volatile free oxides by using the following formulas.

T_{ML}-LOI = T_M T_{ML}= Total value of major oxides with LOI

T_M= Total value of major oxides without LOI

M/T_M x100 = M_F M_F= Volatile free major oxides

M = Major oxides

The selected major elements free from volatile and trace elements are plotted against SiO_2 on the Harker variation diagrams (Fig. 5.1). The major element compositions of the volatile free and with volatile rock sample show a wide variation (Table5.1). The volatile free rock samples show a range of concentrations SiO_2(48-72.02wt%), Al_2O_3(12.6-18.75wt%), Fe_2O_3(3.05-11.18wt%),CaO(0.93-12.75wt%), MgO(0.57-9.27 wt%),Na_2O(0.17-6.13wt%), K_2O(0.16-4.16wt%) and TiO_2(0.3-1.24 wt%) respectively. The major oxides (MgO, Fe_2O_3, CaO, TiO_2 and Al_2O_3) are negatively correlated with increasing SiO_2 contents (Fig.5.1). This correlation suggests that olivine, pyroxene, Fe-Ti oxides and Ca-rich plagioclase minerals were fractionating phases during evolution of magma (Alene et al., 2000). But K_2O and Na_2O oxides show a scattered pattern in some parts with increasing silica contents because of their mobility behavior during hydrothermal activity (Fig.5.1f and g). The values of CaO and Na_2O are high in some samples (e.g. T3-19, T5-34,T4-29, T5-37) that could be due to the presence of epidote as secondary mineral and diffuse albitization of plagioclase in the rocks (Alene et al., 2000). The analyzed samples (e.g.T3-19, T4-28, T4-32 and T5-34) show high iron oxide contents of Fe_2O_3 (3.04-10.7wt %) in most samples indicates that the abundance of pyroxene, olivine and secondary opaque minerals (Deer et al., 1996). The analyzed samples also show high Al_2O_3 contents (12.2-17.75wt %) values. These rocks are similar to those of calc-alkaline series rocks (Lissan and Bakheit, 2010).TiO_2 values are mostly low except one sample (T2-12 shows 1.17wt %), therefore they are in the range accepted in calc-alkaline lavas (Irvine and Baragar, 1971; Pearce and Cann, 1973; Lissan and Bakheit, 2010).

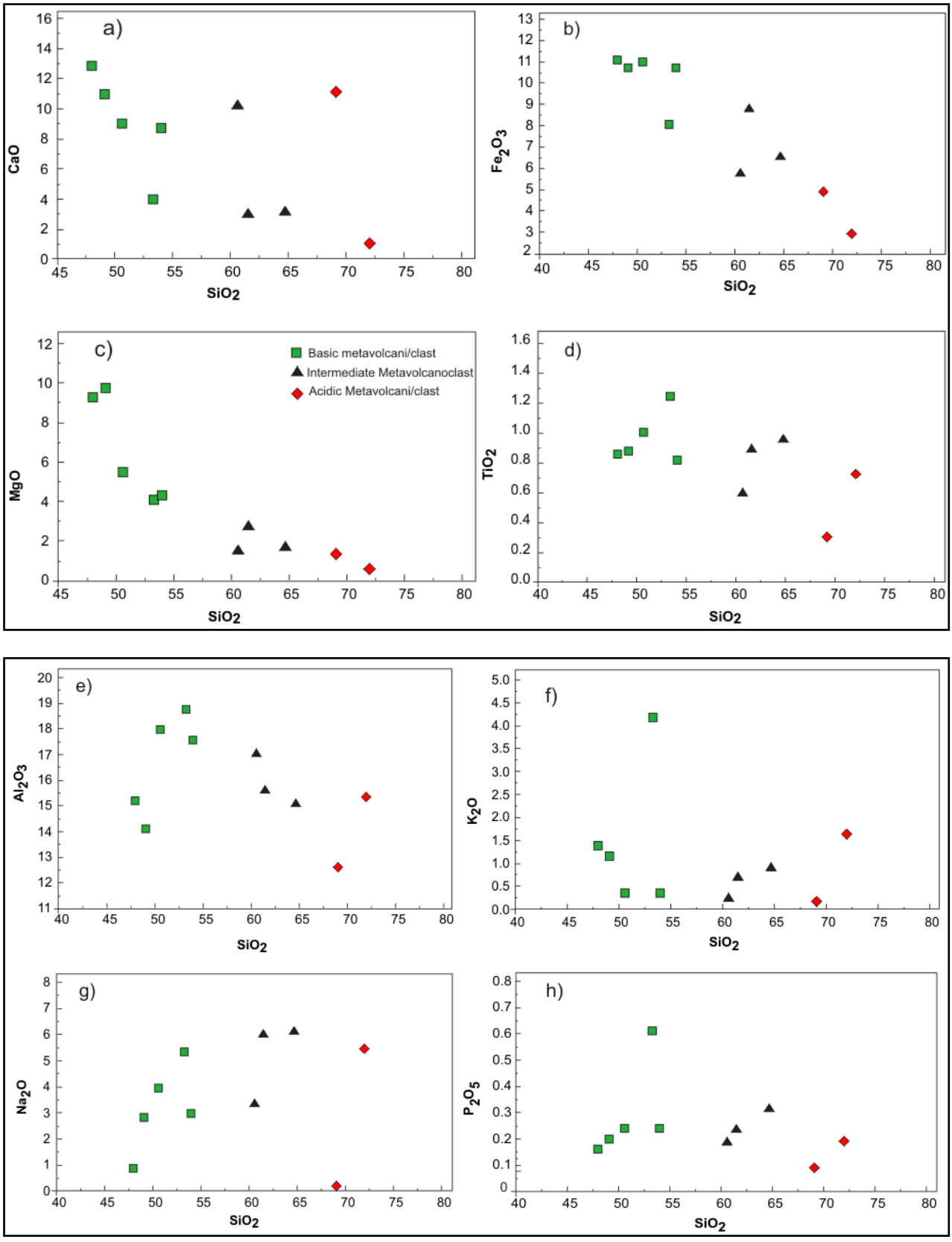

Figure 5.1. Harker variation diagrams showing the variety of major elements (wt%) with respect to SiO_2 for the metavolcanic rocks of the Tahtai Logomti area. The major oxides are volatile free base.

Generally, the analyzed rock samples of the Tahtai Logomti area show a wide variation of MgO contents (0.57-9.38 wt%), Ni (2-89 ppm), Cr (20-470 ppm) and Co (6-42 ppm) in the samples (Table5.1). According to Wilson (1989), primary magma is composed of high MgO (>6 wt%), Cr (500-600ppm) and Ni (250-300 ppm) contents. This indicates that, the metavolcanic rocks were derived from highly differentiated magma sources.

Based on the total alkalis versus silica (TAS) diagram the rocks of the study area plotted in a field of basalt, basalticandesite, andesite, dacite and rhyolite and they are sub-alkaline series (Le Bas et al., 1986, Fig.5.2).

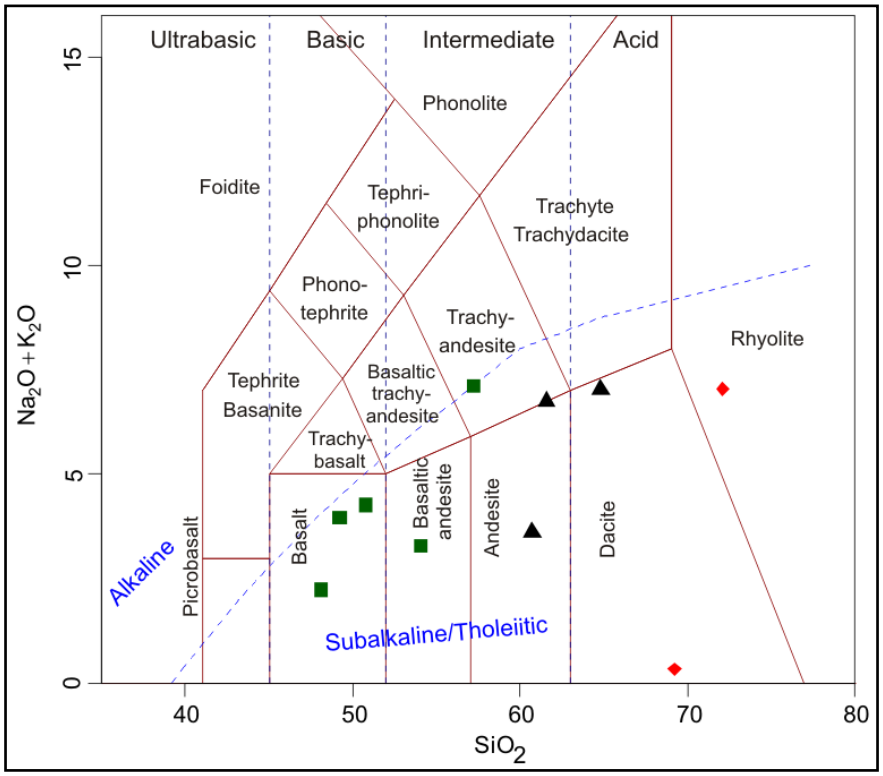

Figure 5.2.Chemical classification and nomenclature of the Tahtai Logomti area rocks using the total alkalis versus silica (TAS) diagram of Le Bas et al. (1986) (Key to symbols is the same as in Fig 5.1).

5.2.2. Trace and rare earth elements characteristics

The selected trace elements (Zr, Ba, Rb, Nb, Ni, Sr, Y and Sc) are plotted against silica in the Harker variation diagrams (Fig.5.3). From these elements, the Ni and Sc show decreasing trend with increasing silica contents because of the partitioning of olivine and pyroxene minerals (Fig.5.3e and c), whereas the other elements (Zr, Y and Nb) are slightly increasing with increasing silica content (Fig.5.3),

indicates that these elements are more resistances to metamorphism and alteration processes, since they are immobile elements (HFSE).Most of the mobile elements such as Ba, Rb and Sr show a wider scatter pattern.

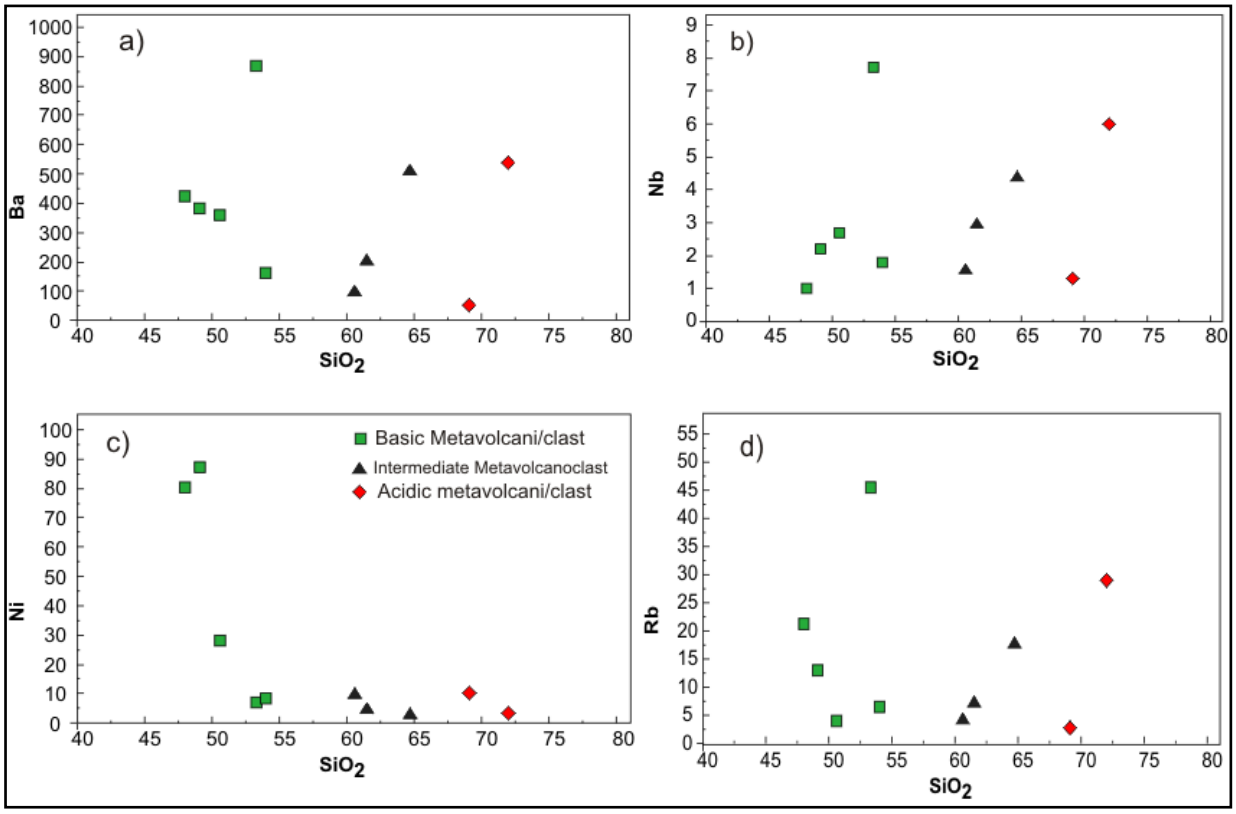

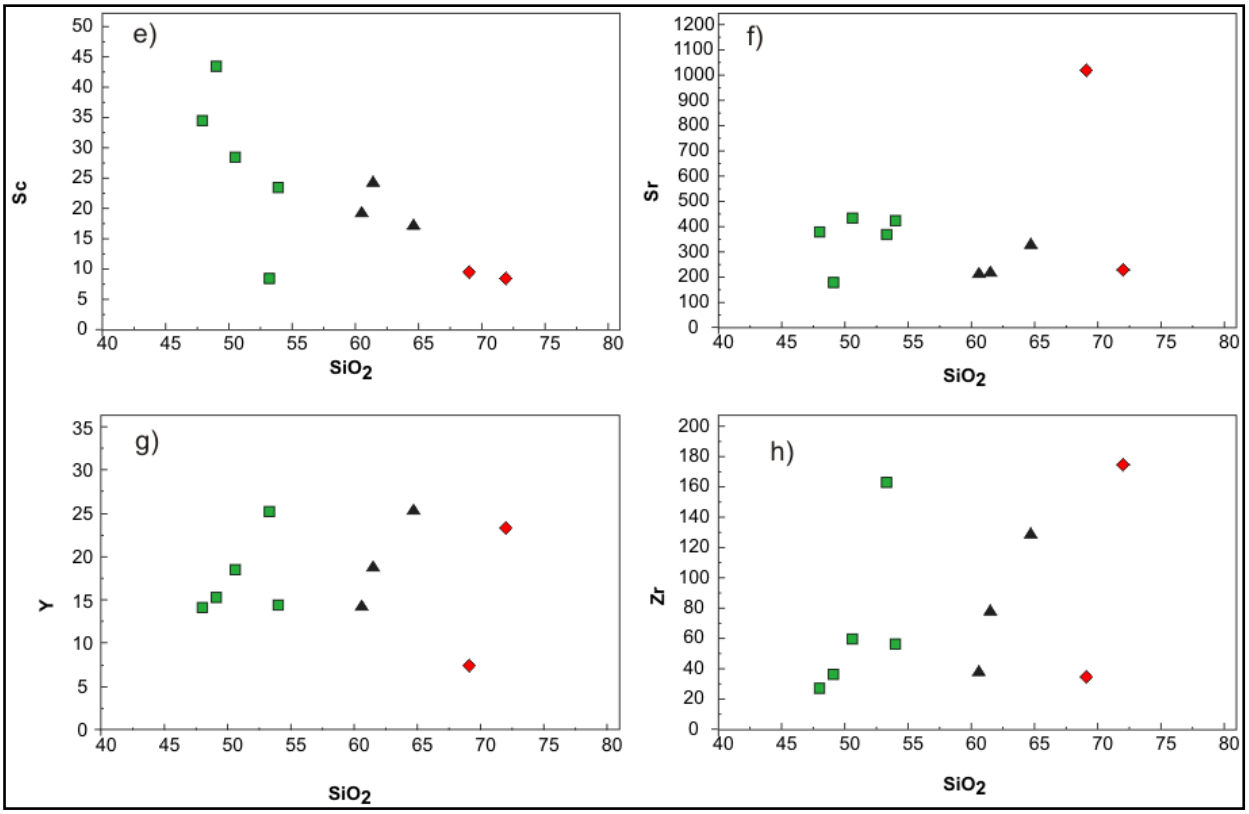

Figure 5.3. Harker variation diagrams of the selected trace elements (ppm) against SiO_2 (wt% and free from volatiles base) for the metavolcanic rocks of the Tahtai Logomti area.

The diagrams plotted for the selected trace elements (Zr, Rb, Nb, Ni, Sr, Y, and Sc elements) against Zr element, in order to evaluate their behavior and establish their relative mobility (Green, 1980). The Ni and Sc elements show decreasing trends with increasing Zr because of the fractionation of olivine and pyroxene minerals, whereas Nb, Y, Th, Ce, La and U elements concentration increased with increasing Zr, and were probably high resistance during metamorphism and alteration processes and indicates that the rocks have a common source(Fig.5.4). The LILE elements (Rb and Sr) show wide scatter that can also be linked with later mobility (Cann, 1970). All the metavolcanic rock samples of the Tahtai Logomti area show the ratio of Y/Nb>3(Table5.1), typical of tholeiitic and calc-alkaline basalt (Gracia, 1978).

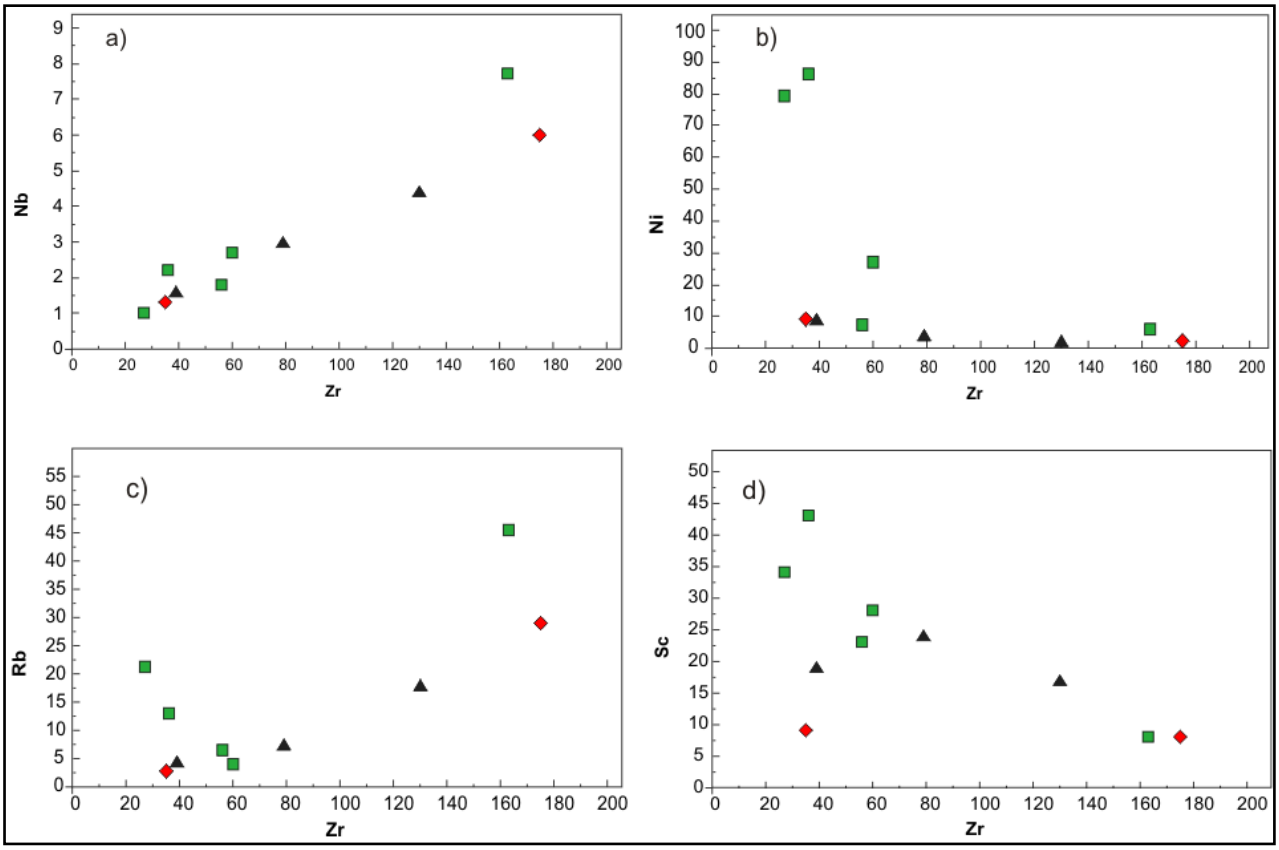
a)
Nb
Zr
b)
Ni
Zr
c)
Rb
Zr
d)
Sc
Zr

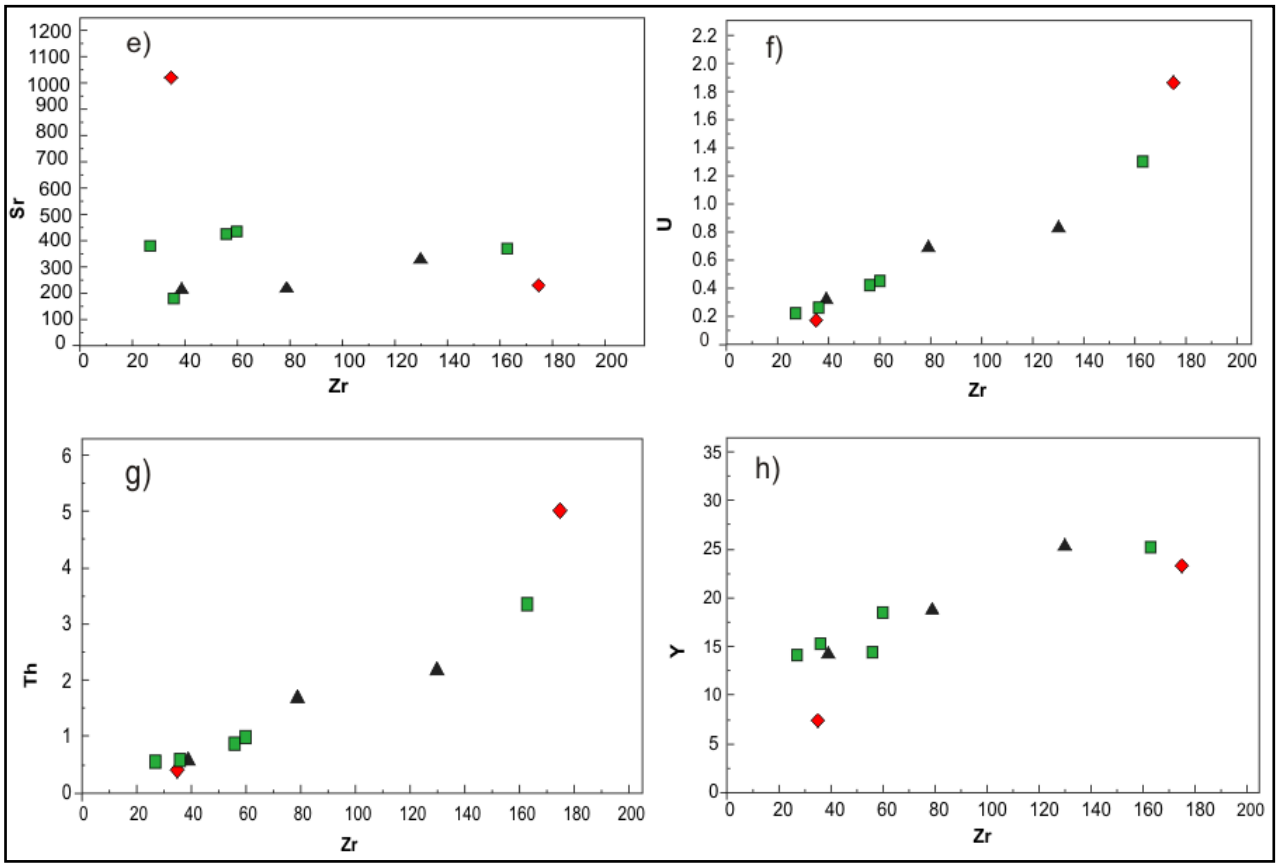
e)
Sr
Zr
f)
U
Zr
g)
Th
Zr
h)
Y
Zr

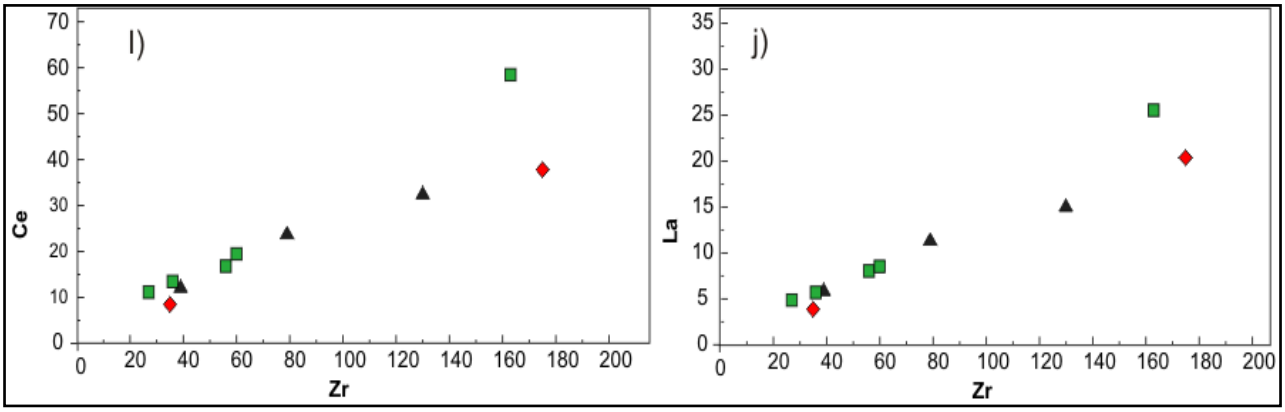

Figure 5.4. Zr variation diagram for various trace elements (ppm) of the Tahtai Logomti metavolcanics (Key to symbols is the same as in Fig 5.1 and 5.3).

In the Chondrite-normalized REE patterns (Fig.5.5A), all the rock samples display slight enrichment in light rare earth elements (LREE) than the heavy rare earth elements (HREE). The parallel REE patterns of all the samples suggest that they are derived from a common source. All the samples do not show any Eu anomaly in the diagram, indicating the absence of feldspar fractionation and the flat HREE pattern is also indicating the samples are free from garnet source. The multi-element spider diagram (Fig.5.5B), normalized to primitive mantle values, the trace elements data show enrichment in some incompatible elements such as Ba, U, Pb, K and Sr and negative anomalies in Rb, Th, Ta, Nb, Pr and Ti. The trough of Nb and Ta relative to the adjacent LILE elements indicates that subduction related magmatic eruption.

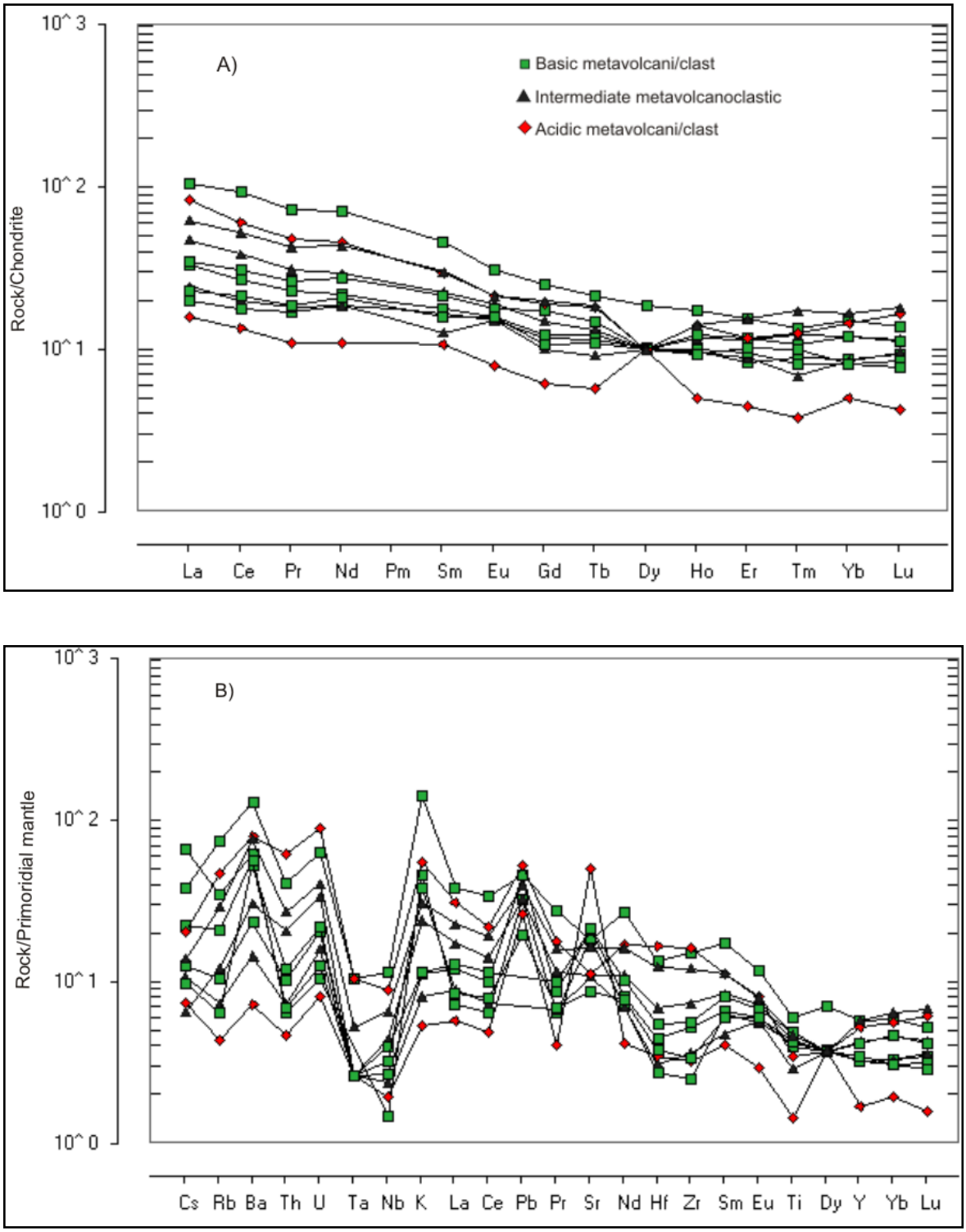

Figure 5.5. A) Chondrite normalized REE patterns of the metavolcanic rocks from the study area, Chondrite normalization values are from Sun and McDonough (1989). B) Primitive mantle normalized multi element diagram of the bulk rock samples from the Tahtai Logomti area, (Mc Donough and Sun, 1995).

5.2.3. Paleotectonic setting of the metavolcanic rocks

The tectonic setting of these metavolcanic rock samples of the area is determined by using the discrimination diagrams of the immobile elements such as Zr, Nb, Ti Y, La, Hf, Ta, and Yb (Pearce and Cann, 1973; Winchester and Floyd, 1975; Wood, 1980).The Ti-Zr-Y ternary diagram (Fig.5.6A) of Pearce and Cann (1973) can be used to discriminate the different types of basalt. The Tahtai Logomti rock samples data plot in the mid-ocean ridge basalt (MORB), calc alkaline basalts (CAB) and some fall in island-arc tholeiites (IAT) field. Most of the basic metavolcanics plot in the MORB and IAT, whereas the intermediate and the acidic metavolcanic rocks plot in the field of calc-alkaline basalt, and there is no sample plot in the within plate basalt field. On the Nb-Zr-Y discrimination diagram (after Meschede, 1986), the metavolcanic rocks plot in both the volcanic-arc basalt and the N-MORB fields (Fig. 5.6B). However, the Th-Hf-Ta diagram (after wood, 1980) (Fig.5.6C) shows that all the samples of the metavolcanics lie on the volcanic-arc basalt field. The Th, Hf and Ta elements are immobile during metamorphism conditions. Those volcanic arc basalt are distributed below the line represented by Hf/Th=3, indicating calc-alkaline magma types.

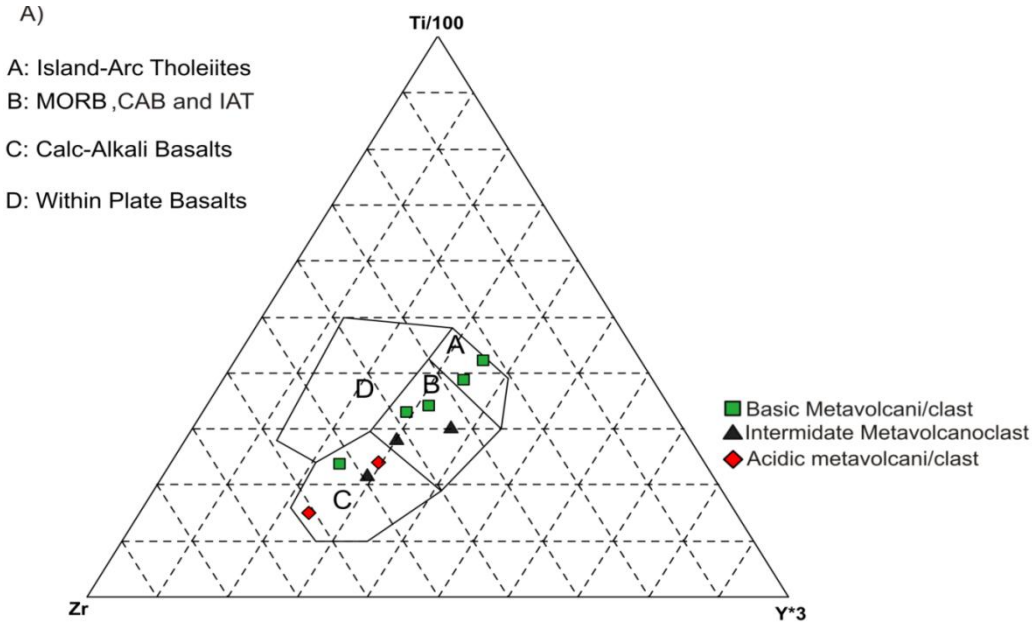

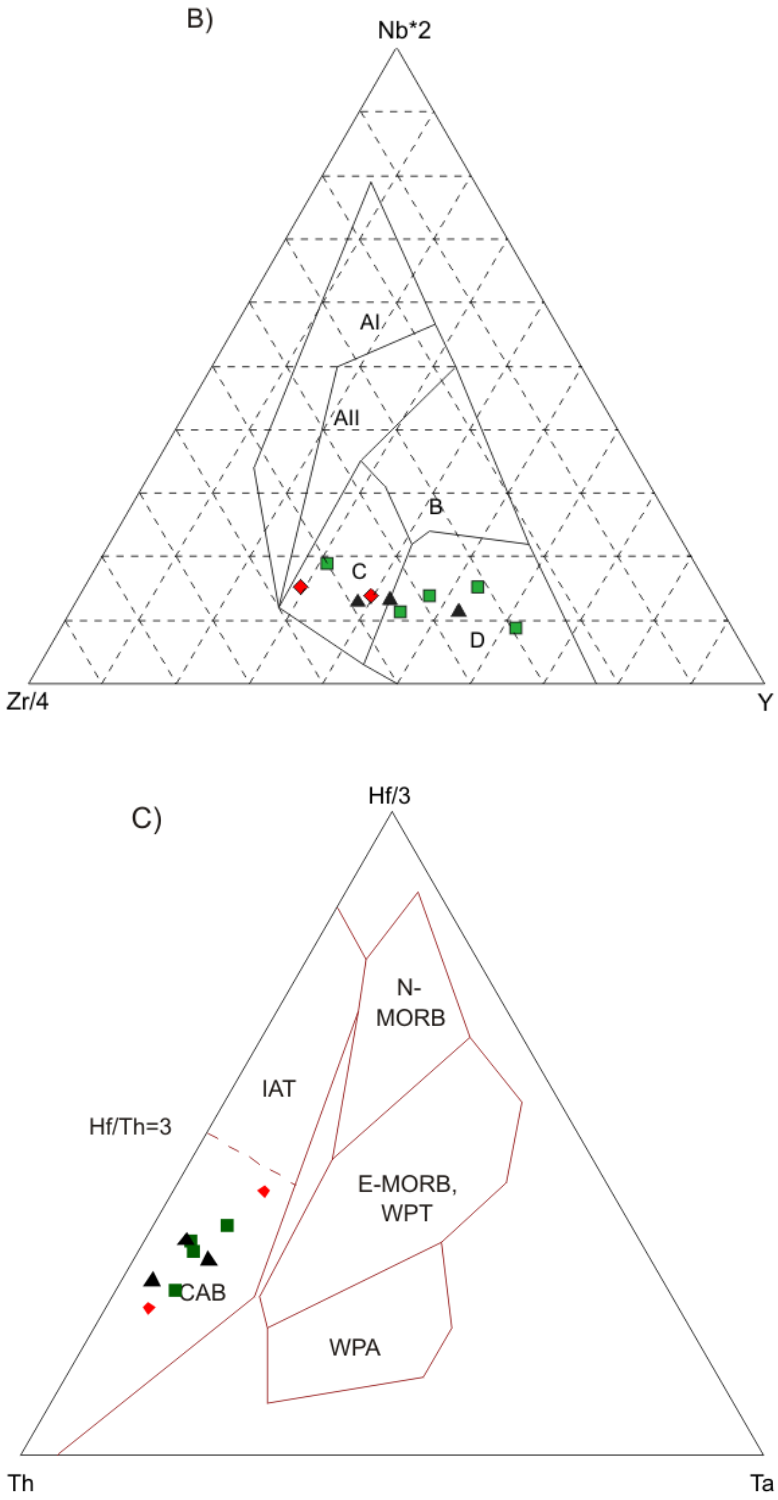

Figure 5.6.Tectonic discrimination diagrams of the Tahtai Logomti metavolcanic rocks. A) Ti-Zr-Y ternary diagram after Pearce and Cann(1973), B) Zr-Nb-Y ternary diagram after Meschede(1986) with the fields (AI: within-plate alkali basalt; AII: within plate tholeiite; B: E-MORB; C and D: volcanic-arc basalt and D: N-MORB), and C) Th-Hf-Ta ternary diagram after Wood (1980). Abbreviation for all plots: MORB= mid-ocean ridge basalt, IAT=island-arc tholeiite, CAB=Calc-alkaline basalt, WPA= within plate alkali basalt, WPT= within plate tholeiite.

Because of the small number of samples analyzed in this study, the discrimination of the tectonic setting may be considered as less conclusive. Broadly, however, the present geochemical data is consistent with the previous results of Tadesse et al. (1999), Alene et al. (2000) and Sifeta et al. (2005) that the Tsaliet metavolcanic rocks of the northern Ethiopia are parts of volcanic-arc basalt having calc-alkaline to tholeiitic affinity.

CHAPTER SIX

6. Conclusion and recommendations

6.1. Conclusion

Depending on the field observation, petrographic interpretation and combined with geochemical data interpretation in the present study the following conclusion has been obtained about the area. Based on the mineral assemblages such as chlorite, actinolite, epidote, muscovite/sericite and albite, the presences of relict igneous texture (porphyritic texture due to the phenocryst of plagioclase and augite minerals) and the preserved primary structures (e.g. cross bedding, bedding, lamination and slump), the rocks of the Tahtai Logomti area and its surrounding area are affected by low grade of metamorphism and belonging to lower greenschist facies metamorphism.

The lithological units of the Tahtai Logomti area have been affected by three phases of deformation such as D1, D2 and D3 deformations. The relationship between metamorphism and deformation is interpreted from mineral assemblages and micro-structural features. The first phase of deformation (D1) is produced by the pencil structure (L1) and regional foliation which is S1 mostly occurred in all lithological units, NE striking and associated with the M1 metamorphic event. The minerals developed during M1event are chlorite, epidote, actinolite, plagioclase (albite), muscovite/sericite, calcite and recrystallized quartz minerals. The second phase of deformation (D2) is produced by the kink band folds, low plunging folds and en echelon array veins, whereas the later phase of deformation D3occurred because of the formation of joints and faults structures.

The geochemical characteristics of the Tahtai Logomti metavolcanic rocks show calc-alkaline magma affinity and they were formed in volcanic arc tectonic setting.

6.2. Recommendation

From the obtained results and conclusion made by this study the following recommendations can be forwarded:

- ✓ Geochemical data with more samples is required in order to have a better understanding in terms of petrogenesis and tectonic evolution of the rocks.
- ✓ Isotope data is recommended to determine the age and to reconstruct the stratigraphic sequence of the metavolcanic rocks.
- ✓ Geothermobarometry study is also required to determine the pressure and temperature conditions of these metamorphic rocks by using microprobe analysis.

Reference

Abdelsalam, M.G. and Stern, R.J. (1996). Sutures and shear zones in the Arabian-Nubian Shield. *Journal of African Earth Sciences*, 23: 289-310.

Alemu, T. (1998). Geochemistry of Neoproterozoic granitoids from the Axum area, northern Ethiopia. *Journal of African Earth Science*, 27:437-460 pp.

Alene, M. (1998). Tectonomagmatic evolution of the Neoproterozoic rocks of the Mai Kenetal-Negash area, Tigrai, northern Ethiopia. Unpublished Ph.D. Thesis, University of Turin, Italy.

Alene, M. and Sacchi, R. (2000). The Neoproterozoic low grade basement of Tigrai, northern Ethiopia. Abstracts: 18th Colloquium of African Geology, Graz. J. *Afr. Earth Sci*., 30 (4), 5-6.

Alene, M., Ruffini, R. and Sacchi, R. (2000). Geochemistry and geotectonic setting of Neoproterozoic rocks from northern Ethiopia (Arabian-Nubian Shield). *Gondwana Res*. 3: 333-347.

Alene, M., Jenkin, G.R.T., Leng, M.J. and Darbyshire, D.P.F. (2006). The Tambien Group, Ethiopia: An early Cryogenian (ca. 800-735 Ma) Neoproterozoic sequence in the Arabian-Nubian shield. *Precambrian Research*, 147: 79-99.

Allen, A. and Tadesse, G. (2003). Geological setting and tectonic subdivision of the Neoproterozoic orogenic belt of Tuludimtu, western Ethiopia. *Journal of African Earth Sciences*, 36: 329-343.

Asrat, A. (1997). Geology and geochemistry of the Negash Pluton and their metallogenic significance, Central Tigrai. Unpublished M.Sc. thesis, Addis Ababa University, Ethiopia, 159pp.

Asrat, A., Barbey, P. and Gleizes, G. (2001). The Precambrian Geology of Ethiopia: a review, *Africa Geoscience Review*. 8: 271-288.

Asrat, A., Gleizesc, G., Barbey, P., and Ayalew, D. (2003). Magma emplacement and mafic–felsic magma hybridization: structural evidence from the Pan-African Negash pluton, Northern Ethiopia. *Journal of Structural Geology*.25: 1451-1469

Asrat, A., Barbey, P., Ludden, J., Reisberg, L., Gleizes, G. and Ayalew D.(2004). Petrology and isotope geochemistry of the Pan-African Negash pluton, Northern Ethiopia: Mafic-felsic magma interactions during construction of shallow-level calc-alkaline plutons. *Journal of Petrology*, 45(6): 1147-1179.

Avigad, D., Stern, R.J., Beyth, M., Miller, N. and McWilliams, M. (2007). Detrital zircon U-Pb geochronology of Cryogenian diamictites and lower Paleozoic sandstone in Ethiopia (Tigrai): age constraints on Neoproterozoic glaciation and crustal evolution of the southern Arabian-Nubian Shield. *Precambrian Research* 154, 88-106.

Ayalew, T., Bell, K., Moore, J.M., and Parrish, R.R., (1990). U-Pb and Rb-Sr geochronology of the Western Ethiopian Shield. *Geological Society America Bulletin* 102, 1309-1316.

Ayele, B. and Gangadharan, R. (2016). Study on geological and structural characterization around Mai Kenetal, Central Tigrai in Northern Ethiopia. *International Journal of Engineering and Applied Sciences (IJEAS)*, 3:30-35.

Barker, A.J. (1998). Introduction to metamorphic textures and microstructures, 2nd ed. Stanley Thornes, United Kingdom, 263pp.

Berhe S.M. (1990). Ophiolites in northeast and east Africa: Implications for Proterozoic crustal growth. *Journal Geological Society London* 147: 41-57.

Beyth, M. (1971). The Geology and Central and Western Tigrai. Min. Mines, Addis Ababa, unpublished report.

Beyth, M. (1972). The Geology of the Central and Western Tigre. Unpublished PhD Thesis, University of Bonn, Germany, 155pp.

Beyth, M., Avigad, D., Wetzel, H.U., Mattews, A. and Seife, M.B. (2003). Crustal exhumation and indications for Snowball Earth in the East African Orogen: north Ethiopia and east Eritrea. *Precambrian Research*, 123: 187-201pp.

Cann, J. R. (1970). Rb, Sr, Y, Zr, Nb in some ocean-floor basaltic rocks. *Earth Planet Sci. Lett.*, *10*, 7-11.

Collins, A.S. (2006).Madagascar and the amalgamation of Central Gondwana. *Gondwana Research*, 9: 3-16.

Cox, G.M., Lewis, C.J., Collins, A.S., Halverson, G.P., Jourdan, F., Foden, J., Nettle, D., Kattan, F. (2012). Ediacaran terrane accretion within the Arabian-Nubian Shield. *Gondwana Res*. 21: 341-352.

Deer, W.A., R.A. Howie and J. Zussman, (1996). An Introduction to the Rock-Forming Minerals. Pearson. Prentice Hall, Harlow.

DeWit, M.J. and Chewaka, S. (1981). Plate tectonic evolution of Ethiopia and origin of its mineral deposits: An overview In Chewaka, S., de Wit, M.J. (Eds.), Plate Tectonics and Metallogenesis: Some Guidelines to Ethiopian Mineral Deposits. *Ethiopian Institute of Geological Surveys, Bulletin* 2:115-129 pp.

Fritz, H., Tenczer, V., Wallbrecher, C.A., Hauzenberger, E., Hoinkes, G., Muhongo, S., Mogessie, A. (2005). Central Tanzanian tectonic map: a step forward to decipher Proterozoic structural events in the East African Orogen. Tectonics 24, TC 6013.

Fritz, H., Abdelsalam, M., Ali, K.A., Bingen, B., Collins, A.S., Fowler, A.R., Ghebreab, W., Hauzenberger, C.A., Johnson, P.R., Kusky, T.M., Macey, P., Muhongo, S., Stern, R.J. and Viola, G. (2013). Orogen styles in the East African Orogen: A review of the Neoproterozoic to Cambrian tectonic evolution. *Journal of African Earth Sciences*, 86:65-106. 78

Garcia, M. O., (1978). Criteria for identification of ancient volcanic arc. *Earth and Planetary Science Letters*.14: 147-165.

Garland, C.R. (1980). Geology of the Adigrat Area. Ministry of Mines, Addis Ababa Memoir No.1, 51 pp.

Gebresilassie, S. (2009). Nature and characteristics of Metasedimentary rock hosted gold and base metals mineralization in Werkamba area, central Tigrai, northern Ethiopia‖ PhD thesis, Ludwing-Maximilian University, Munich, Germany, 134pp.

Gerra, S. (2000). A short introduction to the geology of Ethiopia. *Chron. Rech. Min.*, 540: 3-10.

Green, T.H. (1980) Island arc and continent-building magmatism - A review of petrogenic models based on experimental petrology and geochemistry. In: Banks, M.R. and Green, D.H. (Eds.), Orthodoxy and creativity at the Frontiers of Earth Sciences (Carey Symposium). *Tectonophys.*, v. 63, pp. 367-385.

Irvine, T. N. and Barager, W. R. A. (1971). A guide to the chemical classification of the common volcanic rocks. *Canadian Journal of Earth Science*, 8: 523-548.

Jacobs, J., Fanning, C.M., Henjes-Kunst, F., Olesch, M., Paech, H.J. (1998). Continuation of the Mozambique Belt into East Antarctica: Grenvilleage metamorphism and polyphase Pan-African high-grade events in Central Dronning Maud Land. *The Journal ofGeology*, 106, 385-406.

Jamicic, D. (2002). The Relationship between Tectonic Stylolites and Fold Morphology in Limestones of the "Croatica Deposits" (Croatia).*Geologia Croatica/zagreb*, 55/1, 79-81

Johnson, P.R., Kattan, F. (2001). Oblique sinistral transpression in the Arabian Shield: the timing and kinematics of a Neoproterozoic suture zone. *Precambrian Research*, 107, 117-138.

Johnson, P.R. and Woldehaimanot, B. (2003). Development of the Arabian-Nubian Shield. Perspectives on accretion and deformation in the northern East African Orogen and the assembly of Gondwana. In. Yoshida, M., Windley, B.F., Dasgupta, S. (Eds.). Proterozoic East Gondwana, Supercontinent Assembly and Breakup. *Geological Society, London, Special Publication*, 206: 290-325.

Johnson, P.R., Andresen, A., Collins, A.S., Fowler, A.R., Fritz, H., Ghebreab, W., Kusky, T. and Stern, R.J., (2011). Late Cryogenian-Ediacaran history of the Arabian-Nubian Shield. A review of

depositional, plutonic, structural, and tectonic events in the closing stages of 65 the northern East African Orogen. *Journal of African Earth Sciences*, Volume 61, Issue 3,167-232.

Johnson, T.E., Brown, M., Kaus, B.J., VanTongeren, J.A. (2014). Delamination and recycling of Archaean crust caused by gravitational instabilities. *Nat. Geosci*. 7 (1), 47-52.

Kazmin, V. (1971). Precambrian of Ethiopia. Nature, 230: 176-177pp

Kazmin V. (1972). The geology of Ethiopia. *Ethiopian Institute of Geological Surveys.* Note No. 821.

Kazmin, V. (1973). The geological map of Ethiopia, 1:2,000,000. Geological Survey of Ethiopia, Addis Ababa. Note No. 821-051-12: 211.

Kazmin V. (1975). The Precambrian of Ethiopia and some aspects of the Geology of Mozambique Belt. *Geophysical Observatory of Addis Ababa Univ*.15, 27-43.

Kazmin V., Alemu S. and Tilahun B. (1978). The Ethiopian basement, Stratigraphy and possible manner of evolution. *Geo/. Rundschau*., 67, 531-546.

Kroner, A. (1985). Ophiolites and the evolution of tectonic boundaries in the late Proterozoic Arabian-Nubian shield of northeastern Africa and Arabia. *Precambrian Research*, 27, 277-300.

Kroner, A., Linnebacher, P., Stern, R.J., Reischmann, T., Manton, W. and Hussein, I.M. (1991). Evolution of Pan-African island arc assemblages in the southern Red Sea Hills, Sudan and in southwestern Arabia as exemplified by geochemistry and geochronology. *Precambrian Research*, 53: 99-118.

Kroner, A., Hegner, E., Collins, A.S., Windley, B.F., Brewer, T.S., Razakamanana, T. and Pidgeon, R.T., (2000). Age and magmatic history of the Antananarivo Block, central Madagascar, as derived from zircon geochronology and Nd isotopic systematic. *American Journal of Science* 300, 251-288.

Kroner, A., Stern, R.J., (2004). Africa: Pan-African orogeny. In: Selley, R., Cocks, L.R.M., Plimer, I.R. (Eds.), Encyclopedia of Geology. Elsevier, vol.1, pp. 1–12

LeBas, M.J., LeMaitre, R.W., Streckeisen, A., Zanettin, B. (1986). A chemical classification of volcanic rocks based on the total alkali-silica diagram. *Journal Petrology*, 27, 745-750.

Lissan, H.N and Bakheit, K.A. (2010). The Geology and Geochemistry of Metavolcanic Rocks from Artoli Area, Berber Province, Northern Sudan: An Implication for Petrogenetic and Tectonic Setting. *Journal of American Science,* 6(8): 1-13.

McDonough, W. F. and Sun, S. S. (1995). The composition of the earth. *Chemical Geology*, 120: 223-253.

McWilliams, MO. (1981). Palaeomagnetism and Precambrian tectonic evolution of Gondwana. *InPrecambrian Plate Tectonics.* Amsterdam: Elsevier, ed. A Kroner, pp. 649-87.

Meert, J. (2003). A synopsis of events related to the assembly of eastern Gondwana. *Tectonophysics*, Elsevier 362, 1-40.

Meschede, M. (1986). A method of discrimination between different types of mid-ocean ridge basalts and continental tholeiites with the Nb-Zr-Y diagram. *Chem. Geol*., v. 56: 207-218.

Miller, N.R., Alene, M., Sacchi, R., Stern, R.J., Conti, A., Kroner, A. and Zuppi, G. (2003). Significance of the Tambien Group (Tigrai, Northern Ethiopia) for Snowball Earth events in the Arabian-Nubian Shield. *Precambrian Research*, 121: 263-283.

Miller, N.R., Stern, R.J., Avigad, D., Beyth, M. and Schilman, B. (2009). Cryogenian slate-carbonate sequences of the Tambien Group, northern Ethiopia (I): Pre-"Sturtian" chemostratigraphy and regional correlations. *Precambrian Research*, 170: 129-156.

Miller, N., Avigad, D., Stern, R.J. and Beyth, M. (2011). The Tambien Group, Northern Ethiopia (Tigre). In: Arnaud, E. et al. (Eds.), The geological record of Neoproterozoic glaciations, Memoir, vol.36. *Geological Society, London*, pp.263-276.

Patchett, P.J., Chase, C.G., (2002). Role of transform continental margins in major crustal growth episodes. Geology 30, 39-42.

Pearce, J.A., Cann, J.R. (1973). Tectonic setting of basic volcanic rocks determined using trace element analysis. *Earth and Planetary Science Letters* 19, 290-300.

Rollinson, H. R. (1993). Using geochemical data: Evaluation, presentation, and interpretation. John Wily & Sons, New York, 352.

Shackleton, R. M. (1979). Precambrian tectonics of north east Africa. In: *Evolution and Mineralization of the Arabian-Nubian Shield* (Edited by Toheun, S. A.) 1-6.

Shackleton, R.M., (1996). The final collision zone between East and West Gondwana: where is it? *J. Afr. Earth Sci.* 23, 289-310.

Sifeta, K., Roser, B.P. and Kimura, J.I. (2005). Geochemistry, provenance, and tectonic setting of Neoproterozoic metavolcanic and metasedimentary units, Werri area, Northern Ethiopia. *Journal of African Earth Sciences*, 41: 212-234.

Stern, R.J. and Dawoud, A.S. (1991). Late Precambrian (740 Ma) charnockite, enderbite, and granite from Jebel Moya, Sudan: a link between the Mozambique Belt and Arabian-Nubian shield? Geology 99, 648-659.

Stern, R.J. (1994). Arc assembly and continental collision in the Neoproterozoic East African Orogen: implications for the consolidation of Gondwanaland. *Ann. Rev. Earth Planet. Sci.* 22: 319-351.

Stern, R.J. (2008). Neoproterozoic crustal growth: the solid earth system during a critical time of earth history. *Gondwana Res,* 14:33-50.

Stern, R.J. and Johnson, P.R. (2010). Continental lithosphere of the Arabian Plate: A geologic, petrologic, and geophysical synthesis. *Earth Science Reviews* 101, 29-67.

Stoeser, D.B. and Camp, V.E. (1985). Pan-African micro plate accretion of the Arabian-Nubian Shield (ANS). *Geol. Soc. Am. Bull*. 96:817-826.

Sun, S. and McDonough, W.F. (1989). Chemical and isotopic systematic of oceanic basalts: implications for mantle composition and processes: In Sunders, A.D., and Norry, M.J. (eds), Magmatism in ocean basins. *Geological Society Special*, 42:313-345.

Swanson-Hysell, N. L., Maloof, A. C., Condon, D. J., Jenkin, G. R., Alene, M., Tremblay, M. M., Tesema, T., Rooney, A.D. and Haileab, B., (2015). Stratigraphy and geochronology of the Tambien Group, Ethiopia: Evidence for globally synchronous carbon isotope change in the Neoproterozoic. Geology, 43(4),323-326.

Tadesse, T. (1996). The geology of Axum Sheet (ND 37-6). Geological Survey of Ethiopia; Memoir No. 9:186 pp.

Tadesse, T., 1997. The Geology of Axum area (NO 37-6). Ethiopian Institute of Geological Surveys, Addis Ababa. (Memoir No.9), 184 p.

Tadesse, T. Suzuki, K. and Hoshino, M. (1997). Chemical Th-U total Pb isochron age of zircon from the Mareb Granite in northern Ethiopia. *J. Earth Planet. Sci. Negoya Univ.* 44: 21-27.

Tadesse.T, Hoshino, M., and Sawada, Y. (1999). Geochemistry of low-grade metavolcanic rocks from the Pan African of the Axum area, northern Ethiopia. *Precambrian Research*, 99: 101-124.

Tadesse.T, Hoshino, M., Suzuki, K. and Iisumi, S. (2000). Sm-Nd, Rb-Sr, and Th-U-Pb zircon ages of syn and post-tectonic granitoids from the Axum area of northern Ethiopia. *Journal of African Earth Sciences*, 30: 313-327.

Tefera, T. (1996). Structure across a possible intra-oceanic suture zone in low-grade Pan African rocks of northern Ethiopia. *Journal of African Earth Sciences*, 23: 575-381.

Teklay, M., Kroner, A., Mezger, K., and Oberhansli, R. (1998). Geochemistry, Pb-Pb single Zircon ages and Nd-Sr isotope composition of Precambrian rocks from southern and Eastern Ethiopia: implications for crustal evolution in East Africa. *Journal of African Earth Sciences*, 26, 207-227.

Teklay, M., Kroner, A. & Metzger, K. (2001). Geochemistry, geochronology and isotope geology of Nakfa intrusive rocks, northern Eritrea: products of a tectonically thickened Neoproterozoic arc crust. Journal of African Earth Sciences, 33, 283–301

Tsige, L. and Abdelsalam, M.G. (2005). Neoproterozoic-Early Paleozoic gravitational tectonic collapse in the southern part of the Arabian-Nubian Shield: The Bulbul Belt of southern Ethiopia. *Precambrian Research,* 138: 297-318.

Vail, J.R. (1983). Pan-African crustal accretion in north-east Africa. *J. Afr. Earth Sci*., v. 1, pp. 285-294.

Vail, J.R. (1985). Pan-African (late Precambrian) tectonic terrans and the reconstruction of the Arabian-Nubian Shield. Geology, 13:839-842pp.

Wilson, M. (1989). Igneous Petrogenesis a global tectonic approach, Unwin Hyman, London, 480pp.

Winchester, J.A., Floyd, P.A., (1975). Geochemical magma type discrimination: application to altered and metamorphosed basic igneous rocks. *Earth and Planetary Science Letters* 28, 459-469.

Wood, D.A. (1980). The application of a Th-Hf-Ta diagram to problems of tectonomagmatic classification and to establishing the nature of crustal contamination of basaltic lavas of the British Tertiary volcanic province. *Earth Planet. Sci. Lett.*, 50:11-30.

Yihunie, T. and Hailu, F. (2007). Possible eastward tectonic transport and northward gravitational tectonic collapse in the Arabian -Nubian shield of western Ethiopia. *Journal of African Earth Sciences*, 49:1-11.

Appendix

Structural data

No.	Structural element	Orientation			Location	Unit
		Strike	Dip	Dip direction	Longitude: latitude	
1	S1 &S0	35	73	SE	0496098:1553049	Lower slate
2	S0	220	76	SE	0496098:1553049	Lower slate
3	S0 & S1	90	17	NE	0495770:1553076	Metatuff
4	S0	230	60	SE	0495928:1553075	Lower slate
5	S1	40	47	NW	495380: 1553101	Basic metavolcanic
6	S0	220	75	SE	0495213:1552979	Basic metavolcanic
7	S1	225	63	NW	0492832:1552863	Acidic metavolcanic
8	S1	50	78	SE	0492584:1552807	Acidic metavolcanic
9	S1	190	40	NW	0491497:1552667	Intermediate metavolcano clast
10	S0	185	60	SE	0490287:1552931	Basic metavolcano-clastic
11	S0	35	30	NW	0490779:1553142	Basic metavolcano- clastic
12	S0 & S1	45	45	SE	0492307: 1553950	Basic metavolcanic
13	S0 &S1	45	62	SE	0493917:1553373	Basic metavolcanic
14	S0	198	57	NW	0496995:1549490	Upper metalimestone
15	S0	45	32	NW	0496845:1548429	Upper meta limestone
16	S0 & S1	210	45	NW	0495868:1549474	Upper meta limestone
17	S0	225	65	NW	0496780:1548209	Upper meta limestone
18	S1	65	48	SE	0495414:1549047	Upper meta limestone
19	S0	44	39	SE	0496175:1549128	Upper meta limestone
20	S0	210	34	SE	0495280:1549778	Upper meta limestone
21	S1	60	45	SE	0496388:1553367	Lower slate
22	S0	85	21	SE	0495874:1553214	Metatuff
23	S1	45	17	NW	0495387:1552664	Metatuff
24	S1	230	35	NW	0495001:1553163	Intermediate metavolcano clastic
25	S1	75	42	SE	0496859:1552043	Upper metalimestone
26	S1	80	70	NW	0496894:1549000	Upper metalimestone
27	S1	235	72	NW	0496568:1548390	Upper metalimestone

28	S1	47	31	SE	0495010:1548480	Upper metalimestone
29	S1	77	36	SE	0495611:1550071	Upper metalimestone
30	S1	210	56	SE	0495070:1550026	Upper slate
31	S1	231	40	SE	0494068:1549168	Upper slate
32	S1	200	80	SE	0494029:1550244	Lower metalimestone
33	S1	33	45	SE	0494786:1550893	Lower metalimestone
34	S1	68	58	SE	0493440:1549712	Lower slate
35	S1	88	70	SE	0492843:1550206	Basic metavolcanic
36	S1	221	60	NW	0493591:1551161	Basic metavolcanic
37	S1	67	43	SE	0491572:1550615	Meta-agglomerate
38	S1	200	46	SE	0491872:1551547	Meta-agglomerate
39	S1	49	34	SE	0491131:1550014	Intermediatemetavolcanoclast
40	S0 & S1	38	78	SE	0494607:1550255	Upper slate
41	S0	30	60	SE	0494493:1550292	Lower metalimestone
42	S0	45	75	SE	0494328:1550634	Lower metalimestone
43	S1	35	33	SE	0494328:1550634	Lower slate
44	S0 & S1	40	65	SE	0494134:1550618	Lower slate
	S0	30	60	SE	0494055:1550509	Lower slate
45	S0	40	65	SE	0494055:1550509	Lower slate
46	S0	32	66	SE	0493702:1550314	Basic metavolcanic
47	S1	40	58	NW	0493268:1550675	Basic metavolcanic
48	S1	40	52	SE	0494712:1551363	Lower slate
50	S0	30	85	NW	0493002:1550418	Basic metavolcanic
51	S1	76	35	SE	0492501:1552355	Intermediate metavolcanoclast
52	S1	66	31	SE	0492422:1552947	Intermediate metavolcanoclast
53	S1	45	85	SE	0491664:1550631	Meta-agglomerate
54	S1	20	75	NW	0492128:1551726	Basic metavolcanic
55	S1	30	85	SE	0492628:1552289	Intermediate metavolcano clast
	Fold axis					
		Trend	plunge			
1		220	10		0496098:1553049	Lower slate
2		202	15		0495429:1549629	Upper metalimestone
3		195	20		0495868:1549478	Upper metalimestone

4		210	35		0495868:1549478	Upper metalimestone
5		183	9		0493603:1553611	Intermediate metavolcanoclastic
Kink bands						
		205	5		0494700:1551365	Lower slate
		189	4		0494700:1551365	Lower slate
Joints						
1	Joint-1	140	30	NE	0496098:1553049	Lower slate
2	Joint-2	170	85	NE	0496098:1553049	Lower slate
3	Joint-3	120	85	NE	0496098:1553049	Lower slate
4	Joint-4	285	88	SW	0496098:1553049	Lower slate
5	Joint-1	330	45	NE	0495928:1553075	Lower slate
6	Joint-2	330	35	NE	0495928:1553075	Lower slate
7	Joint	125	20	SW	0492832:1552863	Acidic metavolcanic
8	Joint-1	70	33	NW	0492307:1553950	Intermediate metavolcanoclastic
9	Joint-2	350	50	NE	0492307:1553950	Intermediate metavolcanoclastic
10	Joint-1	112	60	NE	0494607:1550255	upper slate
11	Joint-2	111	55	NE	0494607:1550255	upper slate
12	Joint-1	120	85	NE	0494328:1550634	lower slate
13	Joint-1	150	85	NE	0494328:1550634	lower slate
14	Joint-2	110	55	NE	0494328:1550634	lower slate
15	Joint-3	295	90	NE	0494134:1550618	lower slate
16	Joint	280	61	SW	0493737:1551140	Basic metavolcanic
17	Joint-1	85	77	NE	0494700:1551365	Lower slate
18	Joint-1	350	30	NE	0494700:1551365	Lower slate
19	Joint-2	150	45	NE	0494700:1551365	Lower slate
20	Joint-3	348	75	SW	0493002:1550418	Lower slate
21	Joint-1	345	70	SW	0493002:1550418	metatuff
22	Joint-2	80	85	NW	0495770:1553076	Metatuff
Veins						
1	Enechelon calcite vein	110	90	SW	0496483:1553011	Lower metalimestone

2	Calcite vein	115	90	SW	0496483:1553011	Lower metalimestone
3	Calcite vein	120	90	SW	0496483:1553011	Lower metalimestone
4	Calcite vein	105	90	NE	0496483:1553011	Lower metalimestone
5	Quartz Vein	110	90	NE	0496098:1553049	Basic metavolcanic
6	Quartz vein	90	60	S	0490287:1552931	Basic metavolcanic
7	En echelon calcite vein-1	120	42	SW	0496995:1549490	Upper metalimestone
8	En echelon calcite vein-2	130	63	SW	0496920:1549452	Upper metalimestone
9	En echelon calcite vein-1	140	46	NE	0496856:1549413	Upper metalimestone
10	En echelon calcite vein-2	100	60	NE	0496856:1549413	Upper metalimestone
11	Calcite vein-1	100	30	NW	0496856:1549413	Upper metalimestone
12	Calcite vein-2	160	45	SE	0496856:1549413	Upper metalimestone
13	Calcite vein	030	43	NW	0496856:1549413	Upper metalimestone
14	En echelon calcite vein-1	090	45	N	0496320:1549402	Upper metalimestone
15	En echelon calcite vein-2	100	38	NE	0496320:1549402	Upper metalimestone
16	calcite vein	350	26	SW	0495280:1549778	Upper metalimestone
17	Quartz vein-1	284	90	NE	0493277:1552544	Intermediate metavolcanoclastic
18	Quartz vein-2	300	90	SW	0493277:1552544	Intermediate metavolcanoclastic
19	Quartz vein-1	300	57	SW	0495802:1553482	Basic metavolcanic